UNIVERSITÀ DEGLI STUDI DELL'AQUILA

Department of Civil, Construction-Architectural and Environmental Engineering

Doctoral Thesis

Simplified multicriteria method for seismic assessment of unreinforced masonry buildings

Ph.D Course in Civil, Construction-Architectural and Environmental Engineering

XXXIV cycle

Candidate

Ilaria Capanna

SSD

ICAR/09

Course Coordinator

Professor Marcello Di Risio

Thesis Tutor

Professor Massimo Fragiacomo

Co-Tutor

Professor Franco Di Fabio

SIMPLIFIED MULTICRITERIA METHOD FOR SEISMIC ASSESSMENT OF UNREINFORCED MASONRY BUILDINGS

Ilaria Capanna

Professor Massimo Fragiacomo

Professor Franco Di Fabio

Reviewers:

Prof. Brando Giuseppe *University G. D'Annunzio, Chieti-Pescara*
Prof. Formisano Antonio *University Federico II, Napoli*

Simplified multicriteria method for seismic assessment of unreinforced masonry buildings

Ilaria Capanna
IDnumber–
Department of Civil, Construction-Architectural and Environmental Engineering-DICEAA
University of L'Aquila

Website: http://diceaa.univaq.it/

Mens immota manet,
lachrimae vulvuntur inanes.

[Blank page]

Abstract

The aims and motivations that were driven this PhD thesis, *Simplified multi criteria method for seismic assessment of unreinforced masonry buildings*, arise from the common interest on the mitigation of the seismic risk, wide field of continuous relevance and of interest for different disciplines. The scientific community, specially in engineering field, reserves attentions on the mitigation of the seismic risk. The human and economic losses, caused by fragilities of the urban centres, manifested in the aftermath of a seismic event, confirm the need of research effort. The PhD thesis presents a multi criteria method for seismic assessment of unreinforced masonry buildings, URMs. The majority of the built environment consists of URMs. The study of their seismic behaviour is exasperated by the ageing of materials, the lack of anti-seismic criteria, construction process, architectural alterations or restorations, and the poor mechanical properties of used materials. Nevertheless, URMs are unique constructions for their historical and architectural value, that need to be protected against earthquakes. The knowledge of structural fragilities of urban centres is a prerequisite to face the mitigation of the seismic risk. Simplified assessment methods arise to overcome the effort and time consuming of analysis at a large scale of the built environment, by means the introduction of several simplifications. The proposed multi criteria vulnerability method provides a quick assessment based on few structural parameters, known from field observations and geometric survey, to overcome excessive computational demand, thanks to two different levels of evaluation. The first level of the vulnerability assessment method, called *empirical method*, bases on the evaluation of few structural parameters to perform a first screening of the seismic fragilities. The second level, called mechanical approach, predicts the seismic capacity of masonry walls more accurately respect to the empirical one, to establish strengthening measures or strategies more accurately.
Therefore, the multi criteria method could support the activities of authorities and stakeholders in the mitigation of the seismic risk of the built environment.
The thesis consists of eight chapters, below briefly reported.

The first chapter *The seismic risk* introduces an overview on the seismic risk, as field of the research activity. Starting from a generic definition of the issue, the chapter describes the parameters that influence on the seismic risk. Part of the chapter is then dedicated to the seismic risk management to highlight the possible applications of the proposed method. A brief paragraph concerns the seismic hazard in Italy, where the test site of the thesis is located.

The second chapter *Structural vulnerability* concerns the state of the art of structural vulnerability. An in-depth classification of seismic vulnerability assessment methods is reported. The chapter includes all the most important evaluation approaches for URMs, on which the research activity focused.

The third chapter *Unreinforced masonry buildings* regards the test-site of the research activity. The area under investigation has been described in terms of seismic hazard. Structural and architectural information underline the main characteristic of the buildings' class. The chapter also discusses the suffered seismic damage of buildings affected by the last earthquake that hit the Central Italy. The first paragraph has been reserved to the seismic swarm and the historical seismic hazard of the area. The last part of the chapter is dedicated to the characterization of the sample of buildings, on which numerous numerical analyses have been carried out. These numerical results conclude the chapter.

The fourth chapter *On the dynamic behaviour of a URM prototype* reports the dynamic campaign on a URM, chosen as representative of the structural class. The aim of this activity was to investigate the influence of a suite of structural parameters influencing the building behaviour. Therefore, the dynamic campaign conducted was presented in detail in the first paragraphs. The following paragraphs discuss the numerical models developed and the related model up-dating process. The last part of the chapter reports the results of a parametric analysis by varying mechanical properties of masonries and floors, to evidence the influence on the URM dynamic behaviour.

The fifth chapter *Empirical Method for Seismic Assessment of URMs* introduces the first level of the predictive multi-criteria method. The empirical method aims to estimate the seismic vulnerability through the evaluation of a few structural parameters, ensuring a quick application. The derivation and validation of the formulations' method are reported. The last part of the chapter compares the method with others available from the literature, to highlight its reliability and advantages.

The sixth chapter *A path to urban resilience strategies* illustrates possible applications of the empirical predictive method. The first paragraph deals with the derivation of typological curves for URMs class. The second paragraph reports the calibration of a simplified vulnerability model, suggested by the scientific literature, based on the seismic safety index provided by the proposed method. In the third paragraph, a fast seismic risk mitigation strategy was proposed and structured, through three sets of structural interventions, with increasing invasiveness order. This application aims to predict the impact, on an urban sector, of various structural reinforcement measures, in terms of losses and economic disbursements reduction. The last paragraph suggests other possible applications and future

developments of the empirical method.

The seventh chapter *Mechanics-based method for seismic assessment of URMs* discusses the second level of the proposed method. It aims to grasp the seismic vulnerability of buildings, with a higher accuracy than the first level. The mechanical method provides a reliable assessment approach, to avoid the resort of a numerical approach. The first paragraph reports the formulations that support the method and its validation. A final comparison between damage curves drawn with the numerical, empirical and mechanical method highlights the advantageous of the multi-criteria method in seismic vulnerability of URMs.

The eighth chapter *Research significance and future outcomes* completes the PhD thesis, with a broader point of view, to explain the results and future developments.

[Blank page]

Sommario

Gli obiettivi e le motivazione che hanno guidato l'attività di ricerca della presente tesi di Dottorato *Simplified multicriteria method for seismic assessment of unreinforced masonry buildings*, hanno radici nell'interesse comune nella riduzione del rischio sismico: settore a largo spettro, di continua attualità e di lavoro per diverse discipline. La comunità scientifica internazionale, soprattutto nel settore ingegneristico, si dedica, ormai da anni e con sollecitudine, al tema della riduzione del rischio sismico. Le perdite umane, materiali ed economiche, le continue fragilità mostrate dai centri urbanizzati a cui si assiste all'indomani di un sisma, corroborano l'appetibilità della tesi di Dottorato. Il fine dell'attività di ricerca è stato quello di sviluppare un metodo predittivo multi-criterio della vulnerabilità sismica delle costruzioni murarie. Le strutture in muratura rappresentano gran parte del tessuto edilizio esistente. La vetustà dei materiali, il mancato rispetto di principi di progettazione antisismica, la non osservanza delle regole dell'arte, le modifiche strutturali subite negli anni, nonché le scarse proprietà meccaniche dei materiali stessi, sono tutti fattori che complicano l'approccio a tali strutture. Al contempo, il loro pregio storico e architettonico è un valore aggiunto per i nostri centri urbani, e come tale va protetto e salvaguardato, anche dalla minaccia di eventuali scosse sismiche. Le autorità e le professionalità, che dovrebbero avviare uno studio conoscitivo della vulnerabilità sismica di un centro urbano, si trovano davanti una vastità del patrimonio costruito tale da richiedere uno sforzo titanico in termini di tempi e risorse. I metodi di valutazione di vulnerabilità sismica semplificati (così denominati dalla letteratura scientifica di settore) sopperiscono a queste necessità, consentendo l'avvio di studi di vulnerabilità sismica anche estesi ad una vasta scala del costruito. Con il metodo proposto nella tesi si intende proporre un approccio multi criterio che, sulla base di una rapida valutazione di un edificio murario, sia in grado di restituire una stima della vulnerabilità sismica, con due definizione diverse per onere richiesto e accuratezza. Tale connotazione rende il metodo uno strumento ibrido facilmente implementabile in attività di gestione e riduzione del rischio sismico, soprattutto quelle che abbracciano porzione del costruito con decine di edifici da dover analizzare. In virtù dei diversi livelli di valutazione, il metodo valutativo proposto offre due approcci diversi a seconda della accuratezza desiderata nella restituzione del livello di vulnerabilità sismico. Il primo approccio, meno accurato ma più speditivo, è in grado di offrire uno screening della vulnerabilità sismica di un'area costruita, per poi consentire la derivazione di scenari di danno attesi al variare dell'intensità sismica. Tali valutazioni ne guiderebbero anche altre

finalizzate a minimizzare le perdite provocate da un sisma, aumentando così la resilienza dei centri urbani. Il secondo approccio, grazie alla maggiore accuratezza nella valutazione dello stato di capacità sismica, consentirebbe di modulare strategie di messa in sicurezza del patrimonio costruito. Tale informazione sarebbe di grande ausilio per le autorità competenti per stimare tempi e costi degli interventi strutturali da mettere in opera. Pertanto, la strutturazione multi criterio rende il metodo proposto deputato a soddisfare esigenze di diversi *stakeholders* delle attività di mitigazione del rischio sismico del patrimonio costruito.

La tesi è stata strutturata in otto capitoli, di seguito brevemente descritti.

Il primo capitolo *The seismic risk* introduce una panoramica sul rischio sismico, macro-settore dell'attività di ricerca. Partendo dalla più generica definizione del tema, si giunge a descrivere i parametri che concorrono nella definizione del rischio sismico. Una parte del capitolo è dedicata alla gestione del rischio sismico per presentare il campo di applicazione dell'attività di ricerca. Un breve paragrafo è riservato alla pericolosità sismica in Italia, essendo il test-site della tesi ricadente in tale territorio.

Il secondo capitolo *The structural vulnerability* è dedicato allo stato dell'arte. È stata approfonditamente descritta la classificazione dei metodi di valutazione della vulnerabilità sismica. Poiché il metodo valutativo proposto è destinato alle costruzioni in muratura, nel capitolo vengono annoverati tutti gli approcci di valutazione di maggior rilievo per questa classe costruttiva, per offrire anche un metro di paragone dell'attività svolta.

Il terzo capitolo *Unreinforced masonry buildings* presenta il test-site utilizzato nell'attività di ricerca. Dapprima è stata descritta l'area oggetto di indagine è in termini di pericolosità sismica. Siccessivamente, la classe stutturale di analisi è stata caratterizzata dal punto di vista architettonico e strutturale. Il capitolo offre anche una disamina delle evidenze strutturali e comportamenti sismici manifestati dal tessuto edilizio, che è stato recentemente colpito dall'ultimo sisma che ha scosso il Centro Italia nel 2016. La restante parte del capitolo è dedicata alla caratterizzazione numerica del campione di edifici, su cui sono state svolte numerose analisi statiche non lineari, i cui risultati concludono il capitolo.

Il quarto capitolo *On the dynamic behaviour of a URM prototype* descrive la campagna dinamica che è stata condotta su un edificio scelto come rappresentativo della categoria strutturale oggetto di ricerca. Scopo di questa parte di attività è stato quello di indagare l'influenza di alcuni parametri strutturali sul comportamento globale dell'edificio prototipo. Pertanto nei primi paragrafi è stata presentata nel dettaglio la campagna dinamica condotta. I paragrafi successivi discutono i modelli numerici sviluppati e il relativo model up-dating. L'ultima parte del capitolo riporta i risultati dell'analisi parametrica, evidenze che hanno guidato il prosieguo dell'attività di ricerca della tesi.

Il quinto capitolo *Empirical Method for Seismic Assessment of URMs* è dedicato al primo livello del metodo multi criterio predittivo, che può esser definito empirico. Il primo livello si prefigge la stima della vulnerabilità sismica mediante la valutazione di pochi parametri strutturali, con un limitato onere e una speditiva applicazione, aspetti rilevanti in valutazione che coinvolgono numerosi edifici. Si riporta la derivazione e validazione delle formulazioni sviluppate che giungono a definire il primo livello del metodo di valutazione della vulnerabilità sismica. L'ultimo parte del capitolo riporta il confronto del metodo con altri della medesima tipologia presenti in letteratura, per evidenziarne affidabilità e vantaggi.

Il sesto capitolo *A path to urban resilience strategies* traccia un percorso di applicazioni possibili del metodo predittivo empirico. Il primo paragrafo tratta la derivazione di curve tipologiche per il campione di edifici analizzato, generalizzabile alla macro classe di edifici in muratura ordinari. Il secondo paragrafo riporta la calibrazione di un modello di vulnerabilità semplificato, suggerito dalla letteratura scientifica, sulla base dell'indice di sicurezza sismica restituito dal metodo proposto. Nel terzo paragrafo è stata proposta e strutturata una strategia di mitigazione del rischio sismico speditiva, mediante tre set di interventi strutturali, con ordine di invasività crescente. Questa applicazione si prefigge lo scopo di poter predire, in modo semplificato, l'impatto su un comparto urbano di diverse misure di rinforzo strutturale, sia in termini di riduzione delle perdite causate da un sisma che in termini economici. L'ultimo paragrafo si riserva l'obiettivo di suggerire altre possibili applicazioni come sviluppi futuri dell'attività di ricerca.

Il settimo capitolo *Mechanics-based method for seismic assessment of URMs* approfondisce il secondo livello del metodo proposto, che può esser definito come meccanico semplificato. Il metodo si prefigge di cogliere il livello di vulnerabilità sismica di edifici, con un'accuratezza superiore rispetto a quello di primo livello. Il primo paragrafo descrive le formulazioni che supportano il metodo, per poi discutere nei paragrafi successivi la validazione stessa e l'applicazione al campione di edifici. Un confronto finale tra curve di danno tratte con il metodo numerico, empirico e meccanico evidenzia come l'attività sia giunta allo sviluppo di un metodo multi criterio che sia in grado di stimare la valutazione della vulnerabilità sismica di edifici in muratura con accuratezza e oneri crescenti.

L'ottavo capitolo *Research significance and future outcomes* conclude la tesi di dottorato ripercorrendo l'attività di ricerca, con un punto di vista più ampio, per contestualizzare i risultati ottenuti e suggerire futuri sviluppi.

[Blank page]

Contents

List of Figures

List of Tables

The seismic risk

Chapter abstract

Earthquake represents the most frightening natural event that threatens the human life. Despite the hundreds of seismic events that occurred in the history in all over the world, the complexity of the natural phenomenon is still an open issue. Its knowledge is a prerequisite to attempt the mitigation of the shattering consequences that arise after a seismic event. Different disciplines are involved and required in this study. In this chapter, an overview of the seismic risk is delivered to better understand the role of the structural vulnerability of facilities on which the PhD thesis concerns.

1.1 The seismic risk

The impact of the seismic risk on human life is well known: earthquakes continue to represent a serious threat for the seismic prone areas, particularly for Mediterranean bordering countries. In the last centuries and decades, casualties, suffered buildings' damage, homeless, and economic losses confirmed the need of evaluation the seismic risk to prevent future catastrophic consequences. Therefore, seismic risk is the main natural risk to face by several countries, deserving attention of the public authorities to introduce resilience policies and mitigation measures of the existing facilities. According to the definition proposed by United National Disaster Relief Office (U.N.D.R.O., 1979), the seismic risk R_{sv} can be expressed as the result of the mathematical relationship between hazard, vulnerability, and exposure, see Eq.1.1:

$$R_{(ie|T)} = |(H_i V_e)E|_T \tag{1.1}$$

Where: R is the probability of exceedance of a certain level of loss of an exposed element e, as a consequence of the occurrence of a seismic event of certain intensity I; H is the probability of exceedance of a certain level of seismic activity of intensity i during a specified recurrence period T; V is the vulnerability of a certain element e; and E is the exposure of the elements at risk Vicente et al. (2011). In general, seismic risk is the possibility of adverse effects, derived from the interaction of social and environmental processes, from the combination of physical hazards and the vulnerabilities of exposed elements, see Fig. 1.1.

1.1.1 Seismic Hazard

Seismic Hazard expresses the probability of occurrence within a specified period, at a given area, of a potentially damaging phenomenon of a given intensity Coburn et al. (1994). The analysis of a seismic hazard aims to estimate the ground shaking motion for a given magnitude earthquake expressed in terms of a set magnitude parameter. Hazard assessment involves studies of historical data, topographical and geological maps. Two methods are available in literature to perform a macro-seismic hazard assess-

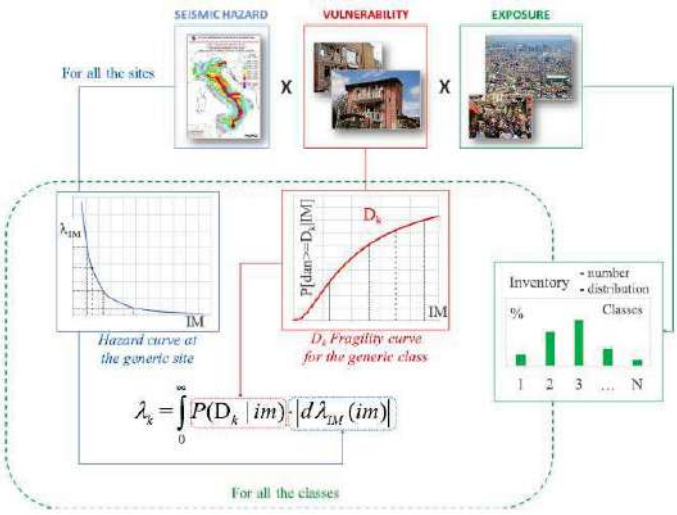

Figure 1.1. Main elements contributing to seismic riskDolce et al. (2021).

ment: (i) the Deterministic Seismic Hazard Assessment (DSHA); (ii) the Probabilistic Seismic Hazard Assessment (PSHA). DSHA method aims to derive the maximum credible intensity of ground-motion at a given site by means of the evaluation of a maximum likely earthquake of occurring at the site or near its proximitySuckale et al. (2005). The method consists of four steps: (i) the identification and characterization of all seismic sources based on seismic historical data events, geological configurations, faults, and magnitude of the maximum historical earthquakes. A grid map divides the territory into cells of which center represents a seismic genetic source. (ii) Selection of the source-site distance parameter; (iii) selection of a controlling earthquake calculating by using an attenuation relationship to estimate the ground shaking within the area of interest; (iv) the hazard has been defined as the maximum expected value. The PSHA predict the earthquake ground motion parameters like peak ground acceleration, peak ground velocity and peak ground displacement. PSHA consists of three steps: (i) specification of all earthquake sources contributing to the seismic hazard of a study area; (ii) attenuation relationships to predict the distribution of ground motion intensities; (iii) probabilistic calculation based on the total probability theorem Du (2020). The PSHA method is affected by uncertainties of earthquake occurrence, like magnitude, location, and recurrence rate. The seismic hazard is defined as the annual rate of seismic events affected by a ground motion amplitude that exceeds the expectation

value at the site. The amplitude is a random variable that represents an arbitrary parameter to quantify the ground shaking, like the Peak ground Acceleration (PGA). The probabilistic approach, that bases on the Cornell Cornell (1967) and McGuire McGuire (2008) formulations, is the most used method in engineering design to characterize the strong ground motion: the overall hazard H is the convolution of the contribution of each source zone I, out of the set of zones I, called $H_i(A)$. Firstly, the seismic hazard is evaluated for each zone separately. Lastly, the probability of the hazard H is evaluated as the sum of the hazard probabilities of each zone, see Eq.1.2:

$$H(A) = \sum H_i(A) = \sum v_i \iint_{mmin}^{mmax} P(a|m,r) f_{(Rj|Mj)}(r|m) f_{MI} dR dm \tag{1.2}$$

where:

- v_i is the annual rate of earthquakes with a magnitude higher than a specified threshold value M_{min} at the zone i;
- P(a—m,r) expresses the probability of exceeding the acceleration value A when an earthquake of magnitude m occurs at a r distance.
- f_{MI} and $f_{(Rj|Mj)}(r|m)$ indicate the probability density function referred to distance and magnitude.

Still, the Poisson expression, see Eq.1.3, evaluates the seismicity as the probability that k events occur, during an interval of time Δt:

$$P(k|K, \Delta t) = \frac{\lambda^k}{k!} \times \exp(-\lambda) \tag{1.3}$$

1.1.2 Exposure

Exposure indicates the element at risk, like population, livelihood, environmental sector, socioeconomic activities, facilities, and lifelines systems that could be affected by an earthquake in a specific area. An analysis of the exposure requires data referred to the analysed area. Exposure may include a single construction with its users and contents or the entire built up of a selected area, depending on the extension of the scope of the analysis. Three different scales of analysis are possible: at the single structure

scale, at the single infrastructure system (e.g. urban lifelines) scale, and at the urban scale. Often, in the application of seismic risk mitigation, a characterization of the exposure in terms of built environment is a preliminary step. The characterization of buildings' typologies aims to investigate, in a qualitative way, the peculiar constructive features. Each country or region preserves its construction techniques, sometimes changed over the time due to the local culture and conditions, affecting the structural characteristics of the built up and its seismic behaviour. A standardization of the inventory of exposure assets facilitates the information collection of the existing facilities in a region. At this aim, an inventory has been introduced based on type, occupancy, and function of buildings. Data and documents are gathered from related agencies or census. In Italy, exposure data are provided by the national census investigations, periodically updated by the National Institute of Statistics, ISTAT, that reports metric data for urban areas, like number of buildings, floors, age of constructions, types, and materials. A more accurate method of inventory of the buildings exposed to seismic hazard was proposed in the framework of the RELUIS projects, through the CARTIS approach Zuccaro et al. (2015). The aim of the CARTIS project is to enhance the knowledge of the buildings' taxonomies, in the Italian urban centres, and their territorial distribution at national scale Polese et al. (2019); Zuccaro et al. (2015). A form was proposed to gather information about facilities located in municipal or submunicipal areas, named urban sectors. An urban sector is characterized by typological and structural homogeneity. For each building type (residential buildings, churches, historical monuments, hospital, schools, governmental buildings, and industrial constructions) relevant parameters are collected, in particular:

- Number of floors;
- Construction period;
- Use;
- Vertical structure configurations;
- Horizontal structure configurations;

Table 1.1. Structure of the CARTIS approach for district scale.

Sections	CARTIS 2014-1st Level
0	Municipality and districts statistics
1	Building type identification
2	General features (building type)
3a	Structural classification (masonry type)
3b	Structural classification (R.C. type)

Table 1.2. Structure of the CARTIS approach for building scale.

Sections	CARTIS 2016-2nd Level
0	Building statistics
1	Building identification
2	Building features
3a	Structural classification (masonry building)
3b	Structural classification (R.C. building)

- Type of foundations;
- Conservation state;
- Construction techniques.

Two different levels of the CARTIS form are set. The first level of CARTIS form, see Tab.tab:cartis1, bases on a protocol that recognizes the main parameters of building types within an urban district. The form consists of distinct sections for masonry constructions (MUR) and reinforced concrete (CAR) ones. The second level gathers data relevant for the seismic response of specific buildings for further accurate investigations, like vulnerability assessment. Moreover, the second level of CARTIS, see Tab.tab:cartis2, corroborates, on a large scale of analysis, the assumptions derived from the first level applied on urban scale.

.

.

Still, many scholars deserve attention to CARTIS form applications to enhance its capability to grasp the exposure of the buildings' taxonomiesTocchi et al. (2021).

1.1.3 Vulnerability

Seismic vulnerability of assets is their susceptibility to loss functionality under an earthquake action, as a function of the seismic intensity Dolce et al. (2021). Buildings' vulnerability is the predisposition of structural or no-structural parts to suffer a certain damage after a seismic action. According to an alternative definition, the vulnerability of a construction is its structural behaviour due to a cause-effect law: the cause is the seismic action, and the effect is the suffered damage. Unfortunately, existing buildings exhibits unsatisfactory seismic behaviour due to fragilities of structural and non-structural elements, revealing an urgent need to enhance their structural safety. Several parameters exacerbate vulnerabilities of constructions, especially materials and geometrical features. Many buildings' classifications, finalised to vulnerability models, are proposed in literature. The first attempts to characterise buildings' vulnerability was carried out in the early 1980's in the United States and Central and Eastern Europe in seismic-prone countries like Italy, Romania and Greece Vicente et al. (2011). In the United States, the Federal Emergency Management Agency (FEMA) developed a tool (HAZUS 1999, Parisi (2013)) for assessing earthquake losses in terms of usable facilities and casualties of urban areas. In Italy, the *Servizio Sismico Italiano* GNDT-SSN (1994) developed a rapid screening method of vulnerability which has been corroborated and improved over time by data collected from occurred earthquakes. A fast buildings classification was proposed by the MKS scale that consisted in three class:

- **CLASS A**: building with dry stone, or clay, adobe or mud walls;
- **CLASS B**: buildings with masonry walls made form brick, mortar blocks, stone units;
- **CLASS C**: buildings with metal or reinforced concrete structures.

The Hazus (1999) Hazus (1997) and EMS-98 Grünthal (1998), see Fig.fig:EMS-98, introduced a more accurate buildings' classification by introducing of sub-categories in order to better consider the structural variabilities of the built environment, see Table 1.3.

EMS 98	HAZUS
Unreinforced masonry, URM	**Masonry typologies, M**
Rubble stone	
Adobe (earth brick)	
simple stone	
Massive stone	
URM (old bricks)	
URM (r.c. floors)	URM bearing walls
Reinforced/confined masonry, RCM	**Reinforced/confined masonry**
RCM	RM with flexible floors
RM with precast	
concrete diaphragms	
Reinforced concrete, RC	**Reinforced concrete, RC**
Frame in RC	RC Moment Frame
Shear walls	RC shear walls
	RC frame with URM infill
Steel typologies, S	**Steel typologies, S**
S structures	S moment frame low-rise
	S braced frame
	S light frame
	S frame with Cast C shear walls
	S frame with URM walls
Timber typologies, T	**Timber typologies, T**
T structures	Wood, Light Frame
	Wood, commercial and Industrial
	Pre-Cast typologies, PC
	PC Tilt-up walls
	PC frames with concrete walls
	Mobile homes

Table 1.3. Buildings classification by EMS 98 and HAZUS.

Moreover, HAZUS classification also considers the number of floors and the code level in force at the moment of the construction (high code, moderate code, low-code and pre-code). Vulnerability deserves attention, not only for the physical consequence in the eventual occurrence of a seismic event, but also because is the aspect that is possible mitigate to reduce the seismic risk Vicente et al. (2011). Further considerations about structural vulnerability and its evaluations are reported in chapter.

.

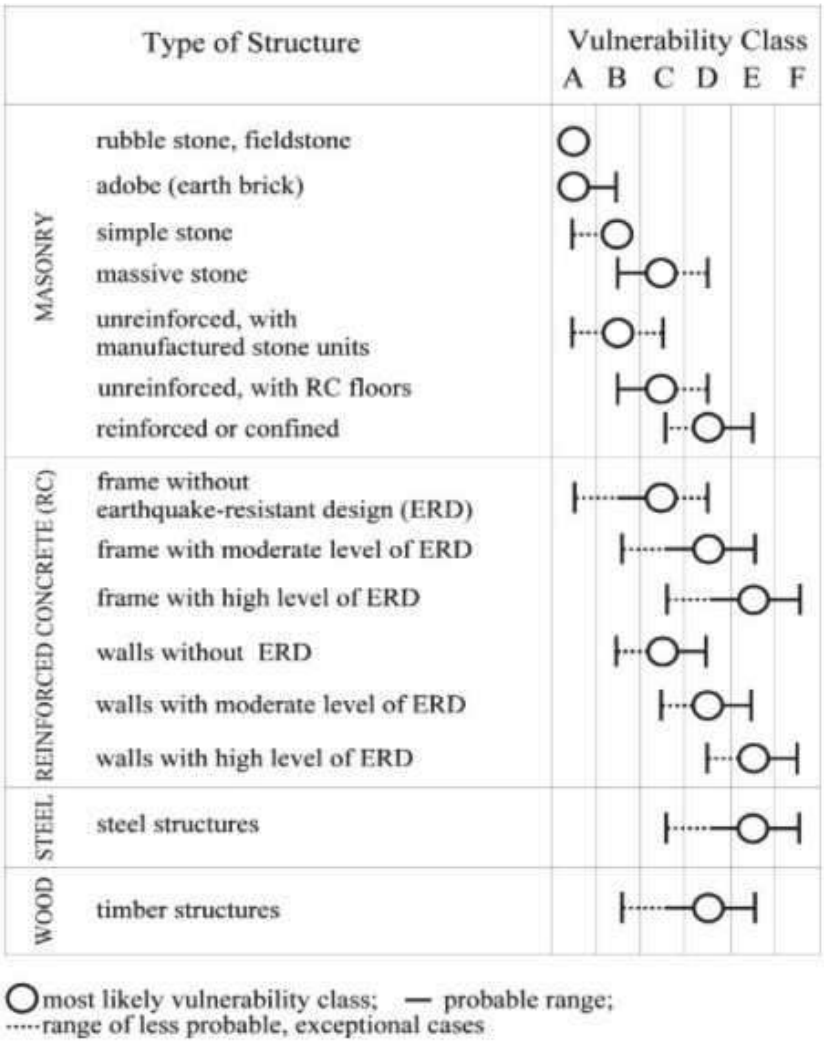

Figure 1.2. EMS-98 Vulnerability classification.

1.2 Management of the seismic risk

Despite the unpredictable nature of seismic events, seismic risk assessment could address appropriate measures to mitigate the devastating consequences on people and facilities that occur under an earthquake. For practitioners and authorities, management policies of the seismic risk are the path to follow in order to improve the resilience of communities towards seismic risk. In fact, in recent years, researchers and system-managers reserved interest to the concept of resilient cities, especially to reduce disaster risk Carpenter et al. (2001); Chelleri et al. (2012); Holling (1973); Ozyetgin Altun and Tezer (2018); Walker et al. (2003). Concept of resilience became relevant also for engineered systems that included infrastructures systems within the built environment: resilient infrastructure systems, particularly "lifeline" services like electric power, water and health care, are fundamental for minimizing the societal impact of extreme events Mcdaniels et al. (2008). In general, resilience indicates the capability of a system or component of standing and recovering the functionality quickly from an event, see Fig.1.3. The main parameters that influence the resilience are the robustness of the system and its rapidity to return to full operational conditions. An alternative definition defines the seismic resilience enhancement as the seismic risk reduction.

The resilience of an urban fabric can be evaluated at three different levels. At the single structure scale, the resilience depends on the structural safety of a single construction, expressed in terms of resisting capacity, ductility, or robustness. The second level focuses on the single infrastructures system scale, like urban lifelines scale, aiming to evaluate the efficiency of the services provided to citizens expressed as robustness and redundancy propertiesBozza et al. (2015). The third level regards the urban scale: the overall complex system is evaluated in terms of efficiency and preparedness of citizens through social and physical capability of the components to return at the full functionality. In the case of occurring an earthquake, the resilience of a city depends on a physical and social network: the built city has to be conceived as linked with social and institutional systems and also with economic and environmental components, embedded within the urban

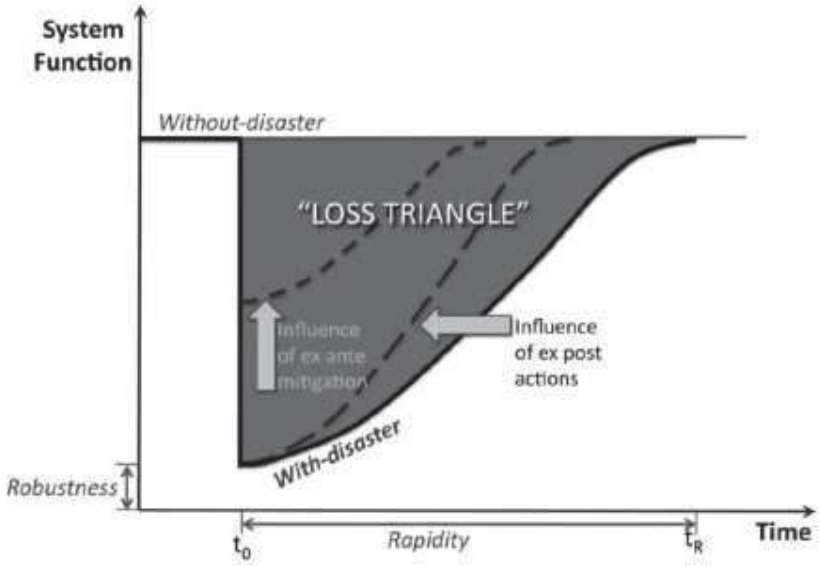

Figure 1.3. Idealization of resilience concept.

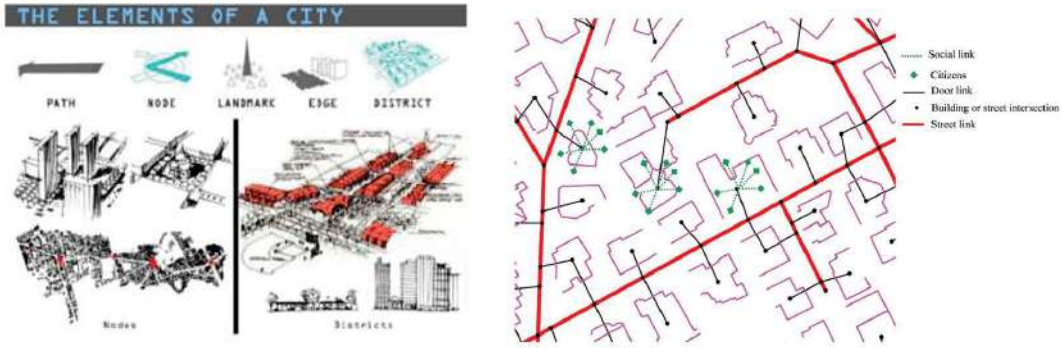

Figure 1.4. Schematic representations of the different ULC.

context, Mcdaniels et al. (2008), see Fig./reffig:network.

Therefore, different methodologies are used to quantify resilience of social and physical networks, in terms of economic, social, and environmental indicators. An important application in this framework is the design of the Emergency Limit Condition (ELC), that is defined as the threshold condition of maintaining the efficiency of the strategic buildings, accessibility, and the connection of the territorial context after an earthquakeBramerini et al. (2014). Emergency plan aims to guarantee the ELC to avoid the interruption of urban functions, see Fig. 1.5.

At this aim, scenario analysis can be performed to support resilience assessment. The enhancement of resilience, which is equivalent to the reduc-

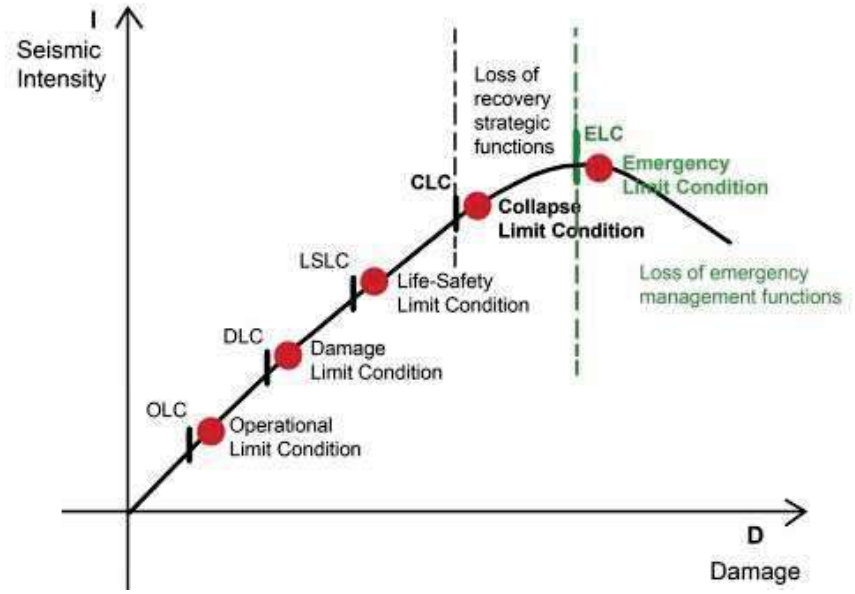

Figure 1.5. ELC curve.

tion of the loss triangle in the Fig. 1.3, needs of two different interventions: ex- ante measures and ex-post actionsChang et al. (2013). The mitigation of the structural vulnerabilities represents an action useful to prevent seismic damage, allowing to enhance the resilience of the built heritage in the ante and post period of a seismic event. The mitigation of the existing facilities is achieved through strengthening measure. Unfortunately, the acclaimed vulnerabilities of the built environment and the high seismic hazard of the earthquake-prone areas lead to an impossibility to resilience enhancing in a widespread manner. An integrated insight is required in planning and decision-making activities to foster built environment components with a more negligible resilience level. Therefore, mapping, vulnerability assessment, economic evaluation, and social studies arise as needful activities to support resilience enhancing strategies and thus, the management of the seismic risk. Below, an overview of the main activities useful for seismic reduction risk is reported.

1.2.1 Mapping to manage the seismic risk

Maps play a fundamental role in seismic risk management, especially at the territorial scale, due to providing the spatial distribution of risk in terms of hazard, exposure, or vulnerability. Seismic risk maps can support the authorities in addressing risk mitigation measures at short, mid, or long

terms. Zanini et al. (2019). The first application of mapping aims to represent the seismic hazard of an analysed area in terms of a ground, peak ground acceleration, peak ground displacement, peak ground velocity, or motion parameter versus return period. Recently, thanks the introduction of a more powerful tools, mapping represents a valuable activity useful to represent different scenarios in terms of damage, costs, vulnerabilities or in general a spatial view of the area under study for a specific parameter of interest. One of the most recent tools is the Geographic Information System (GIS) programme that combines geo-referenced graphical data (vectorised information and orthophoto maps) with buildings' parameters information Ferreira et al. (2017). Nowadays, GIS represents an instrument for multidisciplinary analysis for scenario or risk analysis studies due to the possibility to cross different data and verify the consequences deriving from specific territorial phenomena. Different types of data are implemented in the GIS software like buildings features, survey information, seismic vulnerability indices). Dataset implemented in GIS application can be updated at any time. Particularly, GIS software allows to develop a scenario after a specific seismic event recorder in the seismic catalogues or for future simulated earthquakes to capture damage or unsafety facilities, the interaction from buildings and lifelines, roads in order to manage the post-earthquake emergency. Still, a damage scenario could be performed to evaluate the economic loss.

For this reason, implementation of civil protection and local emergency plans exploit GIS programmes by means of which a spatially integrated analysis could be performed through visualisation of data and results also for different earthquake scenariosGiovinazzi et al. (2021); Mascandola et al. (2021); Narjabadifam et al. (2021).

1.2.2 Loss estimation methodologies

A strong seismic event engenders usability and unsafety of numerous facilities at territorial scale. Loss estimation methodologies allow to predict the consequence in the aftermath of an earthquake in terms of direct and indirect losses, homeless and casualties. The knowledge of homeless' and casualties' amount, monetary-losses, resources for recovery usability may

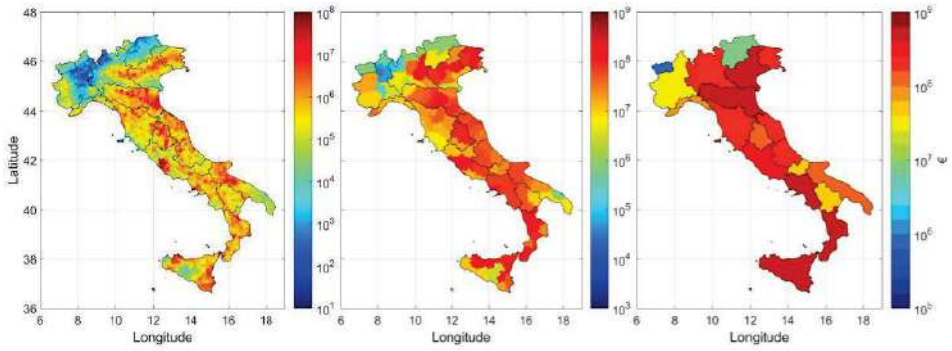

Figure 1.6. The seismic risk map of Italy in terms of: MEAL (left), PEAL (center), and REAL (right).

support stakeholders (owners, authorities, decision makers and insurance companies) to address ex-ante measures and ex-post actions in the mitigation of the seismic risk Cosenza et al. (2018). After an earthquake, the expected damage reveals the amount of facilities that could arise unsafe, supporting emergence plans, enhancing resilience strategies, and forecast of homeless and casualties. Instead, before an earthquake, damage and losses are useful to ascertain the economic disbursements and the reconstruction process to return to fully operational conditions of the hit community. The impact of the seismic risk can be evaluated with different metrics, belonging to three categories (Risk Assessment and Mapping Guidelines for 54 Disaster Management, 2010)Barbalić et al. (2016):

- Human impacts, counting the number of casualties, injuries, homeless, affected population
- Economic and environmental impacts, quantifying disbursements for recovery, restoration buildings, environmental costs, indirect economic losses (like costs due to the disruption of business and economic actives);
- Political and social impacts, evaluated on a semi-quantitative way, due to impacts on public safety, political and social implications.

The Pacific Earthquake Engineering Research Center (PEER) proposed the Performance-Based Earthquake Engineering (PBEE) framework as a robust methodology to perform a loss estimation in four phases: (i) hazard analysis; (ii) structural analysis; (iii) damage analysis; (iv) loss anal-

ysisCornell and Krawinkler (2000); Deierlein et al. (2003). The entire approach aims to quantify the seismic performance of the facilities through decision parameters of interest for stakeholders, like deaths, dollars, downtime, and homeless. According PBEE dispositions, FEMA P-58 Terzic et al. (2020) provided a seismic performance assessment methodology for buildings combining seismic hazard, structural response, damage analysis and indirect losses, in terms of repair costs, repair time and casualties. Moreover, a user-friendly electronic calculation tool, called Performance Assessment Calculation Tool (PACT), provided by FEMA P-58, includes a storage of structural and non-structural component-by-component fragility and data that allows to perform probabilistic assessment of losses De Risi et al. (2019). Still, several researchers reserved attention to the estimation of expected damage and repair cost Cardone et al. (2017); Cremen and Baker (2018); Di Ludovico et al. (2021a). Data gathered after seismic events strengthen the loss estimation methodologies improving their capability in forecasting. In fact, numerous studies have been carried out in the past to appraise typical features of a loss assessment framework on a regional basis using observational from different locations and seismic events Cremen and Baker (2018). Ordaz and Reyes Ordaz and Reyes (1999) compared predicted hazard curves with empirical ones estimated for Mexico city. Booth et al.Booth et al. (2011) corroborated the damage estimation through remote sensing following the 2010 Haitian earthquake. Spence et al.Spence et al. (2003) compared predicted and observed regional losses for the earthquake occurred in Turkey in 1999. Crèmen et al.Cremen and Baker (2018) correlated data from the 2010-2011 Canterbury earthquake sentence to component level loss prediction, see Fig. 1.7.

In Italy, the recent shattering earthquakes, L'Aquila (2009)Capanna et al. (2021); D'Alençon and Rota (2015); DE Martino et al. (2015); De Matteis et al. (2019); Decanini et al. (2010); Formisano et al. (2010); Iervolino et al. (2014); Rossetto et al. (2014), Emilia-Romagna (2012)Ercolino et al. (2016); Formisano (2012); Paupério et al. (2012); Verderame et al. (2014)Acito et al. (2014); Rossi et al. (2019, 2020); Tiberti and Milani (2017), Central Italy (2016)Colonna et al. (2018); Di Sarno et al. (2019); Penna et al. (2019); Risi et al. (2018)Di Ludovico et al. (2019); Fiorentino

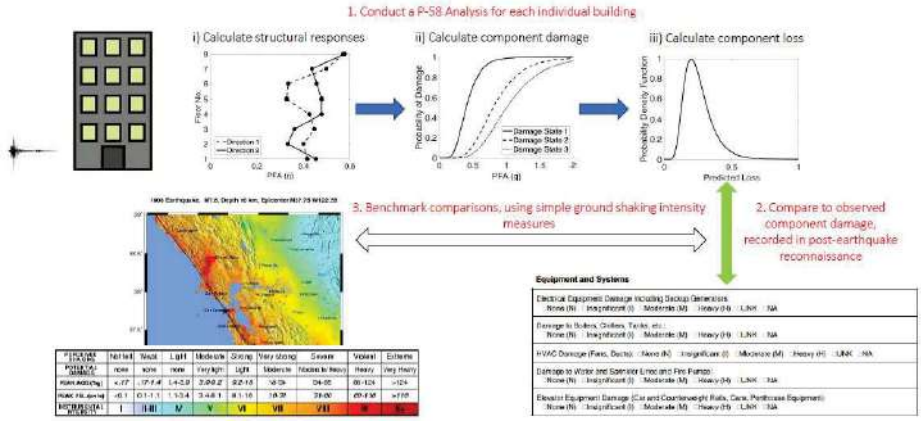

Figure 1.7. Work-flow of the prediction procedure according to FEMA.

Earthquakes	Funding Period	Funding allocated
Valle del Belice	1968-2018	8375
Friuli Venezia Giulia	1976-2006	16917
Irpinia	1980-2023	47470
Marche-Umbria	1997-2024	12284
Puglia-Molise	2002-2023	1300
L'Aquila	2009-2047	17458
Emilia Romagna	2012-2047	8171
Central Italy	20162-2047	13163
Total		125138

Table 1.4. Disaster relief funds and allocation period for Italian earthquakes.

et al. (2018); Sorrentino et al. (2019), highlighted the high vulnerability of the bult Italian heritage. The important losses in terms of homeless, casualties, unsafe and unusable facilities, and the huge economic lead to develop losses estimation methodologies based on data collected after the last earthquakes. An unquestionable need of an improvement of the seismic performance, mostly of unreinforced masonry buildings not designed according to seismic codes, is required. The last seismic swarms occurred caused severe life losses, widespread damage and billion Euros in reconstruction process over the years. Table 1.4, (Servizio Studi- Dipartimento ambiente 2009; Ufficio Valutazione Impatto 2017) reports the disaster relief funds, expressed in MIL euros, and allocation period for major earthquakes in Italy, since 1968.

.

Recent seismic swarms underlined the extended damage suffered in structural and non-structural components also under low intensity events.

Regrettably, the repair cost needed to restore structural and non-structural components represents a relevant part of the total reconstruction cost DE Martino et al. (2017); Del Vecchio et al. (2017); Di Ludovico et al. (2021b, 2017). The expansive economic disbursements justify the interest of the authorities in enhancement of the built seismic safety. The continuous upgrading of the seismic code and the construction process underlines the put effort by the scientific community and authorities in improving the seismic resilience of the built environment. Another important step is carried out for this aim: the Italian "Guidelines for the seismic risk classification of constructions", approved in February 2017 by the High Council of Public Works (Ministry decree n.58 28/02/2017), define the technical principles for exploiting tax deductions for seismic strengthening interventions on existing buildings Cosenza et al. (2018). The tax deduction, called *Sismabonus*, reveal a unique opportunity to improve the seismic safety level of existing buildings. A private householder can take advantage of a tax relief when its building undertakes a retrofit intervention aimed to reduce seismic vulnerability. The seismic risk classes of buildings and the achieved class due to reinforced interventions can be evaluated according to the dispositions of the Guidelines. The components to assess are the expected annual losses (EAL) and repair costs, expressed as a fraction of the Reconstruction Cost, (%RC), see Fig. 1.8.

Two approaches are provided by the code disposition to assign the seismic risk class of buildings and the class up graded through the strengthening interventions: the conventional approach and the simplified approach, respectively.

The conventional approach requires a detailed seismic assessment of the structure at different limit states. In the case of upgrading two or more seismic risk classes, the conventional approach application is requested. The simplified approach, based on the European Macro seismic ScaleGrünthal (1998), proposed for masonry buildings, allows to avoid an in-depth numerical or mechanical assessment of the seismic behaviour of the structure. The seismic risk class is defined as the minimum between the class assigned to the building based on the safety index at the ultimate state and the class established through the EAL. The latter class is correlated to the

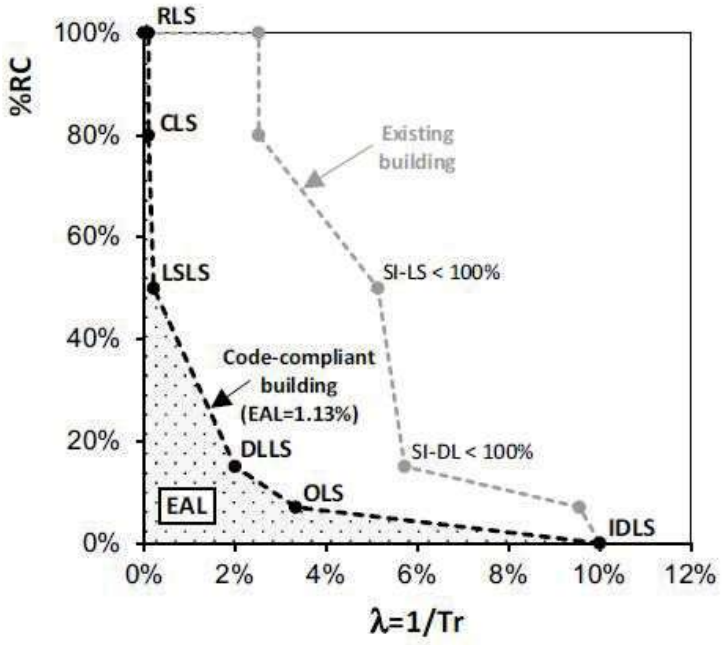

Figure 1.8. Diagramm of the correlation between (EAL) and (%RC).

area under the expected losses curves, obtained by evaluating the safety index converted in the return period (annual frequency) at different limit states and the relevant %RC. The tax deductions represent a unique opportunity to reduce the vulnerabilities of the existing Italian buildings' stock, and thus to mitigate the seismic risk.

1.3 Seismic risk in Italy

Seismic risk in Italy is an open issue due to the high hazard of the area, the increasing exposed level, and the prominent vulnerability of the built heritage. Unfortunately, the history of the Country counts numerous events with shattering consequences in terms of casualties and unusable buildings. The seismotectonic setting of Italian territory is the result of the convergence of the main plates of Eurasia, Adria, Nubia during Cenozoic period Di Bucci et al. (2010). The interaction among the three plates is still ongoing.

The complex geodynamic regional setting and focal mechanisms influence the current Italian seismotectonic Roselli et al. (2018). Shallow extensional focal mechanisms and normal faulting affect the portion of the Apennines from the northern Italy to the northernmost area of Siciliy. In Fig.1.9, the

representation in the top right reports the composite Seismogenic Sources from DISS 3.2.1, coloured according to their kinematics; in the top left the historical earthquake catalog CPTI15 and its area of reliability (green dashed polygon) are depicted. Areas of homogeneous completeness intervals of CPTI15 data are shown by red polygons. In the bottom right of Fig.1.9, focal mechanisms with depth $\leq$40 km are indicated Pondrelli et al. (2020). The representation, in the bottom left, reports the tectonic domains used to compute M_{max}, seismogenic depths, and hypocenter distributions. Compressional and transcurrent tectonics affect the outer front of the Apennines and the eastern part of the Alps. Strike-slip and transpressive earthquakes characterize the outer part of the southern Apennines and southeastern Sicily. Intermediate and deep earthquakes are mainly located in the Calabrian Arc Chiarabba et al. (2005).

The seismotectonic setting of Italy leads to occurring medium and high energy earthquakes. At the aim to reduce the seismic risk, effective mitigation measures are required for the whole country. A reliable estimation of expected ground motion is a required activity to know the seismic hazard of the earthquake-prone areas. At this aim, seismic risk maps play a fundamental role to characterize the seismic risk of the areas. The first seismic classification was performed in 1980 that qualified the 45% of the Italian area as a seismic zone. In 2003, the OPCM 3274 (Ordinanza del Presidente del Consiglio del Ministri) introduced four homogeneous zones to seismically classify the Italian territory. A different value of ag (horizontal maximum acceleration on a rock ground) distinguishes each zone:

- ZONE 1: ag $\bar{0}$.35 g;
- ZONE 2: ag $\bar{0}$.25 g;
- ZONE 3: ag $\bar{0}$.15 g;
- ZONE 4: ag $\bar{0}$.05 g.

Where g is the gravity acceleration constant equal to 9.81 m $\times$ s^2. The recurring earthquakes required to update the seismicity of the territory. In the Table are listed the seismic events occurred in the last forty-five years, with a moment magnitude M $>$ 5. The time of the event, Magnitude (M_L and M_w), geographic coordinated of the epicentre and depth of

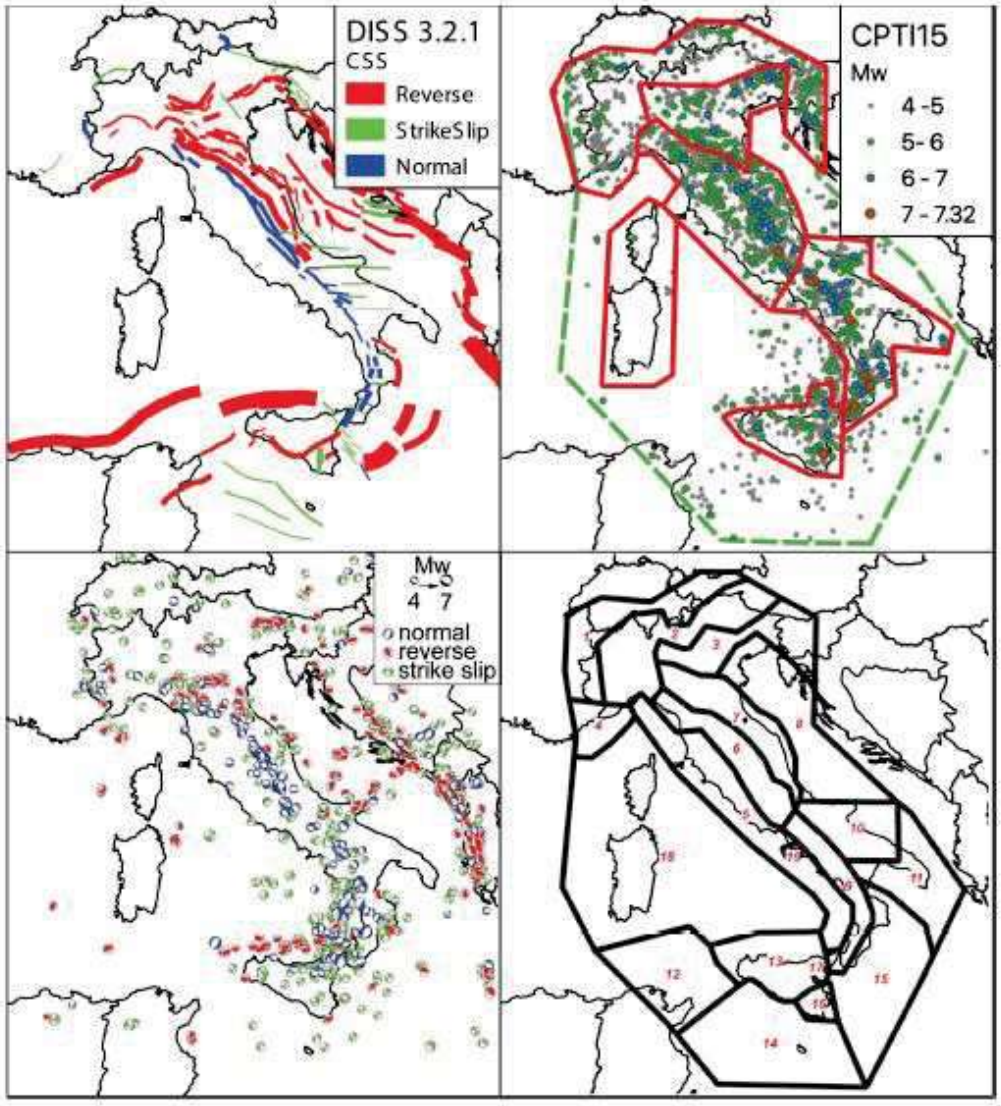

Figure 1.9. Representation of seismogenic conditions of Italian Peninsula

the hypocentre are specified for each seismic event.

Thus, after the publication of the first Technical Italian Guidelines, the Italian territory was divided into squared cells, with a length of five kilometres and identified by geographical coordinates, to define a grid. The zone into a cell is qualified in terms of seismic parameters, referring only to coordinates. After the last seismic events, L'Aquila 2009 and Central Italy 2016, the Italian Government founded the National Program for Seismic Prevention Mauro (2012) to perform an extensive seismic micro-zonation of the seismic hazard level of the national territory, SM Moscatelli et al. (2020). SM is the process of mapping the distribution of site response with respect to ground shaking intensity Mihalić Arbanas et al. (2011). SM allows to mitigate the seismic risk thanks to providing useful information for urban planning, land management, emergency planning and post-seismic reconstruction Pagliaroli (2018). A gradual multi-level approach was adopted to characterize the seismic micro-zonation, according to the Italian Guidelines. The first level, called Level 1, aims to divided the analysed areas into Seismically Homogeneous Microzones (SHMs), at aiming to characterize them, via semi-qualitative way, in three different seismic categories: (i) stable zone, characterized by no amplification of ground-motion; (ii) stable zones with amplifications, characterized by expected ground-motion amplification due to the local seismic-stratigraphical and geo-morphological conditions; (iii) unstable zones, characterized by soil instabilities (liquefaction, landslides, surface faulting, soil densification). The second level evaluates the ground-motion amplification quantitatively, by means a simplified approach. An integral parameter, called Amplification Factor AF, evaluated the amplification expected as an effect of the 1D engineering-geological layering of the specific SHM, as reported in the Eq. 1.4 :

$$AF = \frac{\int_{T1}^{T2} SadT}{\int_{T1}^{T2} SbdT} \tag{1.4}$$

Where T is the period of the considered spectral ordinate,S_a and S_b are the acceleration response spectrum at surface and bedrock, respectively. Three AF values are evaluated referred to short (0.1-0.5 sec), intermediate (0.4-0.8 sec), and long ground vibration periods (0.7-1.1 sec). The third level, named Level 3, deals geological settings affected by significant lateral

variations in the seismic impedance that could engenders soil instabilities. In this case, simplified approaches cannot be applied. Therefore, laboratory tests and advanced numerical modelling are required. The Level 3 focused on restricted area due to the high effort and costs of analyses. According to the ISTAT 2001 census, 61% of Italian residential existing built-up consists of Masonry buildings (M) and 25% of reinforced concrete buildings (RC). The remaining residential constructions, indicated ad other (O), consists of steel or wooden or mixed typology buildings. Fig.1.10 reports the main data on Italian residential assets, derived from the ISTAT census.

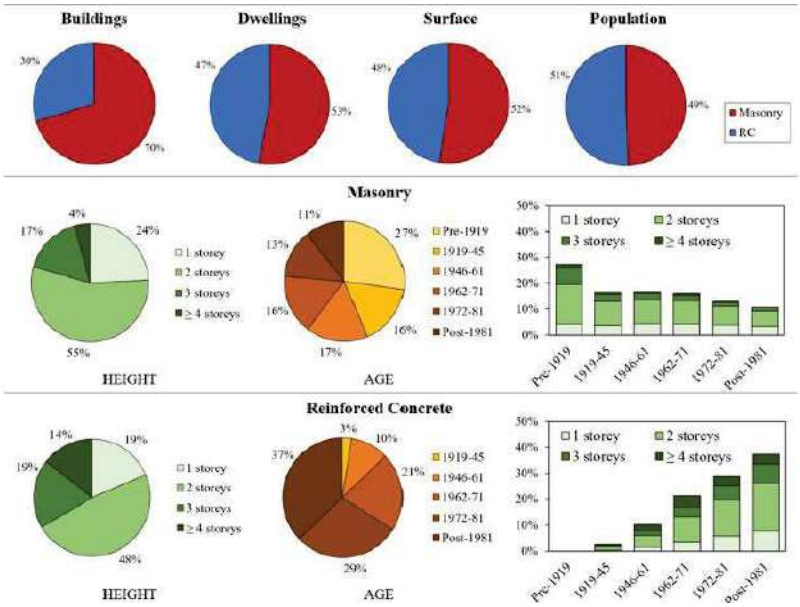

Figure 1.10. Workflow of the prediction procedure according to FEMAda porto et al. (2021).

The first row of Fig.1.10, shows the preponderance of masonry buildings. M and RC are almost equivalent in terms of dwellings, floor surface and population. The reason is that RC buildings have a higher number of storeys, and thus, more housing units per building compared to M buildings, which mostly correspond to single dwellings da porto et al. (2021). The second and third rows in Fig.1.10 underlines the subdivision of the buildings in terms of number of storeys, age of construction and their combination, respectively for masonry and reinforced concrete typology.

Despite the more updated census are available, the ISTAT 2001 dataset is used for National Risk Assessment (ICPD 2018), due to its detail in characterizing some building characteristics.

Structural vulnerability

Chapter abstract

The mitigation of the structural vulnerability of existing constructions allows the reduction of the seismic risk. The assessment of the seismic fragilities represents the first step to protect the built heritage against seismic risk. Furthermore, the seismic vulnerability assessment is an approach that could be followed in different ways, on the basis of scale of analysis and resources available. Several scholars proposed different modelling and methods at varying the complexity and accuracy of the seismic assessment, leading to a wide literature.he aim of this chapter is classifying the assessment methods, based on their level of detail and scale of evaluation. A deeper attention has been deserved to a dissertation of method for URMs, on which the PhD thesis focuses.

2.1 A brief overview of the framework of the research

The majority of the built environment of seismic prone countries exhibits facilities built according to concepts and rules deficient to the seismic context. As reported by Economidou et al. (2011), only 20% of buildings in European areas was built according to anti seismic rules. Furthermore, the 40% of them suffers their aging (over 60 years) Valluzzi M.R. and Saretta (2021), exhibiting an unsatisfactory seismic behaviour. More precisely, among the European built heritage, residential buildings account for 75% of the total stock. In Italy, 87% of residential buildings consist of masonry (URMs) and concrete (RC) constructions: of these, more than 90% of URMs were conceived to withstand only gravitational loads. Therefore, the strengthening of these built heritage is an urgent prerequisite to avoid injuries, casualties, damage or unusable buildings, and economic losses after a seismic event.
The reduction of the seismic risk lays on the mitigation of vulnerability of existing constructions. At this aim, the assessment of the fragilities of existing buildings represents the first activity of the path to follow for the protection of the built heritage against seismic risk. Different modeling and methods are available in literature, at varying the complexity and accuracy of the seismic assessment.
To investigate masonry buildings behavior, the most used modeling strategies are:

- **Full Discrete Models**, which consider the micro-modeling of the different components (units and mortar) and their mechanical interaction based on constitutive laws. The accuracy of this strategy is reserved to single masonry panels analysis.

- **Continuum Models**, which reproduce the mechanical behavior of a representative volume element of a URM, modeled as a continuum body of homogeneous material, based on homogenized constitutive law for units and mortar.

- **Rigid Body and Spring model**, that divides a URM into a finite number of rigid bodies, linked by springs located at contact area of

adjacent bodies.

- **Macro-elements models**, which considers a URM as an assembly of finite elements.

Instead, vulnerability assessment methods are sorted into three different categories, based on their level of detail and scale of evaluation Vicente et al. (2014). The first approach typology, called also *Empirical or observational method*, assess the seismic vulnerability of a construction by introducing building categories and the related vulnerability classes, based on a suite of structural-typological features Brando et al. (2017); Del Gaudio et al. (2019); Lagomarsino and Giovinazzi (2006); Rosti et al. (2021a,b); Ruggieri et al. (2021a, 2020). A vulnerability model is associated to an vulnerability class, that has been calibrated on past seismic damage. Thanks to statistical analyses, empirical methods can be applied on urban scale, requiring limited information. The second typology, also called *Analytical/Mechanical method*, involves simulation procedures on building models to derive vulnerability function between structural capacity and seismic demandDel Gaudio et al. (2015b); Gaetani d'Aragona and Prota (2020). Therefore, this approach needs of a characterization in terms of geometrical and mechanical properties of the structure. The third approach typology, or *Numerical method*, depends on an in-depth knowledge of the structure Kappos et al. (2006). The evaluation of the seismic vulnerability relies on a numerical or analytical method able to reproduce the real behaviour of the structure. Non Destructive Tests (NDT) or semi-NDT are necessary to deliver a comprehensive knowledge of the structure, especially for URMs due to the intrinsic heterogeneity of their features and consequent variety of their mechanical properties. Unfortunately, the resort to this level of assessment is not possible for numerous buildings, due to the effort and time demanding. An other approach, called *Hybrid method*, attempts to calibrate the results of analytical methods, based on post-earthquake observational damage. Still, hybrid methods are particularly advantageous in the cases of absence of damage data and impossibility of calibrating results of analytical methodsJiménez et al. (2018). Due to the reasons explained above, empirical and analytical methods, also called predictive methods,

represent a simplified and quick tool to estimate seismic performance on a large-scale application, see 2.1.

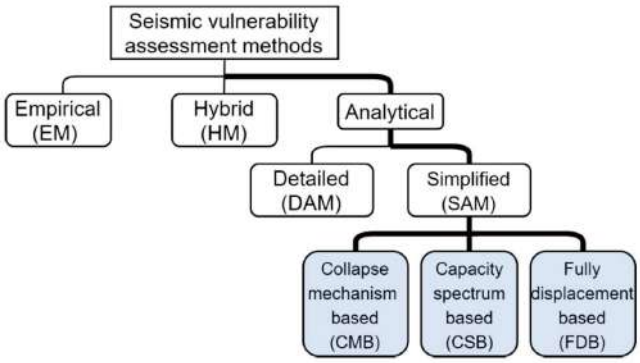

Figure 2.1. Seismic vulnerability assessment methods classificationShabani et al. (2021).

An other classification bases on the scale of the seismic analysis, introducing three levels at varying the required knowledge of the structure and the accuracy of the results. (i) The first level, that bases on a rough knowledge of the structure, return an index representative of the propensity of a building to be damaged under a seismic action with a qualitative study of the problem. (ii) the second level, that bases on a more detailed knowledge of the structure, return an index of the seismic vulnerability representative of the seismic structural behavior. (iii) The third level, basing on an in depth knowledge that supports a refined modeling of the structure, embraces an detailed seismic performance. Despite the incessant effort of researchers to propose novel assessment methods, the availability and accessibility of data, at the large scale, still represents an open issue, leading to the classification of buildings with comparable overall performance into typological-structuresCacace et al. (2018). Each category attempts to be representative of the buildings under investigation in order to ascertain a common taxonomy Lang et al. (2017). After the brief reminders discussed above, valid for any constructions typologies, the chapter carefully illustrates the main methods available to face mostly the vulnerability assessment of URMs at varying the scale of the problem and the accuracy of results. Other approaches are only reported in Tab.2.1, Chever (2012).

.

Scale of analysis		
Thousands	Few hundred/few dozens	Individual
ATC 13	AFPS (2001)	
EMS98	ATC21	
DBELA	FaMIVE	JBDPA Japan
GNDT, I level	FEMA 154	FaMIVE
GNDT, II level	GNDT, II level	FEMA 310
HAZUS model	IEB New Zeland	VC/VM
Risk-UE LM1	NRC-CNRC	Vulnus
Risk-UE LM2	OFEG I level	
Vulneralp	Risk-UE LM1	

Table 2.1. Vulnerability methods at varying the number of buildings.

2.1.1 Empirical assessment methods

An effective reduction of the seismic risk presupposes the assessment of seismic vulnerabilities of entire built areas to define their susceptibility to suffer a certain damage level under a seismic action. A screening of structural fragilities of urban centres is a prerequisite, involving numerous existing facilities. In operative terms, a vulnerability seismic assessment, that focuses on numerous constructions, requires an high effort and time consuming demand. Therefore, empirical methods, also called *Simplified Methods*, arise to overcome these issues by means the introduction of several simplifications that allow to overcome the effort for numerous buildings. In the light of above, empirical methods enable to evaluate the seismic safety of a certain built area, offering an assessment tool for territorial scale. Still, the need to deepen the seismic safety of entire built areas arises from the unsatisfactory structural performance exhibited under the seismic events of the last centuries. Furthermore, the damage revealed allows to better understand the seismic fragilities. At the same time, the detected seismic response of existing buildings suggests valuable information to support predictive methods. In this regard, empirical methods are conceived to provide a rough evaluation of the seismic safety of a structure by means the formulation of engineeristic judgments expressed on the properties of buildings and on the severity of potential damages, referred to *ex-post* or

ex-ante seismic events Rapone et al. (2018). In the light of above, empirical methods, like damage probability method and vulnerability index methods Benedetti and Petrini (1984b); GNDT-SSN (1994), have also been widely employed to foresee the vulnerabilities of a large built scale.

Nowadays, an increasing attention is reserved to the development of empirical tool to foresee damage scenario through predictive methods. A copious number of predictive methods have been proposed in literature. Among these, the more simplified methods aim to simulate damage scenario, and thus to grasp seismic vulnerability, from a statistical observation of the damage revealed during seismic events. For example, Rota et al.Rota et al. (2008) and Del Gaudio et al.Del Gaudio et al. (2015a)predicted the damage scenarios of Italian buildings stocks. In this activity, the availability of seismic data offers a tool to statistically develop or corroborate novel methods. In Italy, the seismic data of past events are collected through the AeDES forms redacted by the Italian Civil Protection. The AeDES forms collect general information of a building (like positions and owner), geometrical data (in plan and elevation), structural typology (URM or RC), topographic and soil condition, and a section reserved to describe the type and intensity of the seismic damage detected, for structural and no-structural components. Fig.2.2 reports an extract of the AeDES form reserved to characterize the structural typologies of horizontal and vertical structures of a URM. The thousands of buildings surveyed in the aftermaths of the last earthquakes led to a large portfolio of recorded information, in terms od structural typologies, constructions and geometric properties. A web-gis database, Da.D.O. (Observed Damage database) Dolce et al. (2017) collect the data of ordinary buildings hit by the earthquakes occurred from the 1976. Still, other research activities led to different empirical methods.

In the 1980s, Benedetti and Petrini Benedetti and Petrini (1984a), within the research activity of the G.N.D.T. (Italian National Group Against Earthquakes), developed a vulnerability function with a deterministic correlation between the seismic action and the damage level, based on detailed information and a geometrical survey of the buildings. The method provided a screening tool, called G.N.D.T. Chart **(G.N.D.T. 1994a, 2001b; S.S.N. 2001)**, based on vulnerability parameters classified by assigned

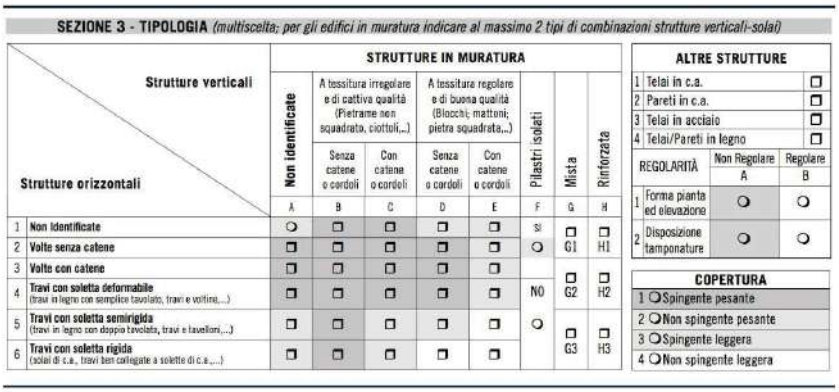

SEZIONE 3 - TIPOLOGIA *(multiscelta; per gli edifici in muratura indicare al massimo 2 tipi di combinazioni strutture verticali-solai)*

Strutture orizzontali \ Strutture verticali		STRUTTURE IN MURATURA								ALTRE STRUTTURE	
		Non identificate	A tessitura irregolare e di cattiva qualità (Pietrame non squadrato, ciottoli,..)		A tessitura regolare e di buona qualità (Blocchi; mattoni; pietra squadrata,..)		Pilastri isolati	Mista	Rinforzata	1 Telai in c.a.	☐
			Senza catene o cordoli	Con catene o cordoli	Senza catene o cordoli	Con catene o cordoli				2 Pareti in c.a.	☐
		A	B	C	D	E	F	G	H	3 Telai in acciaio	☐
1	Non identificate	○	☐	☐	☐	☐	SI	☐ G1	☐ H1	4 Telai/Pareti in legno	☐
2	Volte senza catene	☐	☐	☐	☐	☐	○			REGOLARITÀ: Non Regolare A / Regolare B	
3	Volte con catene	☐	☐	☐	☐	☐		☐ G2	☐ H2	1 Forma pianta ed elevazione: ○ / ○	
4	Travi con soletta deformabile (travi in legno con semplice tavolato, travi e voltine,...)	☐	☐	☐	☐	☐	NO			2 Disposizione tamponature: ○ / ○	
5	Travi con soletta semirigida (travi in legno con doppio tavolato, travi e tavelloni,...)	☐	☐	☐	☐	☐	○	☐ G3	☐ H3		
6	Travi con soletta rigida (solai di c.a., travi ben collegate a solette di c.a.,...)	☐	☐	☐	☐	☐					

COPERTURA
1 ○ Spingente pesante
2 ○ Non spingente pesante
3 ○ Spingente leggera
4 ○ Non spingente leggera

Figure 2.2. Extract of AeDES form.

weights (for the relative importance among the parameters on the global behaviour of the building) and scores (for the increasing vulnerability of each parameter), aimed to yield an index representative of the buildings' vulnerabilities. The methodology was extensively used in earthquake prone areas. Several researchers applied the method to investigate the seismic vulnerability of old historical centres. Ohter authors proposed modified the G.N.D.T. form to consider specific structural features of the built tissue under investigation. Formisano et al.Formisano et al. (2011, 2014) implemented the G.N.D.T. form with five parameters to consider the structural interaction among adjacent structural units of building aggregates. More precisely, five factors, partially derived from previous studies of literature, were introduced: (i) in elevation interaction; (ii) plan interaction; (iii) number of staggered floors; (iv) structural or typological heterogeneity among adjacent units; (v) percentage difference of openings areas among adjacent facades.By means specific numerical parametric analyses, the weights and scores to be assigned to the five additional parameters have been calibrated to achieve a form homogeneous to the GNDT form. Maio et al.Maio et al. (2015)arranged the parameters of G.N.D.T. chart into four groups to emphasize their differences and relative importance. Ferreira et al.Ferreira et al. (2017) investigated 192 URMs in the old city Horta, Azores, by applying the GNDT methods with some modifications, that lead the vulnerability index evaluated based on 14 parameters instead of 11 ones Vicente et al. (2011).

A similar approach was applied on others Portuguese built tissue Ferreira

et al. (2013); Maio et al. (2016); Vicente et al. (2008).

Cavaleri et al. Cavaleri et al. (2017) developed a vulnerability index based on the GNDT method, corroborated by means an application on the Lampedusa Island, in southern Italy, involving 288 buildings (264 URMs and 24 RC).

Starting from the effective application of the empirical seismic approaches, other authors proposed predictive methods based on identification of parameters only requiring a visual inspection of buildings to grasps their potential fragilities. Brando et al.Brando et al. (2017) developed a vulnerability index based on the external visual inspection of a masonry building. The method was calibrated based on the damage observed in the aftermath of the 2009 L'Aquila earthquake, like historical centers of Goriano Sicoli and Poggio Picenze Rapone et al. (2018). Below, the main empirical seismic approaches are briefly discussed. Most of them are proposed by Italian researchers due to the high seismic risk in the Italian regions and the numerous earthquake occurred in the last decades that showed the fragilities of the built heritage.

2.1.1.1 The macroseismic method

The Macroseismic method faces the vulnerability assessment of a set of buildings or of a single building: it delivers a model that bases on the measure of the earthquake from the observation of the damage revealed by buildings. Table 2.2 reports synthetically the European Macroseismic Scale to express the earthquake intensity.

.

Two indexes express the seismic preponderance of the building to suffer seismic damage, evaluated referring to the building typology and its features: (i) a vulnerability index, V; (ii) a ductile index, Q. The earthquake severity, expressed referred to the European macroseismic scale, EMS-98, is considered as a parameter evaluated for a rigid soil condition. The possible amplification effects, due to site soil and topographic conditions, are accounted in the Vulnerability parameter V. Five damage grade, D_k (k=0/5), have been introduced to evaluate the physical damage of structural and no-structural components' damage:

Intensity	Description
I	Not felt
II	Scarcely felt
III	Weak
IV	Largely observed
V	Strong
VI	Sligthly damaging
VII	Damaging
VIII	Heavily Damaging
IX	Destructive
X	Very Destructive
XI	Devastating
XII	Completely devastating

Table 2.2. European Macroseismic Scale (EMS-98).

- D_0, no damage;
- D_1, slight;
- D_2, moderate;
- D_3, heavy;
- D_4, very heavy;
- D_5, destruction.

Fig.2.3 and Fig.2.4 depict the EMS-98 seismic damage for URMs and RCs, respectively .

An analytical function, see Eq.5.16, correlates the seismic input and the expected damage on the base of the vulnerability index:

$$\mu_D = 2.5[1 + \tanh(\frac{I + 6.25V - 13.1}{Q})] \tag{2.1}$$

Where I is the seismic input in terms of macro seismic intensity, Q is the ductility coefficient and V is the vulnerability coefficient, evaluated as reported in Eq.5.17, from the vulnerability index i_v, expressed in a range between 0 and 100:

$$V = 0.58 + 0.0064 i_v \tag{2.2}$$

A binomial distribution estimated the probability p_k of occurrence of

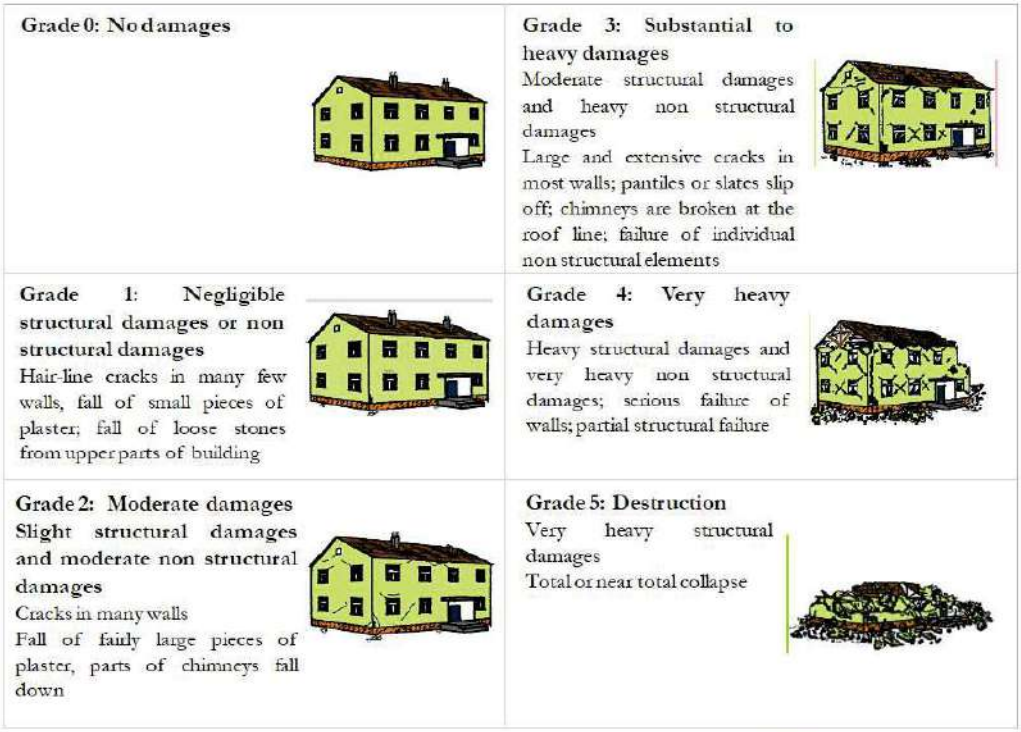

Figure 2.3. Damage classification according to EMS-98 for URMs.

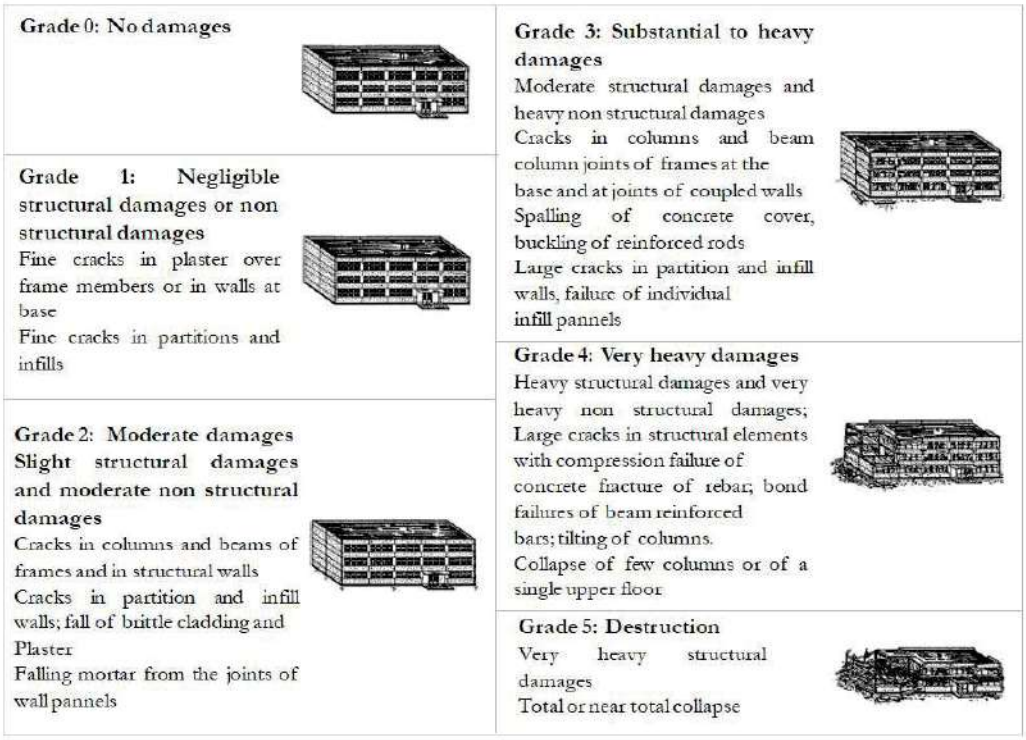

Figure 2.4. Damage classification according to EMS-98 for RCs.

the damage grade D_k (k from 0 to 5) (Grünthal, 1998) as a function of μ_D, according to Eq.5.18:

$$p_k = \frac{5!}{k!(5-k)!}(\frac{\mu_D}{5}^k)(1-\frac{\mu_D}{5})^{5-k} \tag{2.3}$$

where the symbol ! indicates the factorial operator. The scatter for the expected damage distribution, see Eq.2.4, is evaluated as a funtion of the mean damge value μ_D:

$$\sigma_D = \sqrt{\mu_D(1-\frac{\mu_D}{5})} \tag{2.4}$$

The binomial distribution has been adopted for the macro seismic approach, founding a widespread application for the statisical analysis of data collected after the 1980 earthquake occurred in Irpinia, (Italy). The Macro seismic method allows the derivation of vulnerability curves expressed in terms of macro seismic scale intensity and mean damage value or macro seismic scale intensity and the probability of occurrence of a damage grade. This tool founds a meaningful application at a large built scale.

2.1.1.2 DPM, Damage Probability Matrix

Damage Probability Matrix (DPM) is an observational method that expresses the statistical distribution of damage grades for different macroseismic intensities in a matrix form. Every cell of the matrix indicates the probability of the building's damage degrees (located in the columns) at varying macro-seismic intensities (in the rows), defined by the expression) 2.5:

$$DPM(DV, I, T) = P(DV|I, T) \tag{2.5}$$

where:

- DV is a given damage grade;
- T is a specific structural typology;
- I is the earthquake intensity.

Many authors proposed different macro-seismic scales, such as Medvedev-Sponheuer-Karnik (MSK) scale, the Mercalli-Cancani-Sieberg (MSC) scale,

and the European macroseismic scale (EMS-98). The EMS-98 scale introduced five categories of damage and it is the most common used. Therefore, DPM vulnerability model delivers a direct correspondence between vulnerability classes and buildings' typologies for which a similar seismic behavior is expected. In Europe, DPMs refer to the damage classification introduced by Grunthal, indicated in literature as EMS-98. Six different vulnerability levels (called from A to F) are assigned to buildings' typologies, based on their type of structure (masonry, reinforced concrete, steel and wood), see2.5.

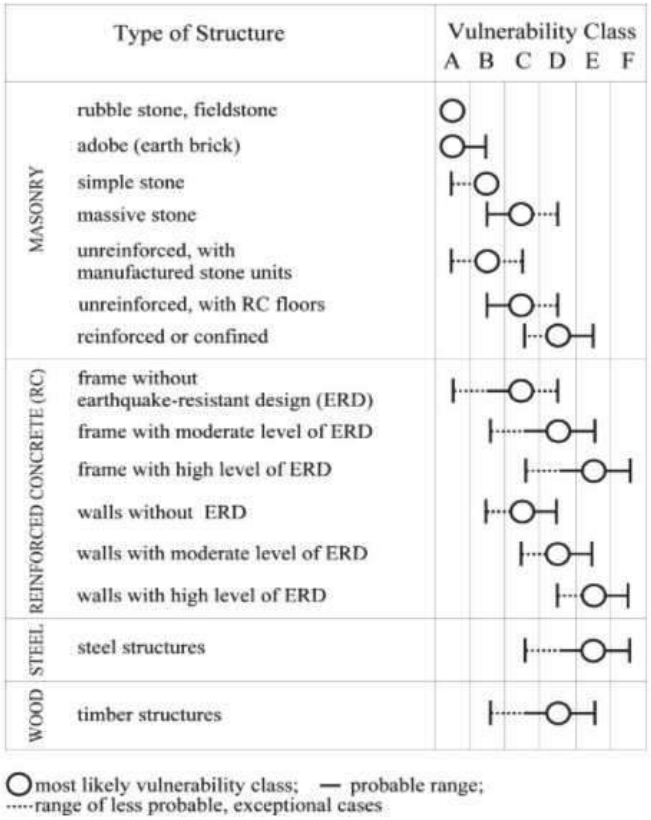

Figure 2.5. EMS-98 Vulnerability classification.

The DPMs represent a reliable and quick tool to predict the probable distribution of damage suffered at varying seismic action, supporting large scale analysis.

2.1.1.3 GNDT methodology: the I and II level.

The **GNDT I** level is an empirical method based on observational and collected data from post-event building' damage detected after Italian seismic swarms, developed by the *National Group for the Earthquake Defence.*

A formulation was proposed to assess a vulnerability index relating the expected damage grade and the microseismic intensity through a vulnerability functions. At this aim, the method was articulated in two levels, distinguishing different buildings typologies (reinforced concrete RC and masonry URMs): (i) the I level GNDT methodology; (ii) the II level GNDT methodology. This methodology aims to express a vulnerability index for the investigated building, laying on the DPMs approach, discussed in the previous paragraph, to express the expected damage through qualitative levels at varying the macro seismic intensity. The robustness of the GNDT DPM probabilistic distributions was extensively corroborated by means the large portfolio of seismic data about the Italian built-up, hit by the recent earthquake of the last century. Particularly, the 1980 earthquake occurred in Irpinia represents the reference seismic event for the development of the method.
The I level GNDT consists of collecting data to qualify the building, filling eight sections:

- General data of the building identification;
- Configuration of the building: isolated or in aggregate, toponymic and site information;
- Geometrical data: area plan, inter-story heights, dimension in plan;
- Use of the building in terms of destination and percentage;
- Age and recent intervention;
- State of the building conservation;
- Structural typology of vertical and horizontal structures;
- Level and extension of previous damage.

The II level GNDT focused on only the structural features of the examined building. An expert judgement provides a seismic vulnerability index, I_v, evaluating the sections reported in the format in Table 2.4, based on a visual inspection that screen the predominant seismic vulnerabilities and deficiencies of the building.

Parameters	class scores	weight
1 Organization of the vertical structures	0 5 20 45	1
2 Nature of the vertical structures	0 5 25 45	0.25
3 Location of the building and type of foundation	0 5 25 45	0.75
4 Planimetry	0 5 25 45	1.5
5 Planimetry compactness	0 5 25 45	0.5
6 Regularity in plan	0 5 25 45	variable
7 Type of slabs	0 5 15 45	variable
8 Roofing	0 15 25 45	0.75
9 Structural details	0 0 15 45	0.25
10 Physical conditions	0 5 25 45	1.00

Table 2.3. GNDT I Level chart.

Parameters	class scores	weight
1 Type and layout of resistant system	0 5 20 45	1
2 Structural system quality	0 5 20 45	0.25
3 Conventional strength	0 5 25 45	1.50
4 Bearing walls and foundations	0 5 25 45	0.75
5 Floor system	0 5 15 45	variable
6 Configuration in plan	0 5 25 45	0.50
6 Configuration in elevation	0 5 25 45	variable
7 Maximum distance between walls	0 5 25 45	0.25
8 Non structural elements	0 5 25 45	0.25
9 State of conservation	0 5 25 45	1.00

Table 2.4. GNDT II Level for URMs chart.

.

Furthermore, two different screening tools are proposed differently for the two most widespread structural types in European countries: reinforced concrete (RC) and masonry (URMs). The format for URMs (topic of this thesis) attempt to evaluate the structural seismic behaviour of a masonry building, considering the main factors that influence the dynamic behaviour. Table 2.4 lists the eleven parameters, classified by assigned weights and scores.

.

The weights (w) are fixed to consider the relative importance among the parameters on the global behaviour of the building. The scores (s) are assigned by the technician to evaluate the increasing vulnerability of each parameter, introducing four classes, called A,B, C and D, where A and D indicate the lowest and highest vulnerability grades. The vulnera-

bility index is evaluated combining the relative weights (w_i) and scores (s_i) assigned to the parameters, according to the equation 2.6:

$$I_v = \sum s_i * w_i \tag{2.6}$$

The I_v value ranges from 0 to 382.02, or from 0 to 100 if normalized respect the maximum value. Due to the robustness of the GNDT methodology, several scholars started from the framework of the GNDT to perform seismic assessment of large scale built areas, spread in different zones. These activities led to calibrate differently the weights of the parameters to better reflects the structural characteristics of the local buildings types. Moreover, other empirical methods arise from the GNDT formats introducing some modifications and suggestions of other parameters representative of peculiar structural conditions.

2.1.2 Analytical/mechanical assessment methods

Analytical or mechanical approaches evaluate a vulnerability function through simulation procedures of buildings' behavior to relate structural capacity and seismic demand. These methods rely on structural parameters to estimate vulnerability functions: the limit states are defined based on mechanical indicators, representative of the structural performance, known from analysis of numerical or mechanical modelingRota et al. (2010). Therefore, analytical methods require a thorough characterization of buildings, which in some cases are burdensome for large scale applications Del Gaudio et al. (2015b); Ruggieri et al. (2021b). Generally, analytical methods are classified into three main approaches, that can be mentioned in this context areShabani et al. (2021):

- **Collapse Mechanics-Based methods**, *CMB*.
- **Capacity Spectrum-Based methods**, *CSB*.
- **Fully Displacement-Based methods**, *FDB*.

Collapse Mechanics-Based methods, *CMB*, aim to evaluate the collapse multipliers for different possible local collapse mechanisms under a seismic action with a given intensity. CMB methods are based on the kinematic

chain to derive the collapse multipliers. Capacity Spectrum-Based methods, *CSB*, compare the capacity curves of selected facilities typological classes with the required seismic demand. Capacity curves are derived through Nonlinear static analyses. The capacity curve is intersected with she seismic demand to detect the performance points for different damage thresholds. CSB is widespread in the last decades as an alternative tool to nonlinear time-history analyses. Introduced in ATC Commission (1996), CSB has been implemented in HAZUS methodology for loss estimationHazus (1997). In FEMA 273 and N2 method Peter (1999, 2000)(nowadays introduced in Eurocode 8-part 3Herrmann and Bucksch (2014)), an other alternative version of CSB method is available. N2 method was formulated in the acceleration-displacement format Peter (1999); Peter and Fischinger (1987). Figure2.6 depicts the main steps of the method. Through non static linear analyses, the capacity curve of a structure is derived and then is transformed from a multi-degree-of-freedom system into an equivalent-single-degree-of-freedom, see step 1 of Fig.2.6. The capacity curve is changed in a bi linear elasto-plastic capacity curve, see step 1 of Fig.2.6. The idealized capacity curve is intersected with seismic demand to detect the performance point of the structure. The seismic demand is evaluated by selecting the ground motion and then, deriving the inelastic response spectrum that evaluate the performance point at inelastic displacement demand for a specific round motion, see step 3 of Fig.2.6.

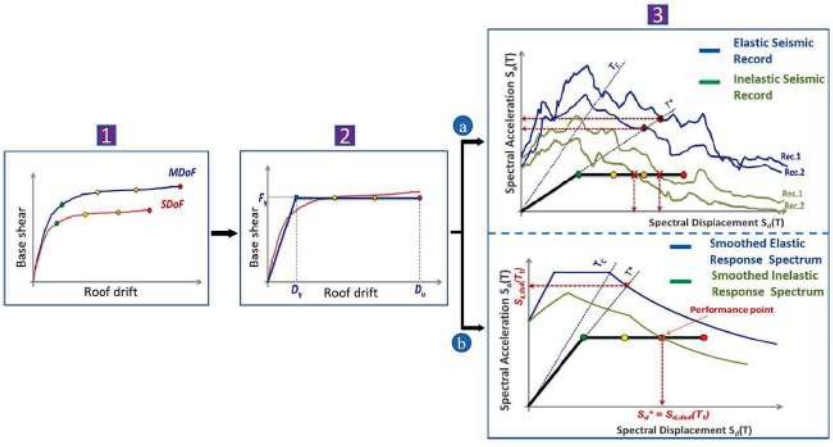

Figure 2.6. Procedure of CSB methods Meslem et al. (2016).

In Appendix A, the formulations of CSB are esaustively discussed due to their use in the research activity. Several researchers proposed simpli-

fied CSB methods to derive simplified capacity curves based on simplified model: FaMIVE id one od the most noteworthy method for out-of-plane failure mechanisms of masonry constructionsD'Ayala and Speranza (2003). Fully Displacement-Based methods, *FDB*. An equivalent single degree of freedom model, *ESDOF*, is derived and the displacement capacity for each damage thresholds is compared to the displacement demand to estimate the possibility of exceeding a damage thresholds Silva et al. (2019); Zucconi et al. (2017). Another classification of analytical methods introduces two groups,Shabani et al. (2021) : (i) detailed analytical methods (DAMs); (ii) simplified analytical methods (SAMs). DAMs face the seismic vulnerability assessment of URMs by means sophisticated and detailed nonlinear analyses D'Altri et al. (2019). Different approaches have been proposed to perform non linear analysis of URMs to deepen the dynamic behaviour under seismic actions. In non linear static analyses (also called Push-over analyses), the seismic action is applied to the structure as lateral static load and it is increased until a displacement target is reached Rota et al. (2010). In the case of Incremental dynamic analyses (IDA), the seismic action is applied to the models as acceleragrams of which intensity are increased until the collapse occurs Meslem et al. (2016).

In the recent decades, simplified analytical methods have been developed to curtail the computational effort of analytical methods involved on large scale applicationLeggieri et al. (2021). Their aim is the performing of a rapid and accurate estimation of seismic vulnerability of URMs considering the uncertainty related to a low knowledge level. Furthermore, in the case of a single URM analyses, uncertainties derives from the lack of knowledge of the structural features: an on-site survey and can achieve an extensive investigation of the structure, reducing the uncertainties. Unfortunately, in the case of a vulnerability assessment at a large scale, a suite of variables affect the knowledge of the URMs, involving capacity, demand and damage thresholds. These evidences drive the resort to an analytical methods based on the scale of the assessment and the complexity level of the methodologies.

2.1.2.1 Vulnus methodology

The Vulnus approach, developed by the scholars of University of Pavia, is a mechanics based method, based on in-plane and out-o-plane collapse mechanisms of URMs. The method reflects the main features of empirical approach: a building survey collect geometrical and structural data to support a qualitative judgement, to estimate the seismic vulnerability of a building through the definition of the collapse multipliers based on the fuzzy theory. A vulnerability index is provided starting from the evaluation of a collapse multiplier, I_1, for the in-plane behaviour, that evaluates the shear collapse of ground floor, see Eq.2.7:

$$I_1 = \frac{min(V_x, V_y)}{W} \tag{2.7}$$

where:

- I_1 is the collapse multiplier for in-plane behaviour assigning a shear collapse at ground floor;
- W is the total structural weight;
- V_x and V_y indicate the strengths at mid-storey height of the ground floor referred to the two directions (X- direction and Y- direction), evaluated according to the Eq.2.8:

$$V_x, V_y = F_x, F_y \frac{f_t}{1.5\omega} 1 + \frac{W}{f_t(F_x + F_y)}^{\frac{1}{2}} \tag{2.8}$$

where:

  - F_x and F_y indicate the resistant area of the walls in the X and Y directions, respectively;
  - f_t is the tensile strength of masonry material;
  - ω is the regularity coefficient plan.

The approach requires the evaluation of a second collapse multiplier, I_2, referred to the out-of-plane behaviour, see Eq.2.9, that expresses the ratio between the out-of-plane flexural strength of the most critical external wall and the total weight calculated as the sum of the resistance of the vertical and horizontal strips, I_2^I and I_2^{II}:

Vulnerability factor	Weight (Wi)	
1	Wall system quality	0.15
2	Soil and foundation interaction	0.75
3	Floors interaction	0.50
4	Elevation regularity	0.50
5	Roof interaction	0.50
6	Interaction of no-structural elements	0.25
7	General maintenance conditions	0.50

Table 2.5. Weights related to the vulnerability factors of the building.

$$I_2 = min(I_2^I + I_2^{II})_i \tag{2.9}$$

A third multiplier, I_3, see Eq.2.10, is evaluated as the weighted sum of the scores assigned to vulnerability factors:

$$I_3 = \sum \frac{W_i * S_i}{45 * 3.15} \tag{2.10}$$

where:

- S_i is the score, that ranges from 0 to 45;
- W_i is the weight of the vulnerability factor, see 2.5.

.

Furthermore, a factor a is introduced to consider the uncertainties that affect the judgement, in order to correct the mean absolute acceleration response A of the building (evaluated as the ratio between the maximum shear and the total weight.)
Finally, the vulnerability index is estimated by means the fuzzy set theory: the probability of exceeding a given limit state is expressed as function of the parameters discussed above $V = f(I_1, I_2, A, a)$.

2.1.2.2 FaMIVE methodology

The FaMIVE (Failure Mechanisms Identification and Vulnerability Evaluation) is analytical method aimed to evaluate the seismic vulnerability of URMs referred to out-of-plane seismic response, of which flowchart is reported in Fig.2.7, Meslem et al. (2016); Novelli et al. (2014).

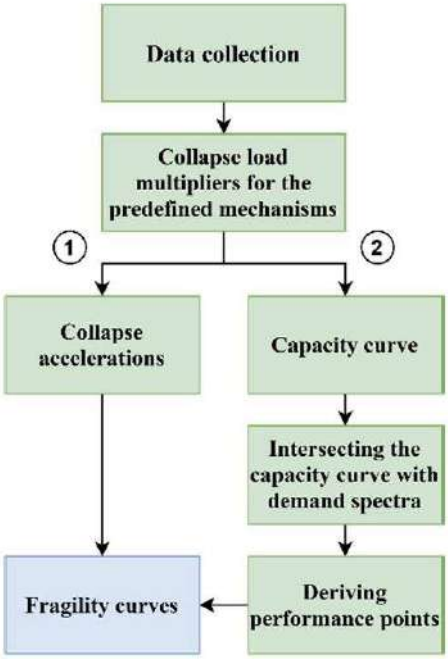

Figure 2.7. Flowchart of FaMIVE methodology to derive fragility curvesNovelli et al. (2014).

The methodology aims to evaluate the ultimate lateral capacity related to the most vulnerable mechanisms, see Fig.2.8 to predict the damage at a specific seismic demand, also in terms of capacity curves. The method requires an on-site survey of the building to collect geometrical and structural data. The first step is the the evaluation of the lateral effective stiffness, K_{eff}, for each wall (that could be involved in an out-of-plane mechanism) and its tributary mass. The K_{eff} is evaluated taking into account the mechanisms attained, the geometrical configuration of the wall and the floors and other portions of walls involved in the mechanisms, see eq.2.11:

$$k_{eff} = k_1 \frac{E_t I_{eff}}{H_{eff}^3} + k_2 \frac{E_t A_{eff}}{H_{eff}} \tag{2.11}$$

where H_{eff} is the height of the portion involved in the mechanism, E_t is the masonry modulus, I_{eff} and A_{eff} are the second moment of area and the cross sectional area, k_1 and k_2 are constants different for edge constraints. The tributary mass is evaluated similarly: it is equal to the volume of the wall involved in the mechanisms plus the the mass of the horizontal structures that participate in the mechanism. Effective stiffness and mass are used to evaluate a natural period T of an equivalent single degree of

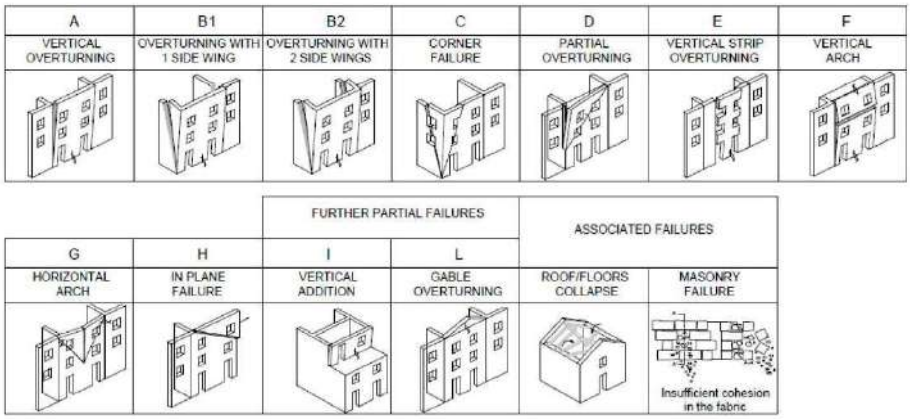

Figure 2.8. Out-of-plane mechanisms considered in the FaMIVE procedure.

freedom oscillator. The mass is applied at the height of the gravity center of the wall.

The second step consists of the calculation of displacement and acceleration at the elastic limit, respectively called D_y and A_y. A_y is considered as the combination of the gravitational load that cause a triangular distribution of compression stresses at the base of the wall, before the onset of the partialisation, see Eq.2.12:

$$A_y = \frac{t_b}{6h_o} g \tag{2.12}$$

The corresponding displacement D_y is evaluated according Eq.2.13:

$$D_y = \frac{A_y}{4\pi^2} T \tag{2.13}$$

where t_b is the effective thickness of the wall, h_0 is the height of the overturning wall. The third step consists of the calculation of displacement and acceleration at the ultimate conditions, respectively called D_u and A_u. A_u is evaluated according to Eq.2.14

$$A_u = \frac{\lambda_c}{\alpha_1} \tag{2.14}$$

where λ_c is the load factor of the collapse mechanism and α_1 is the portion of the mass involved in the mechanism. The corresponding displacement D_u is evaluated according Eq.2.15:

$$D_u = \frac{t_b}{3} \tag{2.15}$$

where t_b is the wall thickness at the base of the overturning portion. An intermediate point,(D_{sd}, A_y), of the capacity curve between (D_y, A_y) and (D_u, A_u) can also identified, as the condition at which the resultant of stresses trigger the fully partialisation of the cross section. Therefore, the capacity curve can be derived. In order to assign a vulnerability level at the structure, the capacity curve could be compared with the EC-8 displacement response spectra (ADRS) to individuate the performance point. The FaMIVE approach delivers also a spreadsheet, see Fig.2.9 to facilitate its application.

Numerous application of the method corroborated its reliability: FaMIVE procedure is useful to ascertain vulnerabilities of URMs for which, an out-of-plane behavior is expected, leading to inexpensive simplified analytical-mechanical analyses on large numbers of buildings.

2.1.2.3 SAVE methodology

The SAVE, Strumenti Aggiornati per la Vulnerabilità sismica del patrimonio Edilizio e dei sistemi urbani, (Updated tool for the seismic vulnerability evaluation of the built heritage and urban suystems) methodology is a simplified procedure developed in the framework of the GNDT Research Project, developed by Mauro Dolce and Giulio Zuccaro GNDT-SSN (1994). The method is an analytical method aimed to evaluate the seismic vulnerability of URMs referred to in-plane seismic response. The procedure evaluates the seismic acceleration for two limit state: (i) Collapse Limit State (CLS); (ii) Operational Limit State (OLS). The authors proposed two spreadsheets to facilitate the analysis, different for RCs and URMs. The spreadsheet consists of four sections:

- **General data**: inter-storey height, geometrical information, loads;
- **Mechanical parameters of masonry walls**;
- **Structural and loading conditions**, for each direction (X and Y), provided by the authomatic procedure implemented in the spreadsheet;

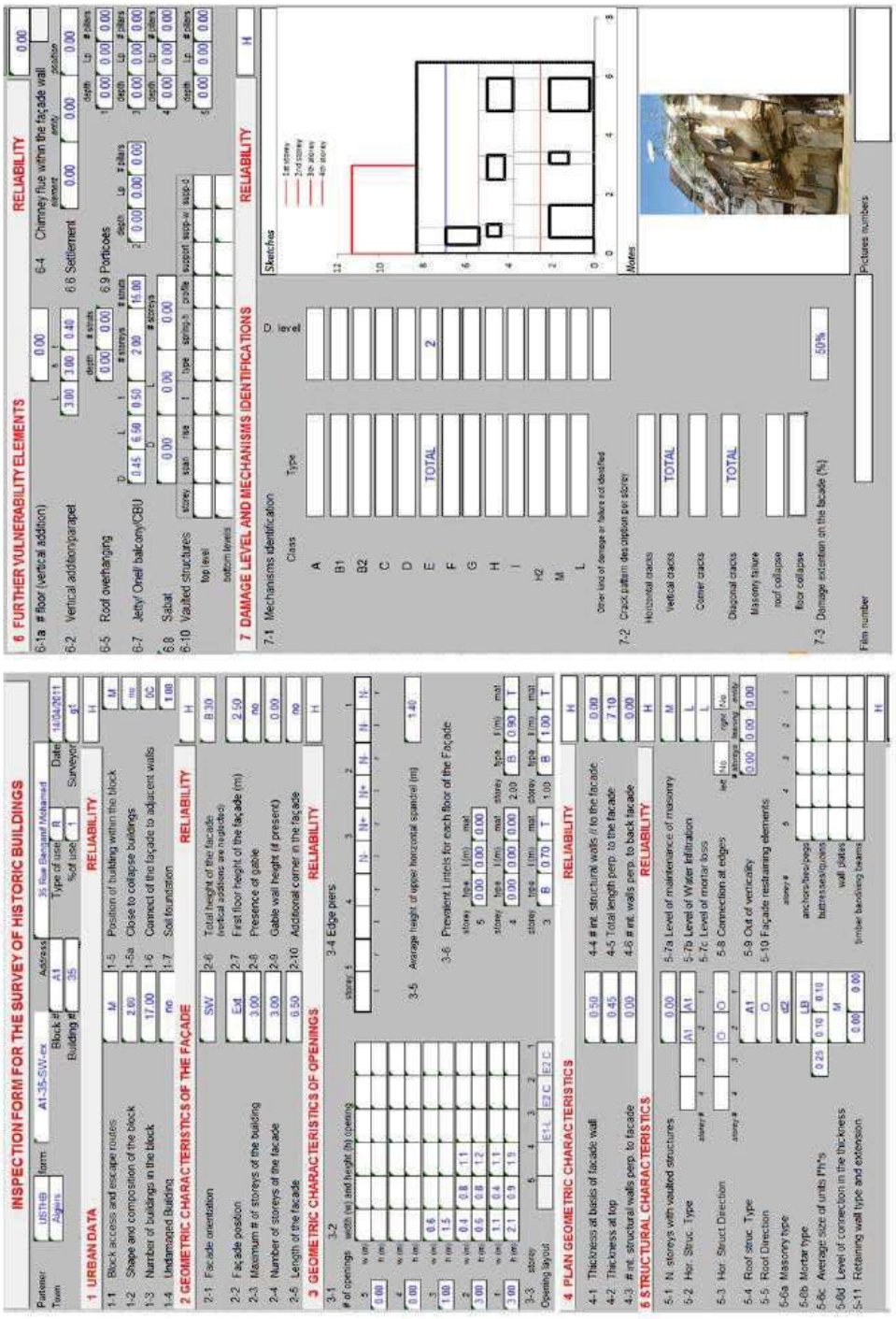

Figure 2.9. Example of a FaMIVE spreadsheet.

- **Result of the analysis**: PGA, a_g and the return period T_r,for each direction (X and Y).

The analysis of the structure could be performed level by level, for the two main seismic directions. For URMs, two collapse mechanisms are considered: (i) the in-plane shear failure; (ii) the compressive-bending failure. The sum of the resistances of each piers, $V_{i,j}$, for a single story and direction, represents the total shear strength, V_t, see Eq.2.16:

$$V_t = \sum V_{i,j} \tag{2.16}$$

The stiffness of each masonry pier is evaluated according to Eq.2.17

$$Ki,j = r\frac{GA}{\psi h_{def}} * \frac{1}{1 + \frac{Gh_{def}^2}{\psi Eb^2}} \tag{2.17}$$

where:

- r (0.5-1) is a factor to reduce the stiffness;
- h_{eff} is the pier deformable height of the pier, equal to openings height;
- b is the pier width;
- $A_{i,j}$ is the section area of the pier;
- ψ is the shear factor.

The Elastic Young and Shear Moduli, E and G respectively, are computed according to Eq.2.18 and Eq2.19:

$$E = 6G \tag{2.18}$$

$$G = 1100\tau_k \tag{2.19}$$

where τ_k is a corrected shear resistance to consider structural irregularities and ductility of the structure that affect the seismic performance, resorting to proper formulations. Finally, the vulnerability index is evaluated taking into account the ratio between the collapse acceleration a_c of the structure and the seismic demand spectra peak accelerations a_{PGA}, see Eq.2.20:

$$I_{save} = 1 - \frac{a_c}{a_{PGA}} \tag{2.20}$$

2.1.3 Numerical assessment methods

Numerical assessment models grasp the mechanical behavior of masonry structures with different level of accuracy at varying the knowledge of the structure. In fact, an in-depth characterization of the geometry, materials and structural details is required to overcome the uncertainties of the structure. Among them, masonry's mechanical properties, the resistance of masonry spandrels, and the in-plane stiffness and resistance of the floors play a crucial role in both the in-plane and out-of-plane seismic response Calderoni et al. (2017); Rizzano et al. (2009). The mechanical properties of masonry markedly affect the damage and the failure of buildings subjected to gravity loads and earthquake actions. The spandrels properties affect the strength degradation and the walls' lateral resistance, influencing the masonry piers' coupling effect Gattesco et al. (2014). The in-plane stiffness and resistance of the floors affect the horizontal force's distribution between the walls and the occurrence of possible out-of-plane phenomena Senaldi et al. (2014). Therefore, the knowledge of the mechanical properties of the masonry material is a prerequisite to perform a numerical model able to predict masonry building's seismic performance. Numerical assessment methods could employ linear and non-linear analysis. However, linear analysis is always performed, before the resorting to more sophisticated approaches, to allow a quick and first assessment of the reliability of the structural model proposedRoca et al. (2010). Recent technological advancement support the researchers in the development of numerical models of increasing complexity and the performing of non-linear analysis. Unfortunately, URMs highlight discrete and heterogeneous nature Calò et al. (2021): computational performance tends to decrease exponentially as a function of the adopted refinement level, thus reserving the applicability of advanced micro-models to reduced-scale problems. Thus, macro-models strategies are undertaken to perform a relatively large number of seismic analyses, or alternatively to limit the cost computational demands.

The research activity presented in this thesis embraces vulnerability as-

sessment at territorial scale. Therefore, for the sake of brevity, in this paragraph, major attention has been deserved to macro-modeling strategies (also called Finite Elements Methods based approaches, FEMs).

The finite element method offers a wide variety of modeling strategy at varying the description of the masonry structures. The possible strategies based on FEMs belong to two main approaches:(i) macro-modeling; (ii) micro-modeling. Macro-modeling is the most adopted approach by practitioners due to the lesser numerical effort than other strategies. In practice-oriented analyses on a full structure, a detailed description of the local behavior of units and mortars could be not considerableRoca et al. (2010). Macro-modeling regards the masonry as a fictitious homogeneous orthotropic material with a proper constitutive laws, see Fig.2.10, Lourenco et al. (1994). Furthermore, a mesh simplification gains a further reduction of the numerical effort of the analysis. Macro-modeling not requires the representation of the constitutive morphology of the structural elements. Instead, micro-modeling considers the separation and collision among unitsPina-Henriques and Lourenco (2005, 2006), yet engendering nodal compatibility issues. Therefore, micro modeling is capable to simulate failure modes that involve the separation or sliding between different parts Roca et al. (2010), capturing the local response of masonry accurately.

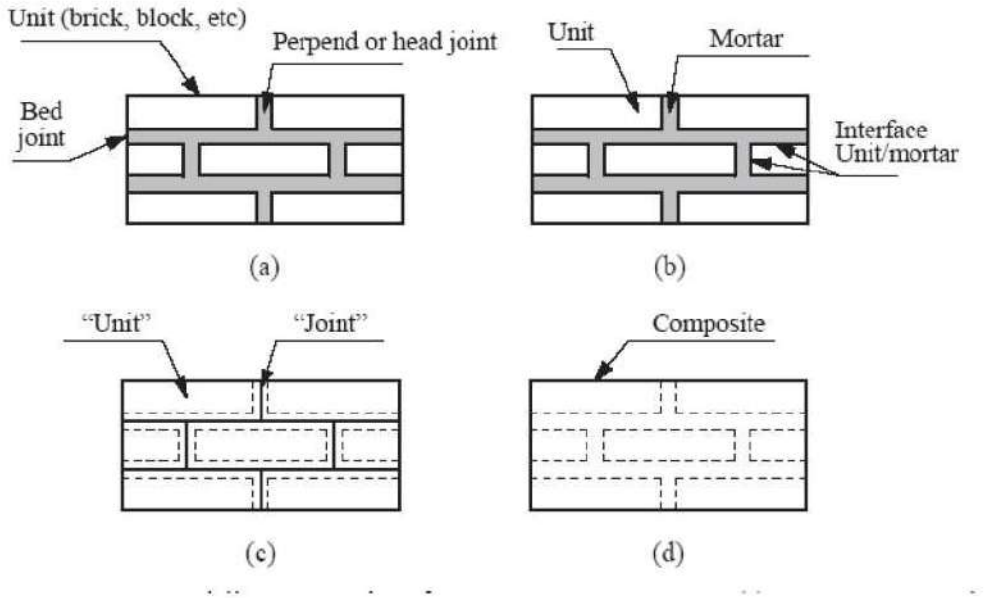

Figure 2.10. Modelling strategies for masonry: (a) masonry texture sample; (b) detailed micro-modelling; (c) simplified micro-modelling; (d) macro-modelling.

Still, thanks the recent performing numerical tools and their numerical power, further micro-modeling strategies are proposed. Among them, Discrete Element micro-models(DEM) is a numerical technique that ensures an high level of complexity and detail. This method was conceived for rock mechanisms application and than applied to structural engineering field, including reduced-scale masonry problems. The DE approach consists in modeling each units separately and connected to each other through zero-thickness interface springs located where damage could occurLemos (2007). The DE micro-modeling approach allows to capture the fracture propagation, as well as both local and global collapses, see Fig.2.11 Pulatsu et al. (2016). However, the DE modeling of a URM is unfeasible in many cases due to the computational and user skills demands. In the current literature, several researchers are working on the development of simplified DE micro-models to extend their use for further applications. Nevertheless, in the framework of vulnerability assessment of URMs, the resort to DE is seldom uncommon.

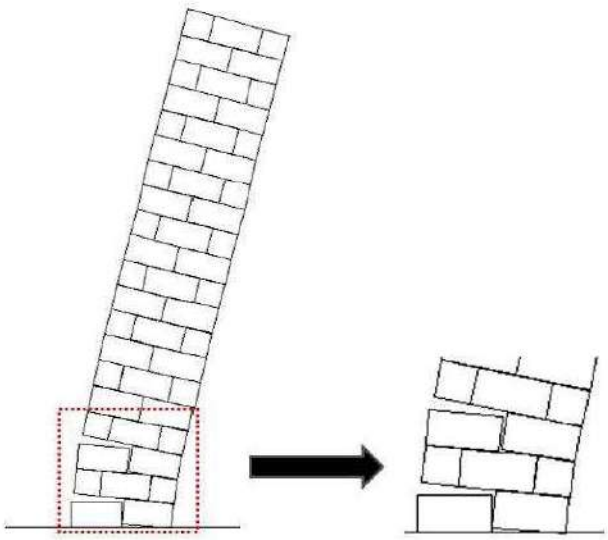

Figure 2.11. Collapse mechanism of masonry wall under nonlinear static analysis using DEM.

Therefore, macro-modeling provides strategies able to grasp the behavior of a full structure through homogenized macro elements (in general one or two dimensional), Finite Elements (FEs). The most applied modeling strategies for the analysis of a full structure considers the in-plane response

of masonry walls with openings as a discretization into three structural compounds: (i) vertical panels, also called piers, that support dead and seismic loads; (ii) horizontal panels, also named spandrels, that links the vertical panels; (iii) rigid nodes that are the masonry portions confined between vertical and horizontal panels, undamaged under seismic actions Gambarotta and Lagomarsino (1996, 1997), see Fig.2.12.

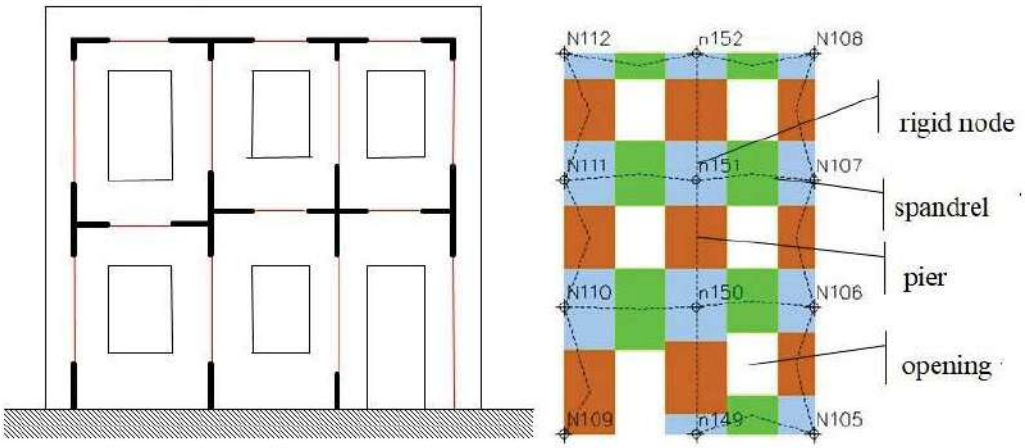

Figure 2.12. Equivalent frame model of a masonry wall and its mesh in the software-package 3Muri, STADATA.

A reference method is the so-called *Equivalent Frame Method*. The model approach consists in modeling piers and spandrels as non-linear beams, connected to each other by rigid links. Masonry portions confined between piers and spandrels are modeled as rigid nodes. The model formulation considers two damage modes, see Fig.2.13: (i) rocking, see Fig.2.13(a); (ii) diagonal shear cracking, see Fig.2.13(b); (iii) sliding shear, see Fig.2.13(c).

The non-linear mechanical behaviour could be considered thorough different constitutive laws. A recurrent approach used is the so-called lumped plasticity approach Pasticier et al. (2008). The masonry elements are modelled as elasto-plastic with two rocking hinges located at the ends of each frame and a shear hinge located at the mid-height. The masonry piers may suffer in-plane failure for bending-rocking and shear sliding mechanisms. Several constitutive laws can be described the failure criteria, that, for Italian and European applications, follow the Eurocode 8 (EC8-1) dei

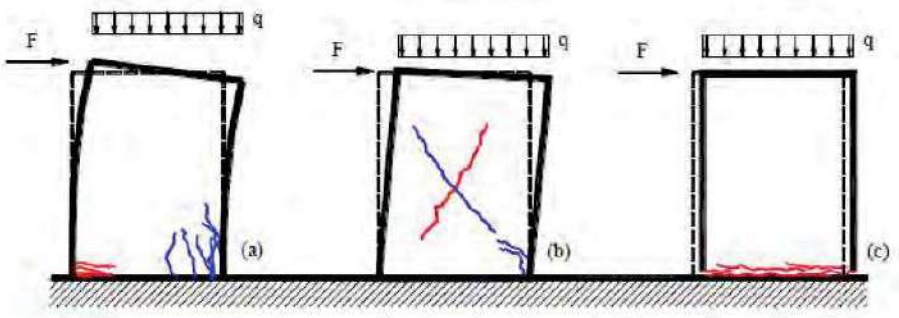

Figure 2.13. Failure mechanisms of a masonry pier: (a) rocking; (b) diagonal shear cracking; (c) sliding shear.

Trasporti e delle Infrastrutture (2008) and the Italian Design Code dei Trasporti e delle Infrastrutture (2008); per le Costruzione (2018). The relationship A.1 evaluates the ultimate moment of the rocking hinges and the relationship 5.7 evaluates ultimate strength of shear hinges.

$$M_u = 0.5\sigma_0 t D^2 (1 - \frac{\sigma_0}{0.85 f_d}) \tag{2.21}$$

$$V_u = \frac{1.5 f_{v0} t D}{\epsilon} \sqrt{1 + \frac{\sigma_0}{1.5 f_{v0}}} \tag{2.22}$$

where σ_0 is the mean vertical stress for gravitational loading, D and t are the width and the thickness of the wall, respectively, f_d is the design compression strength f_{v0} indicates the design shear strength with no axial force and ϵ is a coefficient related to the element geometrical ratio, assumed as H/D, where H is the height of the vertical masonry element.The ultimate shear displacement is equal to 0.4% of the deformable height of the masonry element and the ultimate rotation, for bending moment, is equal to 0.6%. Despite its large application, in presence of irregular opening layouts into masonry walls, the equivalent frame idealizations may lead to epistemic modeling errors due to the non-unique identification of the effective wall height and deformable regions. Therefore, several scholars deserve effort to propose more refined computational techniques for assessing the response of more articulated URMs under seismic actions.

Unreinforced masonry buildings

Chapter abstract

The core of the research activity lays on the structural vulnerability of un-reinforced masonry buildings (URMs). This structural typology is widespread in many built areas, particularly in Italy. Fifteen URMs have been selected in order to better grasp the fragilities that affect the dynamic behavior. The case study is located in Central Italy, recently hit by shattering earthquakes. The investigated URMs show structural characteristics representative of the ordinary existing heritage. Therefore, the sample of buildings mirrors the entire class of URMs, with an overall point of view. Firstly, a brief description of the seismic swarm, occurred in 2016, is delivered. The seismic damage exhibited by these buildings during the 2016 earthquake is deeply discussed. Then, the selected building's seismic performance were investigated via non-linear static analysis. The presented seismic assessment arose from a deep knowledge of the case study, providing a deep characterization of structural parameters and their scatter, known from the suffered damage, the gathered information during the post-earthquake surveys and diagnostic material campaigns. Still, the assessment of the structural archetypes' structural response may be of great help for the understanding of the expected seismic behavior of URMs. Finally, the proposed overview is used to support the research activities of this thesis.

3.1 An overview of URMs

A significant part of the scientific literature focuses on evaluating the seismic behaviour of the built heritage. Furthermore, several existing facilities reveal similar structural response after a seismic event, which leads to classifying buildings based on typological characteristics. The first classification of buildings bases on the construction typologies: masonry, reinforced concrete, wood, steel, and pre-cast. After that, a more detailed classification leads to refine the investigation or evaluation of the seismic performance of a specific typology of constructions. This thesis focuses on un-reinforced masonry buildings' (URMs) seismic behaviour. Masonry buildings built before seismic codes exhibit high vulnerability in almost seismic-prone areas, receiving thus an increasing attention from researchers and authorities. In addition, URMs are a common constructions' typology in many countries in the world. The prediction of URMs seismic response is a rather complex problem due to the uncertainties in the characterization of the masonry and the structural configuration. The discussion of these buildings' seismic response deserves attention due to the predominant non-linear behaviour under a seismic action. Despite the intrinsic differences between masonry buildings, a limited set of structural parameters affect the seismic response the most. Among them, masonry's mechanical properties, the resistance of masonry spandrels, and the in-plane stiffness and resistance of the floors play a crucial role in both the in-plane and out-of-plane seismic response Calderoni et al. (2017); Rizzano et al. (2009). The mechanical properties of masonry markedly affect the damage and the failure of buildings subjected to gravity loads and earthquake actions. The spandrels properties affect the strength degradation and the walls' lateral resistance, influencing the masonry piers' coupling effectGattesco et al. (2014). The in-plane stiffness and resistance of the floors affect the horizontal force's distribution between the walls and the occurrence of possible out-of-plane phenomena Senaldi et al. (2014). Other parameters, also non-structural ones, influence the seismic performance. Nevertheless, their evaluation is more difficult to achieve. The current research, developed in the thesis, focuses on the seismic response of ordinary buildings (two/ three stories), of which a con-

spicuous sample was taken in reference. To the authors' knowledge, seismic response of unreinforced ordinary buildings received interest also from other authors Aşıkoğlu et al. (2020); Angiolilli et al. (2021); Basar et al. (2021); Fragomeli et al. (2017); Saretta et al. (2021); Sorrentino et al. (2019)Augenti and Parisi (2009); Croce et al. (2019); D'Ayala (2013). The Italian built environment exhibits typical features for each region, in term of materials and structural configurations, often requiring a classification at local or regional scale Vettore et al. (2020). This thesis deserves attention to the seismic performance of the masonry buildings typical of the Central Italy, hit by the last seismic swarm occurred in the 2016. The proposed methodology can be addressed to any buildings' typology by considering structural features of the analyzed facilities, as done by other authors Chieffo et al. (2019) . Therefore, the authors attempted to mirror to the entire class of ordinary masonry buildings. In addition, the last suffered damage of the buildings' sample, under the last seismic swarm occurred, allows to better understand the main fragilities of the built environment that could exasperate an unsatisfactory structural performance under a seismic action.

3.2 The 2016 Seismic Sequence

A seismic swarm struck the Central Italy, involving four regions: Lazio, Abruzzo, Marche, and Umbria. On 24 August 2016, the mainshock, with a magnitude M_w= 6.2, occurred with an epicentre located in the municipality of Accumoli (Rieti, Lazio). Other events followed the main shock event. On 26 October 2016, a seismic event of a magnitude M_w=5.9 took place in Castelsantangelo sul Nera (Macerata, Marche). On 30 October 2016, another shock was recorded with a magnitude M_w=5.5, with an epicentre close to Norcia (Perugia, Umbria) and 9.4 km depth Fiorentino et al. (2018). Unfortunately, the seismic sequence continued. On 18 January 2018, a shock hit the municipality of Capitignano (L'Aquila, Abruzzo) already severely damaged by the previous earthquakes. Figure 3.1 displays the horizontal components of two events of the seismic sequence Sorrentino et al. (2019): Amatrice, AMT, and Norcia, NRC, records for the two main events of seismic sequence, on August 24th and October 30th, respectively. Overall, about 6500 aftershocks occurred in the area, with a M_w until 5.5.

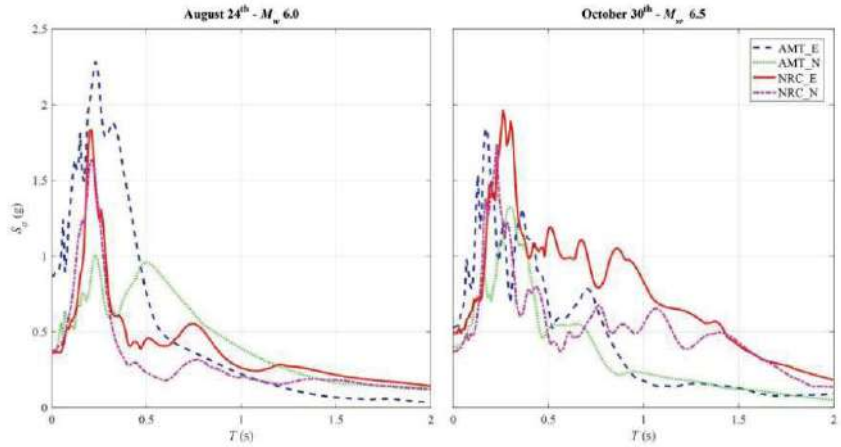

Figure 3.1. Pseudo-acceleration spectra. Sorrentino et al. (2019).

The seismic-genetic area denotes the presence of different faults with a complex structural configuration Galadini et al. (2018). Active extensional tectonics, that characterize this area since the Upper Pliocene, drive the actual morpho-structural setting of Central Apennines. Mostly, this area consists of outcropping of deposits from the Monte della Laga formation and Meso-Cenozoic limestones and marlsForte et al. (2019); Martino et al. (2020). The stratigraphic and topographic configurations revealed strong local site effects causing damage concentration in certain areas, see Fig. 3.2 Sextos et al. (2018).

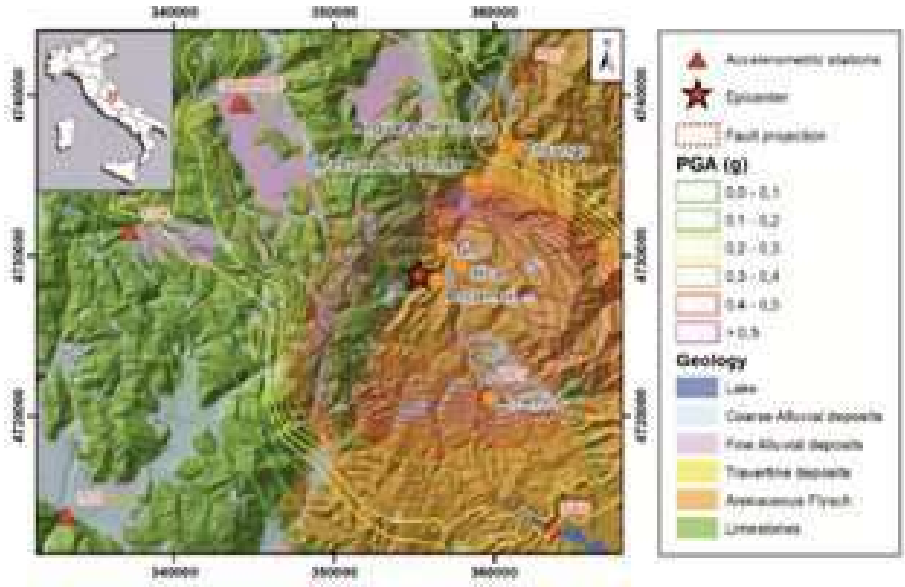

Figure 3.2. Simplified geologic map of the area with the PGA distribution of the 24th August 2016 earthquake (INGV ShakeMap) Forte et al. (2019)

After the seismic swarm occurred, the Italian National Institute of Geophysics and Volcanology (Istituto Nazionale di Geofisica e Vulcanologia, INGV) derived a ShakeMap of the seismic events
(*http* : *//shakemap.rm.ingv.it/shake/index.html*), through the software package ShakeMap, developed by the U.S. Geological Survey Earthquake Hazards Program. The real time maps were obtained from data provide mainly by the INGV broadband stations in addition to strong motion data gathered from the Italian Strong Motion Network (Rete Accelerometrica Nazionale, RAN). Fig.3.3 reports a ShakeMap of the area hit by the 2016 earthquake in terms of peak ground acceleration (PGA) of the event of 24th August 2016 Del Gaudio et al. (2017).

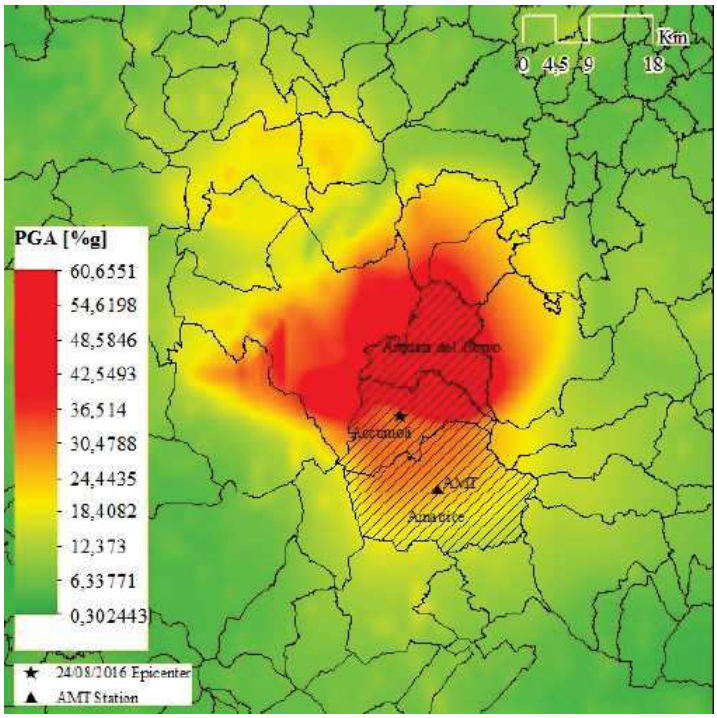

Figure 3.3. ShakeMap in terms of PGA of the hit areaDel Gaudio et al. (2017).

3.2.1 Historical sismicity of the area

The earthquakes occurred in August and October 2016 are among the strongest seismic events occurred in Central Italy. The maximum intensity recorded in the epicentral area reached a value of X-XI grade of the Mercalli-Cancann-Sieberg scale. An earthquake occurred in 1639 was similar to the mainshock of the 2016: the epicentre was far 4km from Amatrice, with a $M_w = 6.2$, and a slightly lower of IX-X MCS intensity Fiorentino

et al. (2018).

Other shattering events occurred near the seismic crater over time. In 1703, a strong earthquake, with a $M_w = 6.6$, hit L'Aquila and in 1730 another strong earthquake, with a $M_w = 6.0$, hit Valnerina, at distances of about 26 km from Amatrice. Recently, the last shattering event in this area was the 2009 L'Aquila earthquake, with a $M_w = 6.3$, that caused 309 victims, 1600 injured and about 60000 homeless. For example, Fig.3.4 reports the historical seismicity in Amatrice expressed according to MCS intensity, starting from year 1500 A.D. Fig.3.5 reports the historical seismicity in Norcia expressed according to MCS intensity, starting from year 1200 A.D.

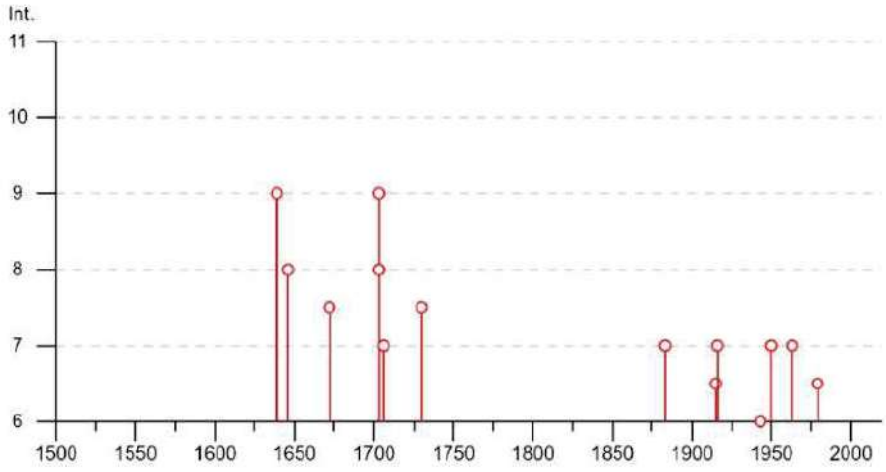

Figure 3.4. Historical seismicity of Amatrice MCS Intensity (above VI degree) versus year of occurrence Locati et al. (2016)

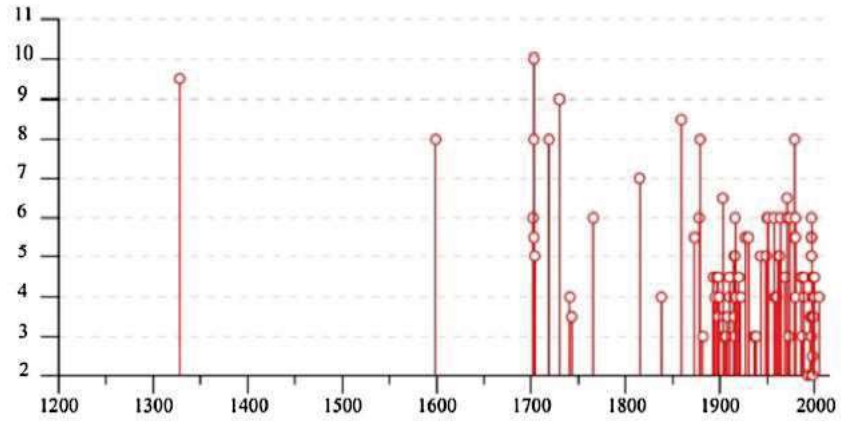

Figure 3.5. Historical seismicity of Norcia MCS Intensity versus year of occurrence

According to the report of the Italian Department of Civil Protection

(Italian Department of Civil Protection 2017,
$http://www.protezionecivile.gov.it/jcms/it/terremoto_centro_italia_2016.wp$),
the event of August 24 caused 299 victims, 384 injured, and about 4800 homeless. At the end of the seismic sequence, 200000 damaged buildings and 11600 homeless could be counted. The most severely damaged area was Amatrice and the surrounding municipalities, belonging to the Lazio region. The historical centres of Amatrice, Accumoli and Arquata del Tronto were almost destroyed. The built heritage proved to be un-safe and severely damaged, see Fig. 3.6 taken by the Italian Fire Department in the aftermath of the seismic events.

3.3 Urban Layout and General Features of the Masonry Built-Up

The municipalities involved in the seismic swarm are located in four regions in the Central Italy (Abruzzo, Lazio, Umbria, and Marche). Among them, the most extended and populated are Amatrice, Accumoli, Cittareale, and Arquata del Tronto. Del Gaudio et al.Del Gaudio et al. (2017) provided a brief description of the main hit municipalities in terms of built-up characteristics. Accumoli is a municipality located in Lazio region with an area of 87.3 square kilometres and a population of 653 inhabitants. The number of buildings is equal to 1382, of which 849 with a residential scope. URMs represent the 94% of the residential buildings, RC the 5% and the 1% is composed by other typologies. The 36% of the residential buildings were built before 1919, 23% between 1919 and 1945, 19% between 1946 and 1961, 12 between 1961 and 1981, and 9% after 1981. Furthermore, 11% of residential buildings consists of a single storey, 45% of two-storeys, 42% by three storeys and the remaining 2% by buildings with at least four floors. Amatrice is a municipality located in Lazio region with an area of 174.4 square kilometres and a population of 2646 inhabitants. The number of buildings is equal to 5288, of which 4103 used to a residential use. URMs represent the 86% of the residential buildings, RC the 5% and the 9% is composed by other typologies. The 27% of the residential buildings were built before 1919, 18% between 1919 and 1945, 16% between 1946 and

(a)

(b)

(c)

(d)

Figure 3.6. Damage suffered during the 2016 earthquake seismic swarm: (a)Collapsed Buildings in Amatrice; (b) Damage along the main way of Amatrice; (c)Damage in Pescara del Tronto; (d) Damage in Accumoli. Taken by Italian Fire Department

1961, 27 between 1961 and 1981, and 12% after 1981. Furthermore, 12% of residential buildings consists of a single storey, 47% of two-storeys, 39% by three storeys and the remaining 2% by buildings with at least four floors. Arquata del Tronto is a municipality located in Marche region with an area of 92.2 square kilometres and a population of 1287 inhabitants. The number of buildings is equal to 1315, of which 1245 used to a residential use. URMs represent the 28% of the residential buildings, RC the 9% and the 63% is composed by other typologies. The 32% of the residential buildings were built before 1919, 31% between 1919 and 1945, 13% between 1946 and 1961, 20 between 1961 and 1981, and 4% after 1981. Furthermore, 3% of residential buildings consists of a single storey, 26% of two-storeys, 57% by three storeys and the remaining 14% by buildings with at least four floors. On the local urban fabric, real fifteen buildings have been selected to sort a representative buildings' sample on which this research activity focuses. The selected buildings, see Fig.3.7, are located in Cittareale. It is a Municipality of Rieti Province (Lazio, Italy), near Umbria and Abruzzo Regions, covering an area of approximately 58.97 km^2. It was located near the Municipalities of Accumoli and Amatrice. It is located along the Falacrina valley, where the Tito Flavio Vespasiano emperor was born in the 9^{th} century. The most accredited chronological hypothesis is that the municipality was founded in 1261 on the ruins of an ancient centre called Apolline, for the will of the Carlo I d'Angiò king. The built heritage exhibits mainly ordinary constructions.

In the light of the above, the built-up of the entire area, struck by the earthquake swarm, mainly consisted of rubble stone masonry and ordinary reinforced concrete buildings, including churches and monuments of a high architectural value. Un-reinforced masonry buildings, composed of two or three storeys, represent the prevailing typology of the local built-up. In the historical centre of the municipalities, buildings were built along the streets, attached to each other, with different heights and storeys' number. The recurrent layout of the local buildings aggregates consists of two or three buildings, built side by side, like a repetition of different structural units: i.e. buildings called B1, B2, B3, B13, and B14 in Fig.3.7. The built-up, immediately near the historical centre, represents an expansion of

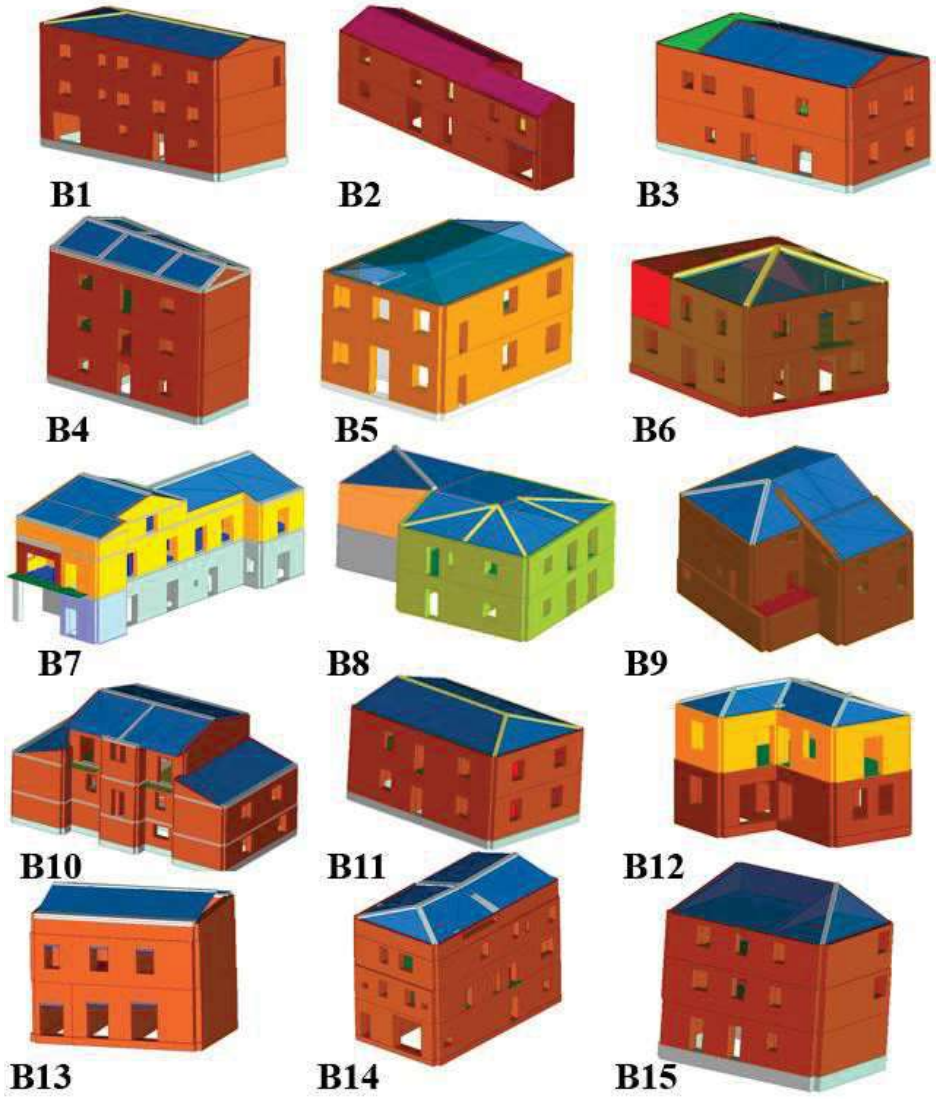

Figure 3.7. Views of the geometrical model of the buildings.

the first core of the municipality: buildings (i.e. buildings called B4, B7, B8, B9, and B13 in Fig.3.7) stand almost isolated, preserving the architectural and historical values. Most of them underwent refurbishments that led to structural extensions (such as horizontal and vertical structures), often realized with different materials, and seldom with a more irregular shape. In the surrounding area, built in recent decades, masonry buildings stand isolated, with a more regular aspect, with a better construction quality. The buildings are generally inaccurately designed and built using poor quality materials, i.e. buildings called B5, B6, B10, B11, B12, and B15 in Fig.3.7. Figure3.8 reports pie charts for the selected buildings to graphically synthesize their structural features.

Two main masonry typologies were detected. The first consists of irregular stone units, like rounded fluvial cobbles, see Fig.**??** (a), with poor and dusty mortar, or like sandstones and travertine limestone material, called Sponga.The second masonry typology consists of tuff units, in forms of cut stones, see Fig.**??**(b), and seldom with scattered clay bricks, see **??**(c). Still, clay masonry bricks and concrete blocks are employed in buildings dated back to 20^{th} century and in refurbishments in the past decades. The masonry units are arranged to build a single leaf wall, without cavity.

The mechanical parameters of the detected masonries' typologies are listed in Table **??**, according to the Italian Standard Code:

Table 3.1. Mechanical parameters of the masonry typologies.

Masonries	f_m, MPa	τ_0, MPa	E, MPa	G, MPa	γ, kN/m^3
Irregular units with no homogeneous thickness	1.00	0.018	870	290	19
Tuff squared units	2.00	0.040	1410	450	16
Tuff units with scattered clay bricks	2.40	0.048	1692	540	16

The lack of wall-to-wall connections triggered out-of-plane mechanisms, see Fig.**??**. Conversely, numerous buildings exhibited a good seismic behaviour. Anti-seismic devices, like iron tires, and connections between structural elements, led to in-plane seismic response, see Fig.**??**.

Floors are generally flexible: can be wooden floors with joists and timber planks, or steel floors with iron beams and clay tiles. Seldom, masonry vaults cover the ground stories. Fig.3.11 depicts three structural cross sections of three floor typologies, most widespread in the Italian built envi-

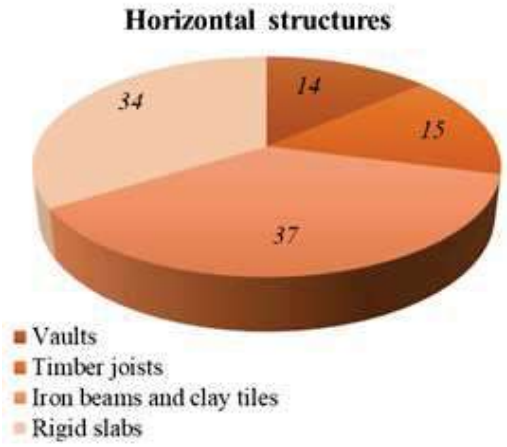

(a) Horizontal structures.

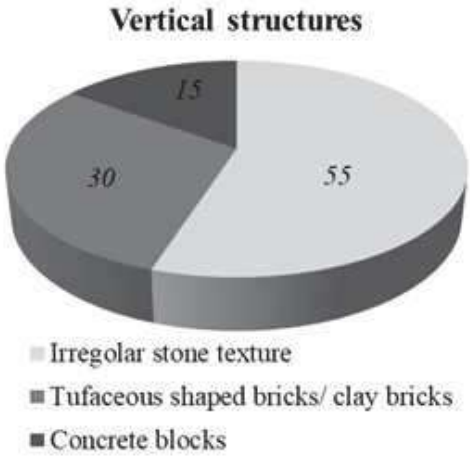

(b) Vertical structures.

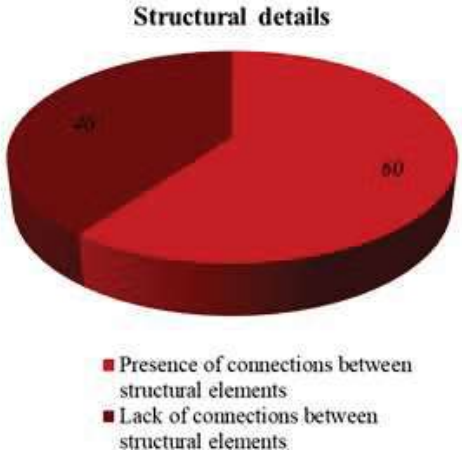

(c) Structural details.

Figure 3.8. Pie charts of some gathered structural features of the building sample.

(a) Rounded fluvial cobble.

(b) Tuff masonry with scattered clay units.

(c) Tuff unit with squared shape.

Figure 3.9. Typical masonry typologies.

(a) Out-of-plane mechanism. (b) In-plane mechanism.

Figure 3.10. Views of observed seismic response.

ronment. Fig.3.11(d) is the photo of the floor of a selected URM, on which a dynamic campaign was carry out to better investigate the structural behaviour (discussed in Chapter 4).

The more traditional roof system consists of wooden pitches, often with thrusting girders. In the last decades, several buildings experienced restoration and alterations, like replacement of roofing system, insertion of tie rods, construction of rigid slabs or large openings. Fifteen masonry buildings have been selected as representative of the local built-up. Visual inspections and geometric surveys allowed an in-depth knowledge of the buildings. Based on the gathered information, numerical analyses of the buildings are performed to investigate the seismic behaviour through non-linear static analysis.

3.3.1 Description of a prototype building

The buildings' sample covers the built area and the availability of data (geometrical, mechanical and structural details) ensures an extensive their knowledge. Nevertheless, a building has been selected as representative of the structural typology to allow more specific investigations, that required effort and time demand difficult to overcome for several buildings: (i) experimental campaigns under environmental conditions; (ii) non-linear dynamic simulations. The selected URM as an archetype of the ordinary masonry heritage, has a nearly rectangular shape, 10.06 m long and 12.23 m wide, and consists of two stories, 3.05 m high. Fig. 3.12 reports the plans of the stories and Fig.3.13 depicts two prospects of the building. The bearing structure consists of irregular stone masonry units with good mortar, recently restored with grout injections, see Fig.3.14. The longitudinal direction consists of three alignments of resistant walls; the transverse one consists of four alignments of walls, of which internal ones are built with clay bricks. The floors are made of steel joists and brick tiles. The openings show the presence of a lintel due to a good layout of masonry units and the presence of tension-resistant element. The roof consists of one layer of timber planks and joists.

Tab.3.2 reports the mechanical parameters of the masonries, assigned according to the Italian Standard Code dei Trasporti e delle Infrastrutture

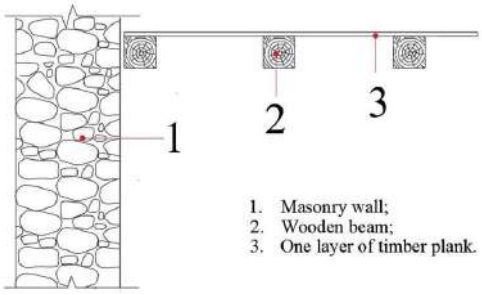

(a) Structural cross sections of the timber floor.

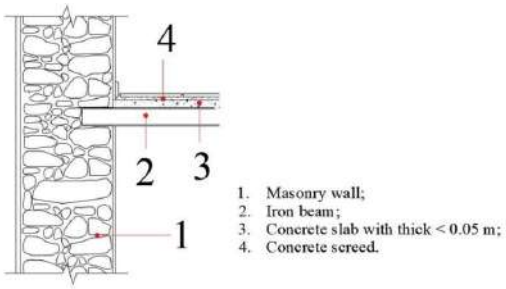

(b) Structural cross sections of the steel joists and brick tiles floor.

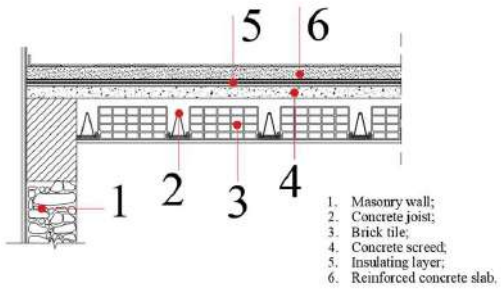

(c) Structural cross sections of the RC floor.

(d) Photo of a steel joists and brick tiles floor.

Figure 3.11. Floor typologies.

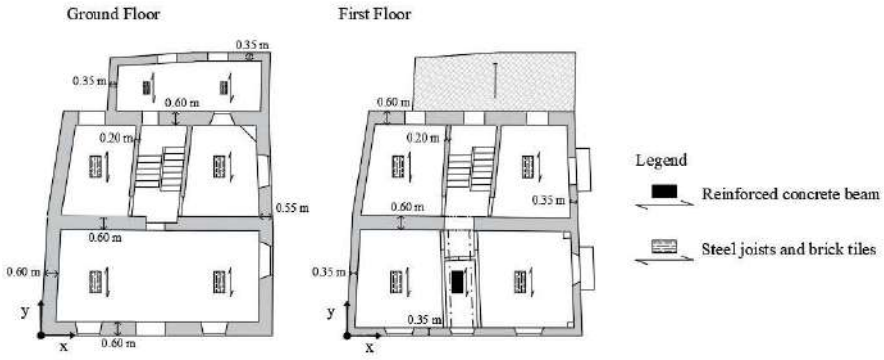

Figure 3.12. Plans of the building with the indication of the warping of horizontal structures.

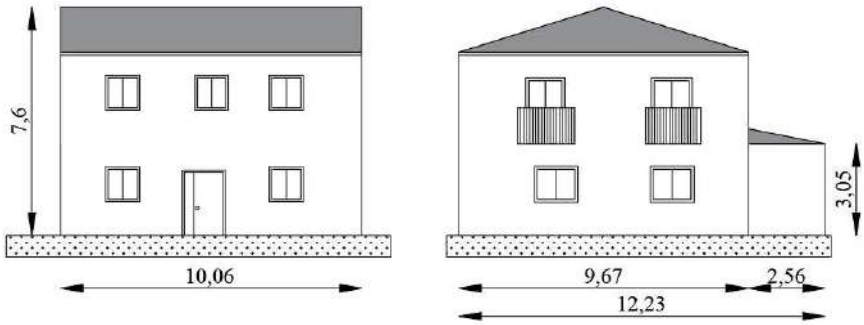

Figure 3.13. Prospects of the building with measures expressed in meters.

Figure 3.14. Texture of the masonry.

(2008); per le Costruzione (2018), where: f_m is the compressive strength average value, τ_0 is the shear strength average value, E indicates the Young Modulus average value, G is the Shear Modulus average value, and γ indicates the specific weight. Three typologies of masonry have been detected: (i) M_{S1}, irregular layout with masonry units embedded with good mortar ;(ii) M_{S2}, reinforced with grout injections; (iii) clay bricks. The masonry walls composed by stone units recently underwent a restoration with grout injections. As suggested by dei Trasporti e delle Infrastrutture (2008); per le Costruzione (2018), the mechanical characteristics are corrected by a correction factor equal to 1.7 to account the effectiveness of the strengthening interventions on the mechanical characteristics of the masonry. This value of the elastic modulus E_m provided the starting value in the model updating process. The floor was modeled as an orthotropic membrane, with the elastic moduli, E_{s1} and E_{s2} of the slab, different for the main direction and the perpendicular direction, respectively Mendes and Lourenco (2010); Yi et al. (2006). The slabs and the load bearing walls have been assumed as perfectly and full connected. The loads of the floors and roof were considered in the model as vertical concentrated forces. The structure was assumed fixed to the foundation.

Masonry	f_m **[MPa]**	τ_0 **[MPa]**	**E [MPa]**	**G [MPa]**	γ **[Mpa]**
M_{S1}	2	0.042	1230	460	13-16
M_{S2}	3.57	0.07	2754	918	13-16
M_{S3}	2.60	0.05	1500	500	18

Table 3.2. Mechanical parameters of masonry.

Tab.3.3 reports the main geometrical and mechanical characteristics of each masonry piers, called respecting the legend reported in Fig.3.15, implemented in the numerical model, where: D indicates the width, t the thickness, H the height, σ_0 the tensional state, $M_{u,t}$ the Ultimate Moment at the top of pier, $M_{u,b}$ the Ultimate Moment at the base of pier M_u, and V_u the Ultimate shear strength.

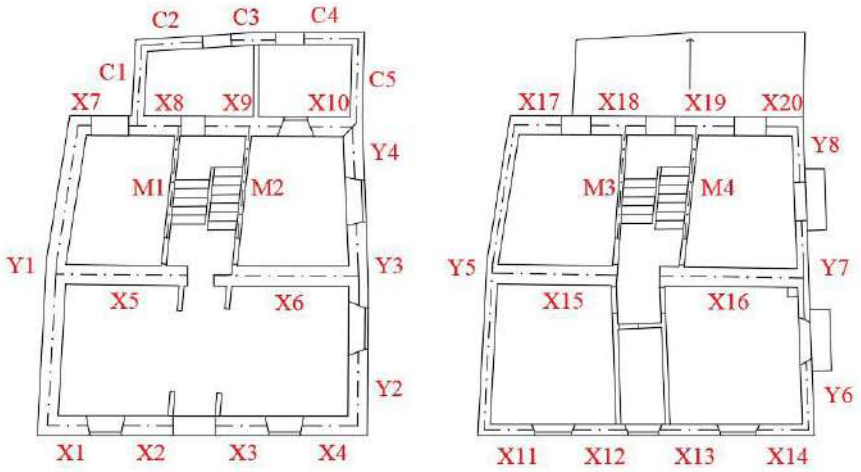

Figure 3.15. Legend of masonry piers (from the left: the first and second floor, respectively).

Piers	**D [m]**	**t [m]**	**H [m]**	σ_0 **[MPa]**	$M_{u,t}$ **[kN*m]**	$M_{u,b}$ **[kN*m]**	V_u **[kN]**
X1	1.22	0.60	1.91	102.37	35.63	48.52	50.80
X2	1.52	0.60	1.45	121.40	67.14	85.42	117.82
X3	1.60	0.60	1.00	118.70	75.51	90.29	180.58
X4	1.70	0.60	2.17	125.24	78.81	116.82	107.67
X5	3.80	0.60	2.70	507.13	1259.86	1411.64	813.53
X6	4.15	0.60	2.70	559.21	1575.55	1760.37	1010.72
X7	0.60	0.60	2.70	97.95	8.69	10.88	8.06
X8	1.60	0.60	2.70	136.38	74.05	112.66	83.45
X9	2.33	0.60	2.70	170.25	183.19	249.73	205.10
X10	1.72	0.60	2.70	118.60	70.24	119.83	88.76
X11	1.52	0.35	1.90	44.29	12.60	21.92	23.07
X12	1.65	0.35	1.00	51.72	20.56	26.76	53.51
X13	1.82	0.35	1.00	51.97	24.76	33.07	66.14
X14	1.55	0.35	2.10	46.60	13.40	24.28	23.13
X15	3.58	0.60	2.70	207.15	470.00	844.16	515.62
X16	4.38	0.60	2.70	239.63	778.37	1414.58	810.97
X17	1.42	0.60	1.90	49.76	17.72	39.85	41.93
X18	1.67	0.60	1.00	49.46	30.26	49.22	98.43
X19	1.80	0.60	1.00	57.86	41.94	65.35	130.70
X20	0.95	0.60	2.10	37.97	6.21	13.67	13.02
Y1	9.15	0.50	3.00	450.09	4648.35	6889.02	3368.74
Y2	2.22	0.50	2.50	109.16	87.44	157.19	125.75
Y3	2.45	0.50	1.00	69.21	78.06	118.27	236.55
Y4	1.60	0.50	2.10	85.99	39.24	76.19	56.44
Y5	9.29	0.35	2.70	175.14	972.47	3354.18	1918.73
Y6	2.07	0.35	2.70	50.73	19.26	53.22	38.42
Y7	3.02	0.35	2.10	27.12	0.00	83.02	79.07
Y8	1.70	0.35	2.70	45.84	12.99	31.47	23.31
M1	3.40	0.15	2.70	69.89	39.24	76.19	56.44
M2	3.40	0.15	2.70	69.89	39.24	76.19	56.44
M3	3.40	0.15	2.70	23.30	0.00	39.24	29.07
M4	3.40	0.15	2.70	23.30	0.00	39.24	29.07
C1	2.64	0.30	2.70	26.13	0.00	52.47	38.87
C2	1.86	0.30	2.70	41.19	11.62	29.53	21.88
C3	1.35	0.30	2.70	34.79	5.76	12.68	9.40
C4	1.58	0.30	2.70	35.94	7.49	18.56	13.75
C5	2.36	0.30	2.70	23.36	0.00	37.65	27.89

Table 3.3. Geometrical and mechanical parameters of masonry piers.

3.4 Numerical analyses of the selected buildings

3.4.1 Static non-linear analysis of the selected buildings

Static non-linear analysis of the fifteen URMs were performed using a commercial software package, 3Muri® software (STA Data)STADATA (2011). In the software, the equivalent frame modelling approach is implemented: the masonry panels, namely the piers (the vertical elements) and the spandrels (the horizontal elements) are modelled as non-linear beams connected to each other by rigid links. Fig. 3.16 reports an idealization of the calculation procedure followed by the software STADATA (2011).

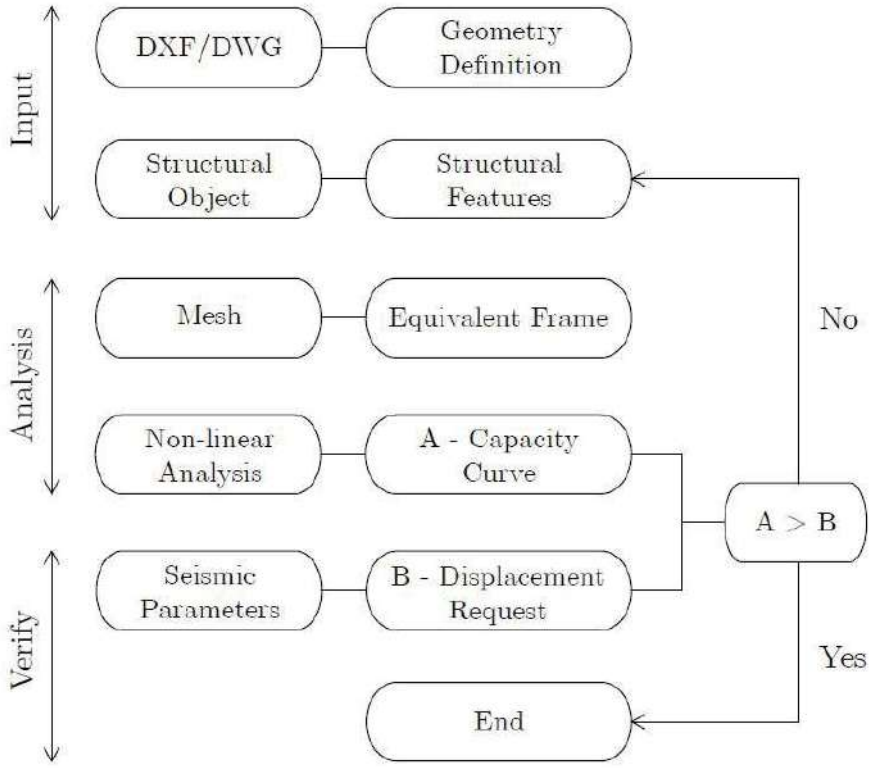

Figure 3.16. Scheme of the calculation path of the 3Muri software.

In Appendix A the formulations implemented in the 3Muri software are discussed more precisely. The piers may suffer two in-plane failure mechanisms: (i) for bending-rocking, and (ii) for shear sliding Gambarotta and Lagomarsino (1996, 1997). The Eurocode 8, EC8-1 Herrmann and Bucksch (2014), and the Italian Design Codedei Trasporti e delle Infrastrutture (2008); per le Costruzione (2018) provide strength criteria for use

in design. The resistant mechanism of the spandrels is not considered if the openings have not resistant structural elements.

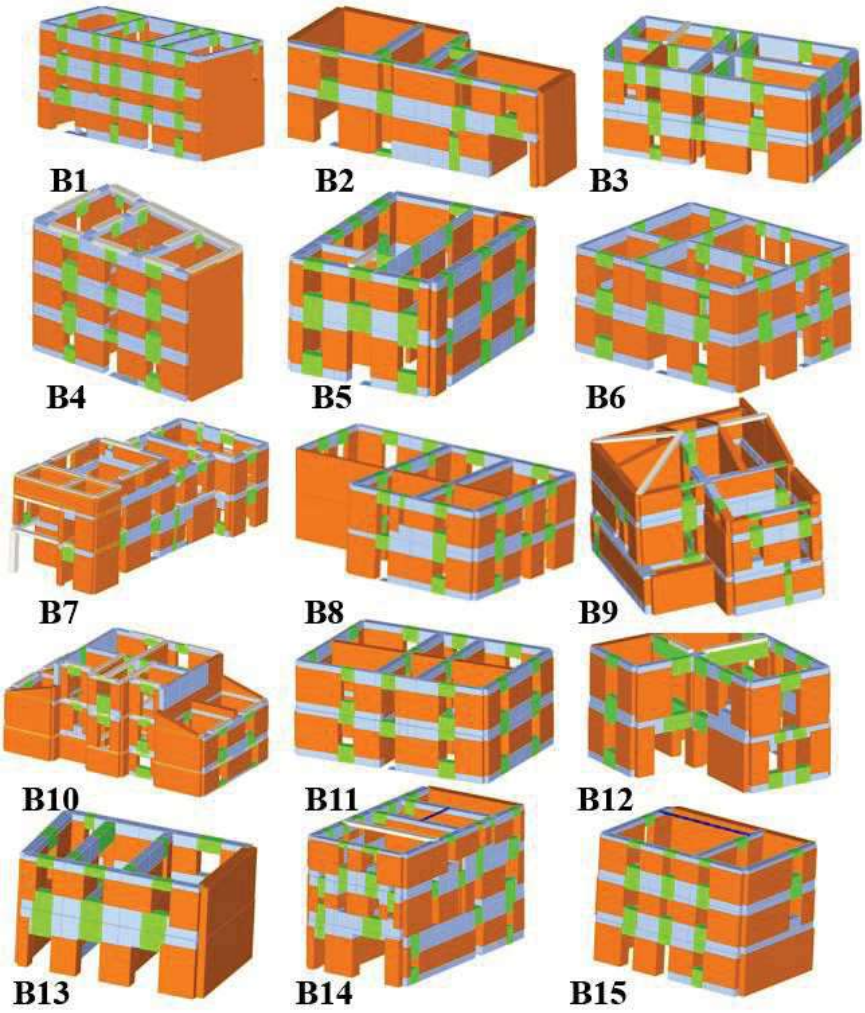

Figure 3.17. Views of the EF model of the buildings.

The seismic action corresponds to the design response spectrum, according to the Italian Seismic Code, defined through the spectral parameters a_g (max ground acceleration), F_0 (max value of the amplification factor for the horizontal acceleration response spectrum) and T_c^* (period of the horizontal onset for constant velocity), reported in the Italian Ministerial Decree dei Trasporti e delle Infrastrutture (2008); per le Costruzione (2018), based on the site geographic coordinates of buildings. Considering the soil and the topographic category of the site, the response spectrum is defined for a return period, T_R, of 30 years, for Operational Limit State, LS1; 50 years, for Damage Limit State, LS2; 475 years, for Significant Damage Limit State, LS3; 975 years, for Collapse Limit State, LS4, Agency (1997), see Table

Limit State	a_g $[m/sec^2]$	F_0	$T_c^*[sec]$
LS1	0.77	2.40	0.27
LS2	1.02	2.33	0.28
LS3	2.55	2.36	0.34
LS4	3.27	2.40	0.36

Table 3.4. Spectral parameters of the selected site.

3.4.

The elastic response spectrum can then be used to derive the Acceleration Displacement Response Spectrum, see Appendix B. Static non-linear analyses were performed for positive and negative orientations of the longitudinal and transversal direction, applying two patterns of seismic loads: (i) proportional to the mass distribution; (ii) proportional to the first vibration mode of the structure. According to the recommendations of the Italian Ministerial Decree dei Trasporti e delle Infrastrutture (2008); per le Costruzione (2018), an accidental eccentricity between the mass and the stiffness centre is considered. Twenty-four push-over curves were derived for each structure, for a total of 360.

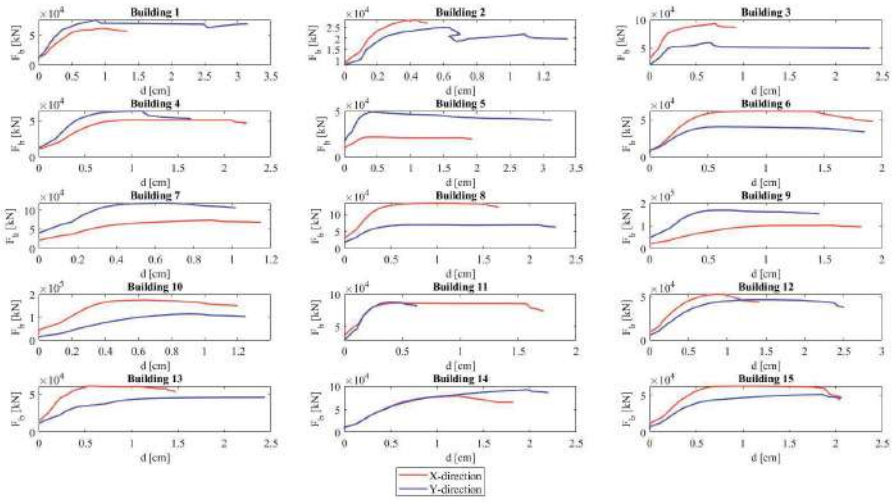

Figure 3.18. Push over curves for each building referred to the lowest safety level.

Tables 3.5 and 3.6 report the main outputs of the pushover analysis, for the lowest safety level,for X-direction and Y-direction, respectively. For each building, tables indicate the yielding force F_y, the yielding and ultimate displacements, d_y and d_u, the vibration period T^* of the of the equivalent single degree-of-freedom (SDOF) system, and the safety factor

Buildings	$F_{y,x}$ $[kN]$	$d_{y,x}$ $[cm]$	$d_{u,x}$ $[cm]$	T_x^* $[sec]$	$\alpha_{u,x}$
B1	503.30	0.45	0.78	0.37	0.23
B2	209.10	0.12	0.40	0.18	0.34
B3	785.00	0.12	0.70	0.14	0.97
B4	396.50	0.43	1.75	0.32	0.47
B5	163.80	0.14	1.54	0.24	0.39
B6	431.00	0.29	1.40	0.21	0.70
B7	653.20	0.29	0.99	0.29	0.39
B8	1075.40	0.25	1.27	0.17	0.96
B9	823.40	0.39	1.24	0.40	0.30
B10	1263.90	0.22	0.87	0.16	0.80
B11	2014.10	0.12	1.35	0.12	1.30
B12	432.60	0.40	1.19	0.25	0.59
B13	655.60	0.34	0.99	0.24	0.46
B14	597.60	0.55	1.40	0.42	0.27
B15	497.40	0.42	1.69	0.30	0.32

Table 3.5. Results of static non-linear analyses, X-Direction.

Buildings	$F_{y,y}$ $[kN]$	$d_{y,y}$ $[cm]$	$d_{u,y}$ $[cm]$	T_x^* $[sec]$	$\alpha_{u,x}$
B1	709.40	0.33	1.00	0.26	0.47
B2	197.30	0.19	0.95	0.22	0.55
B3	548.00	0.15	0.75	0.18	0.65
B4	472.40	0.34	1.00	0.25	0.41
B5	355.40	0.13	2.62	0.16	0.83
B6	336.90	0.25	1.46	0.23	0.54
B7	973.90	0.21	0.81	0.20	0.55
B8	650.80	0.27	1.36	0.24	0.63
B9	1556.10	0.27	1.48	0.23	0.55
B10	872.80	0.45	0.91	0.29	0.39
B11	798.60	0.17	0.56	0.13	0.94
B12	347.70	0.49	1.95	0.30	0.69
B13	356.00	0.23	0.95	0.29	0.31
B14	510.10	1.00	2.45	0.65	0.29
B15	406.30	0.37	1.05	0.31	0.25

Table 3.6. Results of static non-linear analyses, Y-Direction.

α_u referred to the LS3. For each structure, the static non-linear analysis with the lowest safety level were considered.
Fig.3.18 reports the push over curves for each building referred to the lowest safety level.

3.4.2 Dynamic non-linear analysis of a selected building prototype

Non-linear dynamic analysis ensures the most reliable and accurate prediction of the seismic performance of a building. Nevertheless, a deep knowledge of the structure is required. A thorough investigation of morphology, boundary conditions, construction process, architectural alterations or restorations, modeling errors should anticipate any seismic assessment. Unfortunately, extensive knowledge is difficult to achieve due to the lack of historical data and the cost of invasive and destructive tests. Furthermore, non-linear dynamic analysis engenders an high numerical burden and time consuming demand. Therefore, non-linear dynamic analysis were performed only for a single URM, chosen as representative of the case study and called *prototype building*. This paragraph presents only the approach involved in the incremental dynamic simulations of which results have been discussed in the chapter 4.
The chosen modelling approach consists in masonry panels, namely, piers (vertical elements) and masonry spandrels (horizontal elements) as non-linear beams, connected to each other by rigid links. Masonry portions confined between piers and spandrels are modeled as rigid nodes. The nonlinear mechanical behavior derives from a so-called lumped plasticity approach Felice et al. (2017); Pasticier et al. (2008). The masonry elements are modeled as elastoplastic with two rocking hinges located at the ends of each frame and a shear hinge located at the mid-height. The masonry piers may suffer in-plane failure for bending-rocking and shear sliding mechanisms. The constitutive law is represented in Fig. 3.19, and the failure criteria follow the Eurocode 8 (EC8-1) P.Code (2005) and the Italian Design Codedei Trasporti e delle Infrastrutture (2008); per le Costruzione (2018): the **relationship 1** evaluates the ultimate moment of the rocking hinges, see Eq.A.1, and the relationship 5.7 evaluates ultimate strength of

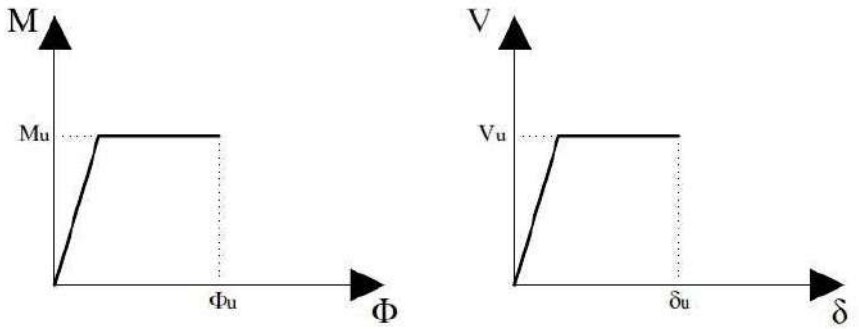

Figure 3.19. Constitutive laws of plastic hinges.

shear hinges.

$$V_u = \frac{1.5 * f_{v0} * t * D}{\epsilon} * \sqrt{1 + \frac{\sigma_0}{1.5 * f_{v0}}} \tag{3.1}$$

$$M_u = 0.5 * \sigma_0 * t * D^2 * (1 - \frac{\sigma_0}{0.85 * f_d}) \tag{3.2}$$

where σ_0 is the mean vertical stress for gravitational loading, referred to the section at the middle of the piers' height; D and t are the width and the thickness of the wall, respectively; f_d is the design compression strength, f_{v0} indicates the design shear strength with no axial force, and ϵ is a coefficient related to the element geometrical ratio, assumed as H/D, where H is the height of the vertical masonry element. σ_0 has been evaluated taking into account loads of the considered floor and the upper ones, at the mid height of the piers. The ultimate shear displacement is equal to 0.4 % of the deformable height of the masonry element, and the ultimate rotation for the bending moment is 0.6 %. Tab.3.7 lists the selected seven seismic events. The story drift was chosen as the target parameter to estimate the structural performance, under different earthquake multiplication factors from 0.1 to 1 in the X and Y directions.

	Name	Areas affected	Year	Mw	PGA $[m/s^2]$
1	El Centro	United States, Mexico	1940	6.9	3.50
2	Erzican	Erzincan Province, Turkey	1939	7.8	5.03
3	Kobe	Japan	1995	6.9	6.76
4	L'Aquila	Italy	2009	6.3	6.63
5	Northridge	Southern California, United States	1994	6.7	5.51
6	Loma Prieta	San Francisco, United States	1989	6.9	6.55
7	Parkfield	California, United States	2004	6.0	4.96

Table 3.7. List of the earthquakes adopted in the analysis

Fig.3.20 reports the frequency spectra of three of the seven accelerograms, used in the Incremental Dynamic Analysis (IDA).

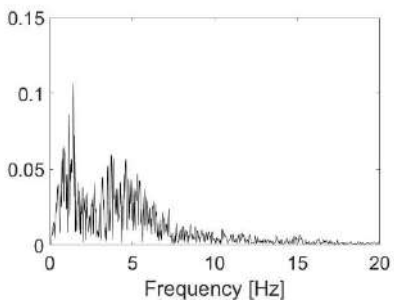

(a) L'Aquila earthquake

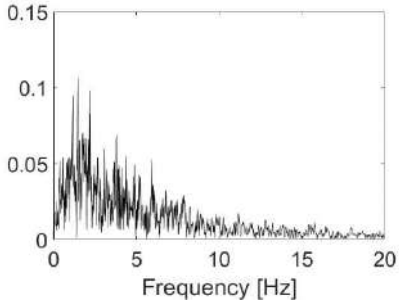

(b) El-Centro earthquake

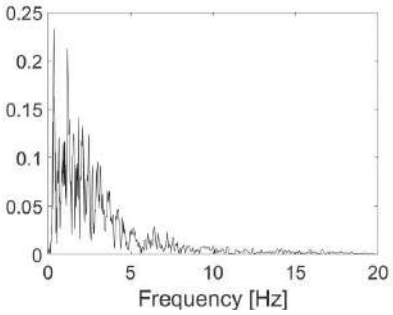

(c) Newhall earthquake

Figure 3.20. Frequency spectra.

The results of the IDA have been reported in the following chapter, that drives the research activity of this PhD thesis.

3.5 Acknowledgements

The author would like to thank S.T.A. DATA company for providing the license of the 3Muri software.

On the dynamic behaviour of a URM prototype

Chapter abstract

This chapter presents experimental and numerical investigations on the dynamic behaviour of an unreinforced masonry building, with two storeys, selected as representative of the entire structural typology of URMs. The experimental campaign consists of two ambient vibration tests to estimate the structure's dynamic behaviour in operational conditions of the structure. Two different aims have been followed: (i) the characterization the local dynamic of the floor, using accelerometers gathered along a row of the first floor; (ii) the characterization the global dynamics of the floor, through a second setup with accelerometers placed at the building corners. Two finite element models are implemented: (i) a single beam with an equivalent section of the floor to grasp the local behaviour of the investigated horizontal structure; (ii) an equivalent frame model of the entire building for the global dynamic behaviour. The model updating process is performed in two phases to seize local and global dynamic responses. Then, a sensitivity analysis underlines the influence of mechanical parameters of floors on the dynamic behaviour of URMs. Therefore, non-linear dynamic analyses are carried out, at varying mechanical characteristics of floors. The notable role of the floor's stiffness in the non-linear dynamic behaviour of URM has been appraised in terms of displacements' trend along its height. Lastly, the fragility curves have been derived predicting the seismic performance in failure probability under a highly severe damage state. The discussed outcomes attempt to deliver an extensive insight of the typological class of URMs to better address the research activity presented in this PhD thesis. In fact, evidences of these

studies highlight the main structural characteristics that influence structure's seismic behaviour. The initial step of the PhD activity researched the prevalent parameters to consider about the seismic capacity of URMs. At this aim, the extensive investigations deeply highlighted the dynamic behaviour of URMs, in order to facilitate the choice of the parameters of the simplified vulnerability assessment method.

4.1 Introduction

The chapter presents the investigation of the dynamic behavior of a URM, chosen as representative of the buildings' class of the research activity: a sensitivity assessment considers different structural features to mirror the entire class. First of all, experimental campaigns of the URM in operational conditions are carried out.

The presence of global failure modes depends on the presence of connection wall-to-wall and floor-to wall and the presence of an adequately rigid and resistant floor Mouzakis et al. (2018). Therefore, through two different setups, global and localized mode shapes have been investigated: (i) the first setup aims at estimating the local in-plane response of the floor; (ii) the second setup aims most at assessing global mode shapes by spreading the sensors inside the building. The chapter has the following objectives: (i) the estimation of the in-plane low-vibration structural response of a typical floor of masonry buildings. An equivalent beam element is updated using the experimental modal parameters to estimate both the equivalent elastic modulus of the floor and its thickness. (ii) The in-plane low-vibration structural response of the entire building using the experimental modal parameters from the second setup and the mechanical parameters of the floor assessed in the first optimization step is deepened. The dynamic behaviour of the building has been numerically estimated by modelling with an equivalent frame model, the most applied approach by practitioners Pasticier et al. (2008). (iii) Lastly, the influence of the floors' stiffness on the global dynamic behaviour of the selected URM is numerically deepened through incremental dynamic analysis by varying a suite of mechanical values according to the variability observed among buildings in Central-Southern Italy. Then, fragility curves are derived aiming at providing a reliable prediction of masonry buildings' seismic performance.

4.2 Dynamic behaviour of URMs

The unsatisfactory performances of URMs, showed under seismic actions, increases attention, in the last decades, on the evaluation of their dynamic behavior. Mechanical characteristics of vertical structures and horizon-

tal ones are the main parameters that influence the dynamic behaviour of URMs. Their role can be investigated through experimental and numerical analysis. Experimental investigations could achieve an-in depth knowledge of masonry buildings. For example, Operational Modal Analysis (OMA) directly evaluates the structural dynamic behavior of a structure allowing an accurate validation of Finite Element models (FE) required by numerical analysis Magenes et al. (2014); Senaldi et al. (2014). Nevertheless, few testing campaigns on full-scale specimens are carried out Brandonisio et al. (2013) Lucibello et al. (2013)Aloisio et al. (2020b), due to several difficulties in their performing. For example, the low-amplitude vibration in operational conditions and the presence of localized mode shapes hinder the estimation of the dynamic response of masonry structures through OMA. The low-amplitude vibration, mainly related to the massive nature of masonry constructions, entails the necessity of adopting sensors of adequate performance in terms of sensitivity and signal-to-noise ratio. Localized mode shapes require installing an adequate number of sensors to achieve a fine discretization of the experimental mode shapes. These difficulties have determined more extensive applications of OMA in reinforced concrete (RC) and steel buildings compared to masonry ones. Therefore, the application of OMA for the identification of the modal parameters of masonry structures as a practice-oriented non-destructive diagnosis technique is limited. Still, dynamic identification using an adequate number of sensors with high-level performance may provide valuable information about the mechanical properties of masonry and the effect of retrofitting interventions. Masonry structures manifest a significant scatter of their mechanical parameters. For URMs, the intrinsic heterogeneity of their features and consequent variety of their mechanical properties require Non Destructive Tests (NDT) or semi-NDT (that give insight into the mechanical properties of a limited area where the tests are executed). However, dynamic tests may ensure comprehensive knowledge into the homogenized mechanical parameters by updating a finite element model using experimental modal parameters (like mode shapes, modal frequencies and damping ratio). The model updating of a masonry structure using the modal parameters estimated from OMA can return an indirect estimation of the Young Modulus, weight and other

structural parameters useful to address and refine structural investigations. As regard numerical investigations, non-linear analysis deliver accurate results on the dynamic behavior of masonry buildings. Nevertheless, they require reliable models for calculating the inelastic response to seismic input of load-bearing masonry structuresMagenes et al. (2014); Moreira et al. (2014), seldom affected by the sensitivity of numerical tools to the input variablesFelice et al. (2017); Whitney and Agrawal (2015). In the light of above, seismic assessment of URMs are sometimes conventional, lacking a solid predictive model of the structural response. Therefore, the dynamic behavior of URMs represents a crucial issue in research for a reliable assessment of their seismic performances.

4.3 Numerical modeling description

The dynamic behaviour of the selected URM (see paragraph 3.4.2) has been appraised through numerical analyses. At this aim, two finite element (FEs) models were developed and implemented in the software package SAP2000. (i) The first FE model attempts to reproduce the local behavior of the floors. A single equivalent beam is introduced with a section equal to the slab portion investigated by the first experimental setup, see Fig. 4.1. In the middle of the equivalent beam, a portion of reinforced concrete models the presence of a flat beams, indicated in purple in Fig. 4.1. The connection with the masonry walls was included in the model introducing linear springs characterized by the stiffness of the supporting walls.

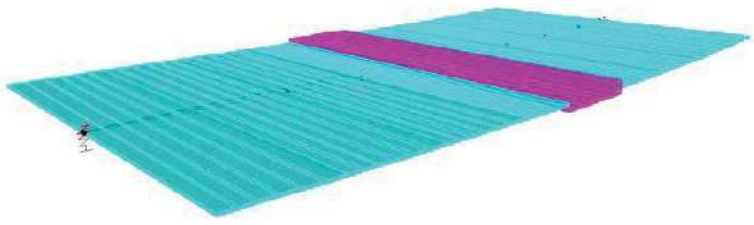

Figure 4.1. View of the numerical model of the equivalent single beam.

(ii) The second FE model aims to grasp the global masonry building,

see Fig. 4.2, (a-b). The masonry elements are represented using a continuum homogenized model with the finite element method, that ensures good results for global analysis of masonry structuresDomaneschi et al. (2019). The slab and the load bearing walls have been assumed as perfect and full connected.

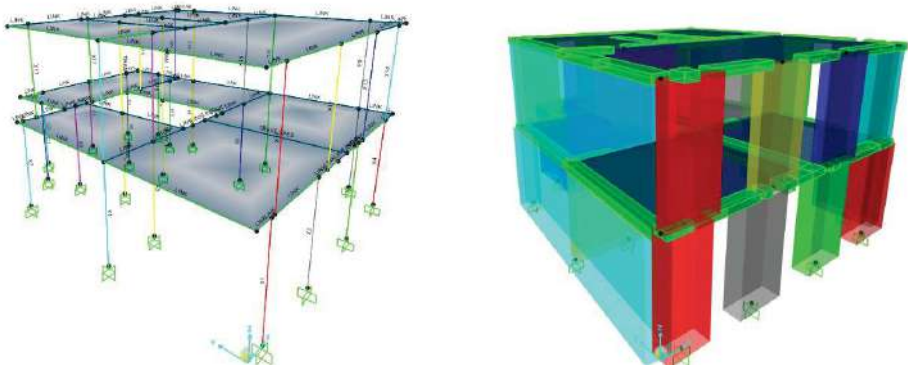

(a) Unifilar view (b) Extruded view

Figure 4.2. Numerical model of the global building

4.4 Ambiental Dynamic Identification

Operational Modal Analysis, OMA Aloisio et al. (2020a); Reynolds et al. (2015), was carried out through the use of ten force-balance mono-axial accelerometers, named SARA Instruments SA10, characterized by a dynamic range higher than 165 dB in the frequency interval 0.1-20 Hz and a 5 V/g sensitivity. The data were sampled at a rate of 200 Hz and the cut-off frequency of the anti-aliasing filter was fixed to 20 Hz. The acquisition system consists of two measurement chains, depicted in Fig. 4.3, each one driven by a master recorder unit and synchronized by a GPS sensor, see Fig. 4.4 (b): (i) the first measurement chain consisted in ten accelerometers located along a row, spaced every 1.05 m, see Fig.4.3 (a) and Fig.4.4 (c), to characterize the global dynamics of the structure; (ii) the second measurement chain consists of four couples of accelerometers, placed at the four corners of the building at the first floor and the remaining couple was located at the middle of the floor, see Fig.4.3 (b) and Fig. 4.4 (a), to identify with high accuracy the mode shapes characterized by a prevalent deformation of the floor.

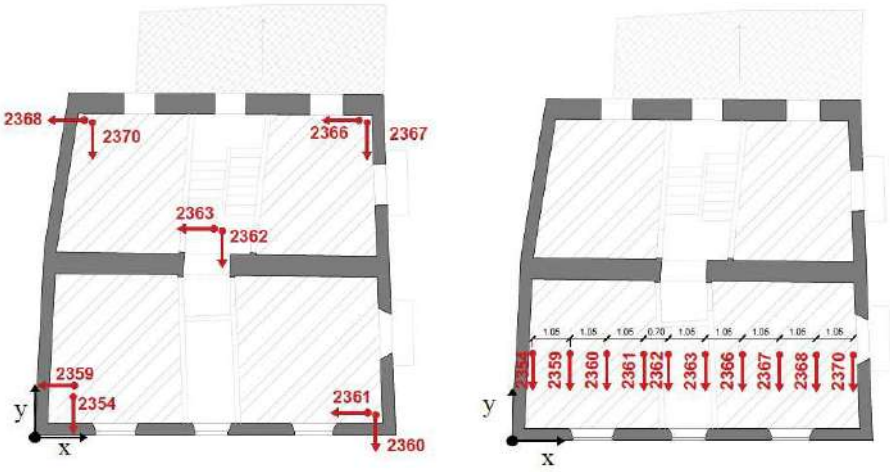

(a) The first setup. (b) The second one.

Figure 4.3. Illustration of the two setups with the measuring direction (indicated by the red rows).

The modal parameters has been estimated from output-only measurements based on the covariance-driven stochastic subspace identification (SSI) method Peeters and De Roeck (2001). The SSI technique represents a classical covariance-driven stochastic realization algorithm, namely the principal component algorithm, also known as covariance-driven SSI algorithm (SSIcov). Stabilization criteria were imposed to graphically verify the stability of the poles as the order of the system increased, see Eq.4.1, 4.2, 4.3:

$$\left| \frac{f_i - f_{i-1}}{f_{i-1}} \right| \leq \delta_f \tag{4.1}$$

$$\left| \frac{\xi_i - \xi_{i-1}}{\xi_{i-1}} \right| \leq \delta_\xi \tag{4.2}$$

$$1 - MAC(\phi_i, \phi_{i-1}) \leq MAC_{thr} \tag{4.3}$$

where f_i, ξ_i and ϕ_i are the natural frequency, damping and mode shape registered for each pole of the i-th order, $i = n_{min} + 1, ..., n_{max}$ from the i-th iteration; the Modal Assurance Criterion (MAC) threshold value is $\text{MAC}_{thr} = 0.02$; $\delta_f = 0.01$ and $\delta_\xi = 0.01$ are the adopted tolerances for the natural frequencies and damping ratios.

Three modes have been identified clearly from the stabilization diagram,

(a) At a corner of the building.

(b) At the middle of horizontal structure.

(c) Along a row.

Figure 4.4. Views of the position of the accelerometers.

which is reported in Fig.4.5. Tab.4.1 summarizes the identified modal parameters.

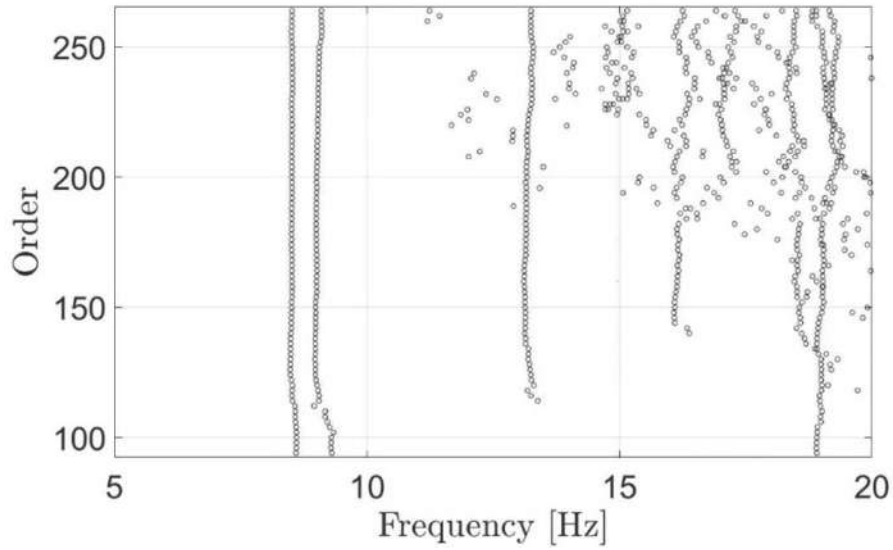

Figure 4.5. Stabilization diagram obtained from SS-I cov analysis on the first setup.

Mode	Frequencies, Hz	Damping ratio, %
1st	8.85	6.49
2nd	9.43	2.17
3rd	12.26	2.90

Table 4.1. Identified modal parameters from the first setup.

The experimental mode shapes from the first setup are depicted in Fig.4.6

4.5 Sensitivity assessment of the dynamic behavior of the structure

The dynamic behavior of the URM has been estimated by varying mechanical properties of walls and floors. In order to curtail the effort of the model updating process, a parametric analysis was performed to address the selection of the parameter for the calibration of the FE models. The parametric analysis involves four mechanical parameters: (i) the elastic modulus of the masonry composed by irregular masonry units, E_m; (ii) the elastic modulus of the masonry composed by clay bricks, E_b; (iii) the elastic

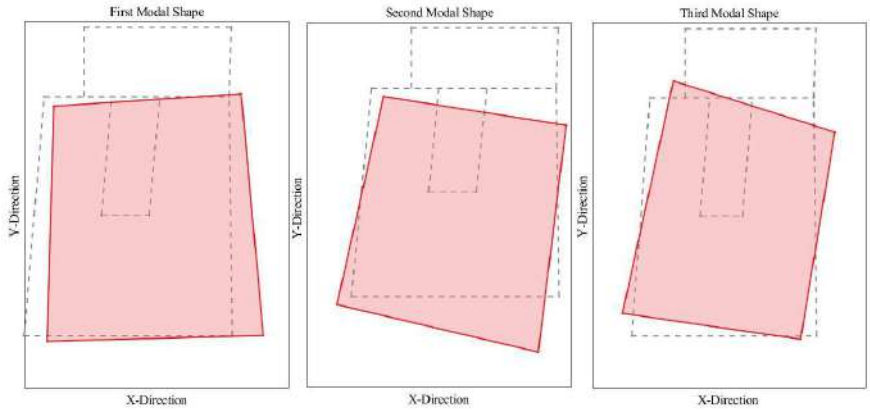

Figure 4.6. Experimental mode shapes.

modulus of the floors for the main direction, E_{s1}, and (iv) the perpendicular direction, E_{s2}. According to the Normative Code and research studies of literatureCapanna et al. (2021), acceptable ranges have been fixed, for each parameter, see Tab.4.2, discretized in 5 spans.

Parameters	**Min. value, MPa**	**Max. value, MPa**	**Mean value, MPa**
E_m	2927.4	5854	4390.7
E_b	1500	3000	2250
E_{s1}	5000	25000	17500
E_{s2}	5000	25000	17500

Table 4.2. Ranges of values considered for the sensitivity analysis.

By varying the mechanical properties in the ranges indicated, the results of the numerical analyses are expressed in terms of frequencies and modal shapes to grasp the influence on the linear dynamic behaviour. The histograms in Fig.4.7 manifest the scatters around the objective function F_{obj} average value, frequency $F_{frequency}$ and modal shape $F_{modalshapes}$ respectively.

The sensitivity analysis highlights the influence of elastic moduli of masonries on the natural frequencies and the modal shapes of the building, mainly. This result justifies the choice of seizing the local behavior of the structure based on the mechanical characteristics of the horizontal structures. Starting from these evidences, the model updating process was set in two phases: (i) the first model updating focused on the local behavior of the building to grasp the horizontal structure influence, involving the elastic modulus E_{s1} of the slab in the in-plane direction, the elastic modulus

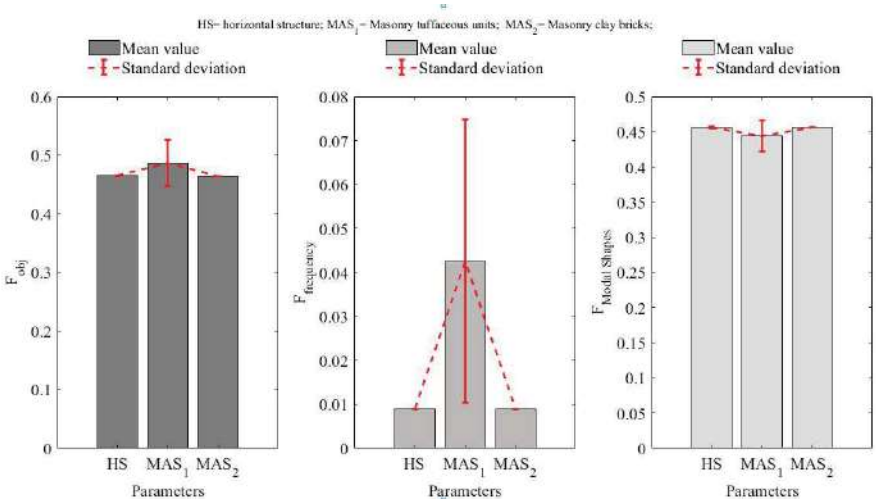

Figure 4.7. Histograms of the modal results by varying: the elastic modulus of horizontal structures, HS; the elastic modulus of irregular masonry units, MAS1; the elastic modulus of brick masonry, MAS2.

E_{s2} in the out-plane direction and the section height of the slab; (ii) the second model updating involved the mechanical parameters of the masonry, the elastic modulus E_m and the specific weight γ_m, focusing on the global behavior of the building.

4.6 Model Updating process of the numerical model

To obtain reliable predictions of the structural behavior, the model updating process attempt to calibrate the finite element model of a structure to match numerical and experimental results Girardi et al. (2018). The model updating process lays on the solution of a constrained optimization problem related to an objective function, that, generally, considers the difference between experimental and numerical natural frequencies and mode shapes of structures. The following selected objective function, see Eq.4.4, measures the distance between the estimated modal parameters and the numerical ones Friswell and Mottershead (1995).

$$C = \sum_{i=1}^{M} \gamma_i \left(\frac{\omega_i^m - \omega_i^c}{\omega_i^m} \right)^2 + \beta \sum_{i=1}^{M} (1 - diag(MAC(\Phi_i^m, \Phi_i^c))) \qquad (4.4)$$

where the apex $(*)_m$ indicates a measured variable and the apex $(*)^c$ a calculated variable; ϕ_i is the mode shape vector; M is the number of modes;

MAC is the modal assurance criterion Allemang and Brown (1982); and γ_i and β are the weighting factors, set equal to 1.00.

4.6.1 Model updating of local behavior

The modal parameters estimated from the second setup are used for the model updating of the floor model. The elastic modulus E_{s1} and E_{s2} of the slab, referred to the in-plane direction and the out-of-plane direction respectively, were assigned according to data of diagnostic campaign on local built-up. The range of both the elastic moduli was equal to 5000-25000 MPa. The height of the section, H, ranges from 0.025 m to 0.05 m. The optimization process was carried out considering the function in Eq.4.4 as the objective function to minimize, and returned a value of 8250 MPa for E_{s1}, 7500 MPa for E_{s2}, and the value of 0.025 m for the height of the slab section. The experimental frequency of the first mode was equal to 8.85 Hz; the numerical one, after the model updating, was equal to 8.83 Hz. The MAC value, evaluated between numerical and experimental mode is equal to 0.84, proving a consistent correspondence. The mechanical and geometric characteristics found were introduced in the global finite element model before to carry out the second phase of the model updating.

4.6.2 Model updating of the global behavior

The modal parameters estimated from the first setup are used for the model updating of the global structural model. An acceptable range for the values of the Elastic Moduli of the masonry were set and investigated. The minimum values of the variation ranges of the mechanical parameters were set in accordance with the Italian Guidelines. Based on the scatter of the mechanical parameters of the irregular stones' material, the maximum values are set slightly higher than the Normative vales. The minimum value of the Elastic Modulus of the masonry was set to 2000 MPa and the maximum values was set equal to 6000 MPa arbitrarily; the elastic modulus E_b of the two bricks alignments ranges between 1200 to 2000 MPa. The specific weight of the irregular masonry units γ_mm varies into the range 12/24 kN/m_3. As in the first parametric identification, the chosen objective function was that in Eq.4.4. The comparison between the numerical

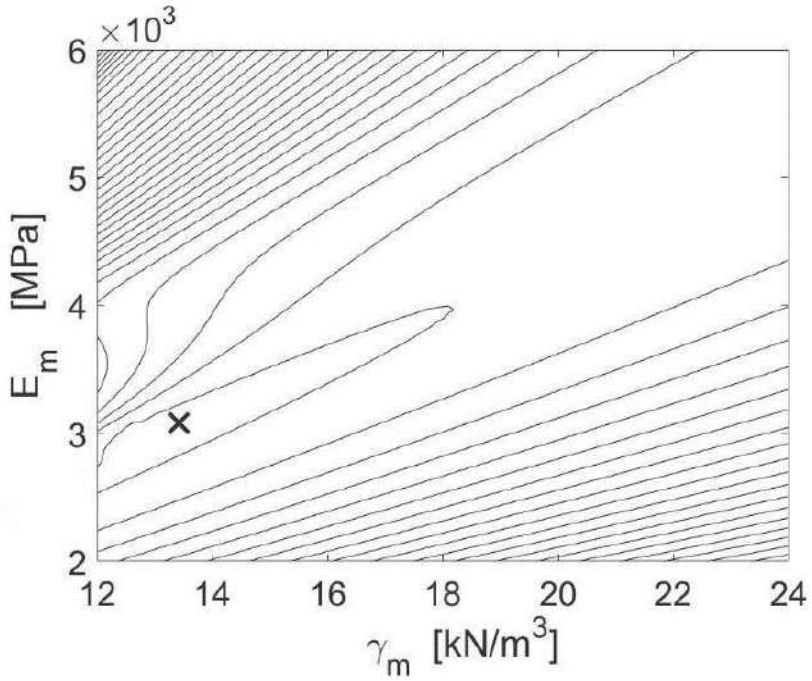

Figure 4.8. Contour plot of the objective function C in the range of variation of parameters E_m and γ_m, at the identified value of E_b

and experimental frequencies of the updated model, called respectively f_e and f_n, and the experimental damping ratio ψ_e, are reported in Tab.4.3.

Mode	f_e**, Hz**	f_n**, Hz**	**Discrepancy, %**	ψ_e [%]
1^{st}	8.85	8.53	3.61	6.49
2^{nd}	9.43	9.30	1.37	2.17
3^{rd}	12.26	13.25	-8.07	2.90

Table 4.3. Comparison between numerical and experimental results.

The optimization process led to a value of 3000 MPa for E_m, 1980 MPa for E_b, and a specific weight of the masonry material γm equal to 13 kN/m^3. The estimated value of the specific weight is very low compared to the expected values for masonry, beyond 18 kN/m^3. This finding reveals that traditional masonry buildings exhibit a significant scatter of the mechanical properties of existing masonry. Specifically, traditional masonry can be characterized by high porosity, evidence of poor masonry quality despite the apparent good texture of the exposed faces. Fig.4.8 reports the contour plot of the objective function for the parameters of masonry composed by irregular masonry units.

The mode shapes revealed by the numerical analysis after model up-

dating process are depicted in Fig.4.9.

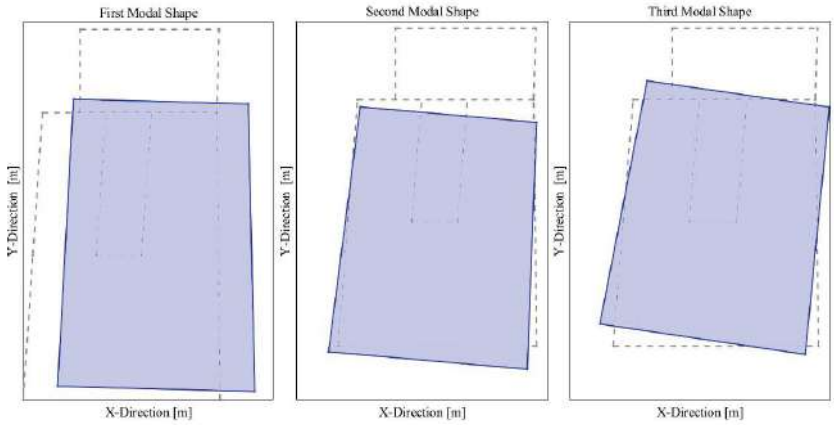

Figure 4.9. Numerical mode shapes after the model updating.

Fig.4.10 reports the MAC values evaluated for the numerical and experimental modes: the diagonal values demonstrate a satisfactory correspondence.

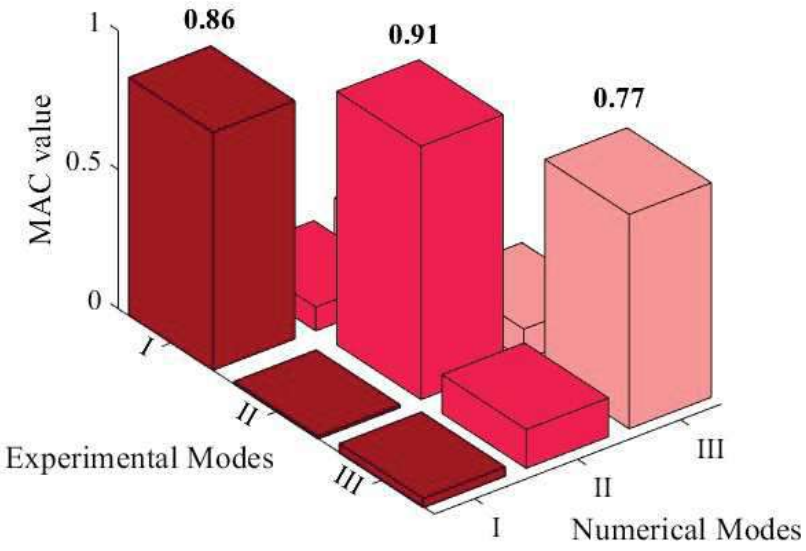

Figure 4.10. MAC representation between experimental and numerical modes.

4.7 Investigation on the role of the horizontal structure in non-linear dynamic field

The sensitivity analysis show the prevalent influence of the Elastic Modulus of the masonry on the dynamic behavior of the URM under environmental

conditions. This paragraph aims to grasp the influence of the floor stiffness on the non-linear dynamic condition. At this aim, non-linear numerical analyses were performed using the updated FEM model. The floor typology of the URM consists of steel joists and brick tiles. To mirror the entire class of masonry buildings, other two floor typologies has been evaluated: a wooden floor consisting of timber joists supporting a timber deck and a traditional RC floor with hollowed tiles. Tab.4.4 reports the Young Modulus value E and the Shear Modulus value G for the selected floor typologies (reported in 3.3), where: (i) HS1 indicates the investigated floor; (ii) HS2 the wooden floor with joists and one layer of timber planks; (iii) HS3 the Reinforce concrete floors.

Floors Typology	**E, MPa**	**G, MPa**
HS1	8250	3437.5
HS2	26	10
HS3	26000	14400

Table 4.4. Mechanical characteristics of floor typologies.

The estimation of the equivalent elastic modulus is based on a mechanical analogy. Specifically, three numerical models different were developed for the typologies of floors: (i) HS1 is the label of the numerical model of the investigated building; (ii) HS2 is the label of the numerical model with timber wooden floors; (iii) HS3 is the label of the numerical model with RC floors. Then, the equivalent elastic modulus has been evaluated for an equivalent slab characterized by evaluated thicknesses, in order to obtain the same in-plane stiffness of the refined FE model of the floor. The choice of this mechanical equivalence aimed at lightening the computational burden of the nonlinear dynamic analyses, by using a single equivalent shell element. Incremental dynamic analysis have been performed resorting to the modelling approach descripted in the paragraph 3.4.2. As a first step, the analyses provide the story drifts under different earthquake multiplication factors from 0.1 to 1 in the X and Y directions, as shown in Fig.4.11.

Then, the outcomes of the nonlinear dynamic analyses are used to estimate the failure probability by comparing the estimated drifts with the target drifts associated with the exceeding of a given limit state, according to Eq.4.5 Agency (1997):

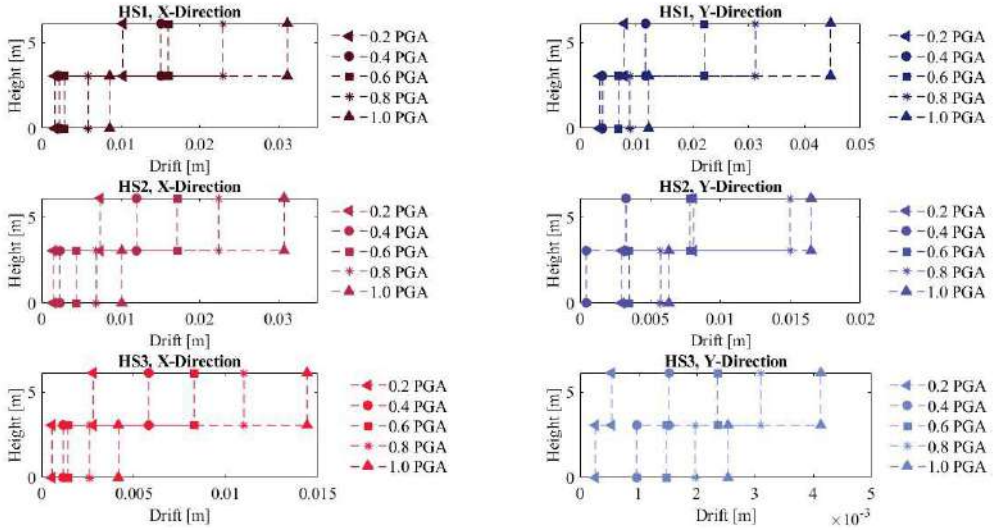

Figure 4.11. Story drifts under different earthquake moltiplication factors for the two main directions, at varying floor typology.

$$S_{d4} = D_u \tag{4.5}$$

Where D_u is the ultimate displacements, defined according to the Normative dispositions. The probability of collapse, P_c, descends from the estimation of the standard normal cumulative distribution function Φ, as expressed in Eq.4.6, used to fit the fragility function with data collected from Non-Linear Dynamic Analysis, Baker (2013):

$$P(C|IM = x) = \Phi\left(\frac{ln(x/\theta)}{\beta}\right) \tag{4.6}$$

Where P(C—IM=x) is the probability of structure collapse due to a ground motion IM=x, ϕ indicates the standard normal cumulative distribution function (CDF), θ is the median of the fragility function (the IM level with 50% probability of collapse), and β is the standard deviation of the ln IM. The parameters θ and β were estimated, following an iterative procedure Aloisio and Fragiacomo (2021) by varying the parameters until a certain likelihood function is maximized, see Eq.4.7.

$$\{\hat{\theta}, \hat{\beta}\} = argmax_{\hat{\theta},\hat{\beta}} \sum_{j=1}^{m} \left[ln\Phi\left(\frac{ln(IM_i/\theta)}{\beta}\right)\right] + [n-m]ln\left[1 - \Phi\left(\frac{ln(IM_{max}/\theta)}{\beta}\right)\right] \tag{4.7}$$

where the symbol ˆ denotes an estimated parameter, $\Phi()$ the standard normal distribution PDF, n the number of ground motion used in the analysis, m the number of ground motions that caused collapse at IM levels lower than IM_{max}, $\Phi()$ the standard normal distribution CDF. Fig.4.12 shows the mean drift values estimated from the response to the seven earthquakes under a specific peak ground acceleration, PGA, value. The X-direction is stiffer than the Y one due to the geometric configuration of the building, characterized by stiffer walls in the Y direction. The effect of the floor stiffness is the redistribution of the internal stresses between orthogonal walls. There is no marked difference between the drift and displacement response in the X direction using the HS1 and HS2 floors. Conversely, the use of the HS2 floor produces a significant reduction of the story drift in the Y direction, compared to the timber floor, higher than 200%. This increment of the story drift value is evident at higher PGAs due to the activation of the plastic hinges. Therefore, the increment of the equivalent elastic modulus between HS1 and HS2 produces a more than 200% decrement of the story drift. The stiffening of the floor by tot percentage does not determine the modification of the response in the X direction, since the floor can be considered stiff due to the reduces free-length in that direction. The comparison between HS1 and HS2 start manifesting if the floor free length is higher than 4 m. If the floor free length is lower than 4 m the effect of the floor typology does not arise, and the displacement associated with a timber floor does not differ with those related to the use of a traditional floor with steel joists and a RC slab with a thickness lower than 0.05 m. If the floor free length exceeds 4m, different floor typologies, even if both are considered not adequately stiff, produce a significant difference in the story drift.

Conversely, using an RC floor made by a slab with more than 0.05 m thickness causes evident effects in both the X and Y direction. Specifically, the use of the HS3 floor determines a reduction of the story drift equal to approximately 100% in both directions. Despite the evident advantages of using rigid diaphragms, recent research shows that substituting traditional wooden floors with rigid diaphragms, i.e., RC floors, can cause unwanted consequences such as cracks on the edges of the two materials or in the

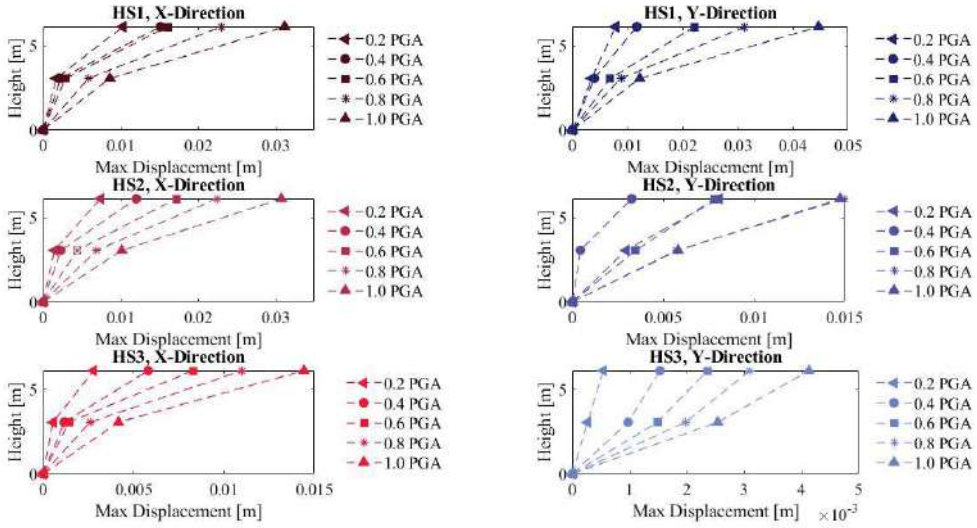

Figure 4.12. Mean drifts values under different earthquake multiplication factors for the two main directions, at varying the floor typology.

worst scenario, disintegration and collapse of the masonry walls Lulić et al. (2021). The use of floors with an equivalent elastic modulus higher than contributes to reducing the inter-story drifts in both directions, even if the floor free length is lower than 4m in the X-direction. Next to reducing the story drift, the use of floors with adequate in-plane stiffness, like the HS3, contributes to regularizing the displacement response along with the height, as evidenced by Fig.4.12. The reduction of the story drift related to using a floor with higher in-plane stiffness determines the reduction of the failure probability. Fig.4.13 shows the fragility functions of the considered building in the two directions. Fragility curves refer to the collapse limit state to better grasp the role of in-plane stiffness of floors, that is negligible for other limit states. Although the HS2 floor is considered not adequately stiff, it significantly reduces the collapse probability compared to HS1. Besides, as expected, the HS3 floor exhibits the most satisfactory seismic performance even at higher PGA values in both the X and Y directions.

4.8 Conclusions

The seismic assessment of URMs is sometimes conventional due to the lack of a solid predictive model of its structural response. Therefore, understanding their dynamic behavior represents a crucial issue in research

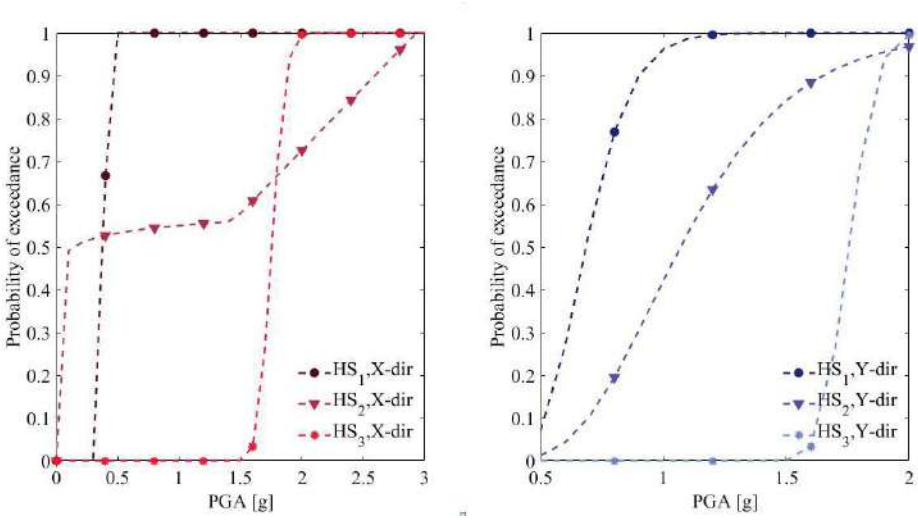

Figure 4.13. Fragility curves of buildings for the two main directions of the building, at varying the floor typology.

for a possible transition between conventional design approaches to ones with a more appropriate mechanical base. The current research attempts to delve into the dynamic behaviour of ordinary residential buildings to strengthen the knowledge of the seismic performance of existing heritage through experimental and numerical analyses. A case study shows the combined application of OMA and a model updating estimates the modal parameters of a traditional masonry residential building. At this aim, an in-depth experimental campaign is carried out through two ambient vibration tests of a representative URM. A parametric assessment addresses the choice of the parameters to be involved in the model updating, reducing the numerical effort. Still, the results of the parametric analysis highlights the more marked influence of the mechanical characteristics of masonries on the linear dynamic response, compared than the floors ones. The results of the dynamic experimental campaign allow to refine and to update numerical models. The model updating process is carried out in two phases, to seize local and global dynamic responses. The diagonal MAC values evaluated between numerical and experimental modes were equal to 0.86, 0.91, and 0.77 respectively, demonstrating the reliability of the numerical model to grasp the seismic performance of the structure. Starting from the achieved dynamic characterization, the influence of the floor has been delved on the non-linear dynamic behavior of masonry buildings by varying a suite of mechanical values according to the variability observed among

buildings of the case study: a wooden floor consisting of timber joists supporting a timber deck, HS1; a floor made of steel joists and brick tiles HS2, and a traditional RC floor with hollowed tiles, HS3. The displacements' trend along the height of the building, derived via non-linear incremental dynamic analysis, evidences the notable role of the floor's stiffness in the non-linear dynamic behavior of the building. There is no marked difference between the drift and displacement response in the X direction using the HS1 and HS2 floors, considering that the X-direction is stiffer than the Y one. Conversely, the use of the HS2 floor produces a significant reduction of the story drift in the Y direction, compared to HS1 floor, higher than 200%. The stiffening of the floor does not determine the modification of the response in the X direction, since the floor can be considered stiff due to the reduces free-length in that direction. The comparison between HS1 and HS2 start manifesting if the floor free length is higher than 4 m. Instead, using an RC floor made by a slab with more than 0.05 m thickness causes evident effects in both the X and Y direction: a reduction of the story drift equal to approximately 100% is revealed in both directions, even in the case of free length lower than 4 m in the X-direction, regularizing the displacement response along with the height, and thus reducing failure probability. Lastly, fragility functions were estimated to evidence the influence of stiffness floors in terms of failure probability under extremely severe damage state. Although the HS2 floor is considered not adequately stiff, it significantly reduces the collapse probability compared to HS1. Besides, as expected, the HS3 floor exhibits the most satisfactory seismic performance even at higher PGA values. The derived fragility curves reliably predict masonry building' failure probability, revealing useful information foresee the influence of strengthening interventions of floors on ordinary masonry buildings. The evidences of this study provide a starting point to drive the following research activity. In fact, the extensive investigations deeply analysed the dynamic behaviour of URMs. The obtained results highlighted the main structural characteristics that influence the dynamic performance, up to facilitate a first choice of the parameters for the simplified vulnerability assessment method.

4.9 Acknowledgements

The study presented in this chapter was published in the Journal *Buildings*, MDPI:

"Operational Modal Analysis and Non-Linear Dynamic Simulations of a Prototype Low-Rise Masonry Building", I. Capanna, R. Cirella, A. Aloisio, F. Di Fabio, M.Fragiacomo, Buildings, 2021, 11(10): 471, 10.3390/buildings1100471.

Empirical Method for Seismic Assessment of URMs

Chapter abstract

The chapter presents a simplified vulnerability assessment method for URMs based on the evaluation of few structural parameters, which can be determined from visual inspection and a geometry survey. The empirical approach proposed, focused on in-plane response of masonry walls, provides a vulnerability index, which is evaluated as the weighted sum of ten parameters markedly affecting the seismic performance. The reliability of the method is investigated through an application on fifteen buildings located in the municipality of Cittareale, in the inner Central Italy, severely damaged by the 2016 earthquake sequence. The mean damage and damage probability distributions were predicted for each building using the proposed method. Then, fragility functions were estimated from the results of non-linear static analysis, and the damage probability distributions were derived. The capability of the simplified method to foresee the damage probabilities was confirmed by a comparison between the damage probability distributions obtained through the different approaches. Finally, the proposed method was compared against other predictive approaches available in literature, showing a satisfying agreement.

5.1 Introduction

The inherent fragility of unreinforced masonry constructions generally leads to extended damage under strong earthquake ground motions. The frequent seismic events occurred in the last decades, highlighted the need to enhance the structural safety of the building heritage, especially in earthquake prone areas. Unreinforced masonry buildings experience considerable damage due to the brittleness of the masonry material, the ageing of the constructions and often the lack of anti-seismic design criteria. Therefore, screening the seismic performance of the building heritage is useful to determine the seismic fragilities before an earthquake occurs. Vulnerability assessment on large scale application involves from dozens to hundreds of buildings. Numerical methods assess the seismic vulnerability accurately if an in-depth characterization of the structure, in terms of mechanical parameters and structural details, is achieved. Furthermore, seismic vulnerability assessment via numerical analysis is very expensive being highly time consuming, leading to a tricky application on a large scale. Thus, simplified vulnerability methods seek to overcome the application effort on a large scale, relying only on few structural parameters known from engineering judgements or via quick evaluations. The chapter presents a novel empirical predictive vulnerability method focused on in-plane seismic response of masonry buildings. The predictive method was applied to buildings located in the municipality of Cittareale, in the inner Central Italy, recently hit by an earthquake ground motion. The seismic behaviour of the buildings was also investigated using a numerical approach: static non-linear analysis was performed to estimate the fragility functions and the correlated damage probability distributions. The reliability of the predictive method to foresee damage probability distributions is confirmed by a comparison with the damage probability distributions derived from the numerical method. Finally, the main advantages and possible developments of the proposed approach are discussed.

5.2 A Novel Vulnerability Predictive Method

Several procedures may be found in literature to assess the out-of-plane vulnerability quickly, by predicting the local damage mechanisms**??**. To the authors' knowledge, less information is available in literature to simplified in-plane vulnerability assessment. In this paper, a method for the in-plane seismic behaviour of masonry buildings is, which consists of two phases: (i) the assessment of the vulnerabilities for each masonry wall of the analysed building, in each main direction; (ii) the derivation of a global index representative of the entire building vulnerability from the masonry walls' indices. The simplified assessment involves ten parameters aimed to capture the in-plane behaviour of masonry walls that depends mainly upon mechanical properties such as shear strength, and geometrical characteristics of more difficult appraisal. The size and the position of openings affect damage and failure modes of the vertical masonry panels**?**, namely the piers, and the seismic vulnerability of walls, as shown by past experimental tests **?** and on-site inspections after past seismic events **?**. Several studies attempted to capture the influence of the openings on the masonry wall behaviour, providing estimation of the stiffness and strength reduction of the wall, based on size and position of the openings **????**. The parameters of the proposed approach are listed in Table 5.1. Three classes of growing seismic vulnerability are introduced, from A to C, with the corresponding scores equal to 0, 50 and 100, respectively. For each parameter, a weight is assigned for the relative importance among the ten parameters on the global in-plane behaviour.

n°	**Parameter of the wall**	**Weight**
1	Quality of the masonry	1.00
2	Amount of openings	0.50
3	Behaviour in plan	0.80
4	Behaviour in elevation	0.75
5	Type of opening	0.20
6	Stiffness of the spandrel beams	0.40
7	Tensional state in plan	0.60
8	Tensional state in elevation	0.60
9	Position of the wall	1.25
10	Site effects	1.05

Table 5.1. Proposed predictive method.

5.3 Description of the parameters

In this section, the description of the ten parameters listed in Table 5.1 and their empirical evaluations, is reported.

5.3.0.1 Parameter 1, P1: quality of the wall masonry

This parameter evaluates the mechanical properties of masonry in terms of material and units' layout. The three vulnerability classes are defined as follow:

- CLASS A: clay bricks filled with lime mortar or concrete bricks filled with cementitious mortar;
- CLASS B:split stone masonry with good layout and good quality of the mortar;
- CLASS C: irregular stone layout.

5.3.0.2 Parameter 2, P2: amount of openings

The parameter P2 evaluates the size of the openings, with a ratio between the sum of the piers' lengths, l_{pi}, and the wall geometric length, l_w, see Eq.5.1:

$$P_2 = \frac{\sum(l_{pi})}{l_w} \tag{5.1}$$

- CLASS A: P2 $>$ 0.75;
- CLASS B: 0.5 $<$ P2 $<$ 0.75;
- CLASS C: P2 $<$ 0.5;

5.3.0.3 Parameter 3, P3: wall behaviour in plan

Two parameters, defined as $P_{3,1}$ and $P_{3,2}$, consider the effect of the openings position on the seismic wall performance. In addition to the resistant area, the resistance strength of a masonry pier depends on a coefficient related to its geometrical shape. The parameter $P_{3,1}$ is defined as the ratio between the max length of the piers and the resistant length of the wall (sum of

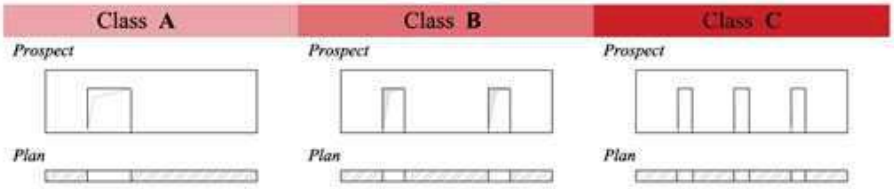

Figure 5.1. Illustration of the vulnerability classes for the parameter P_3.

piers' lengths), see Eq.5.2. The parameter $P_{3,2}$ is defined as the ratio of the difference between the max length and the minimum length of the piers, and their average length value, see Eq.5.3.

$$P_{3,1} = \frac{\max(l_{pi})}{\sum(l_{pi})} \tag{5.2}$$

$$P_{3,2} = \frac{l_{max} - l_{min}}{l_{average}} \tag{5.3}$$

- CLASS A: $P_{3,1} > 0.75$ and $P_{3,2} > 0.7$. The opening is located on a side of the wall, creating considerably different piers in terms of length, like a slender and a squat pier. This class offers the highest shear resistance, provided by the squat pier;
- CLASS B: $0.375 < P_{3,1} < 0.75$ and $P_{3,2} < 0.7$. The position of the openings engenders piers, with different lengths, that offer comparable resistance;
- CLASS C: $P_{3,1} < 0.375$ and $P_{3,2} < 0.7$. The numerous openings lead to slender piers, yielding the lowest shear resistance.

The vulnerability classes are illustrated in see Fig. 5.1.

5.3.0.4 Parameter 4, P4: behaviour of the wall in elevation

Indirectly, the parameter P_4 captures the vertical misalignments of the openings that lead to localized concentrations of strength and displacement demands **?**, starting from the in-plane behaviour evaluation for each floor, according to point 3, see Eq.5.4.

$$P_4 = \Delta P3_{y,k} = P3_y - P3_k \tag{5.4}$$

where $y = k + 1$

- CLASS A: $P_4 = 0$ or $P_4 < 1$ class. This class shows a regular behaviour along the height of the masonry wall;
- CLASS B: $P_4 < 2$ classes.The wall exhibits a not negligible reduction of the shear resistance and stiffness in elevation, leading to a higher inter-story drift.
- CLASS C: $P_4 > 1$ class.This class entails a remarkable increase of stiffness along the height, causing a localized collapse, also called soft floor, leading to a brittle seismic behaviour. The illustration of the vulnerability classes is reported in Fig. 5.2.

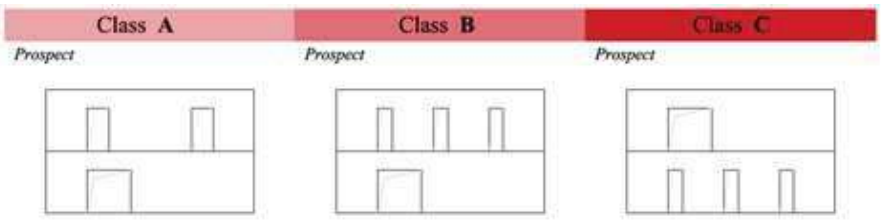

Figure 5.2. Illustration of the vulnerability classes for the parameter P_4.

5.3.0.5 Parameter 5, P5: type of the openings in the wall

The parameter P_5 deals with the type of openings (doors or windows) that affect the height of the piers. The vulnerability classes are defined as:

- CLASS A: windows are predominant. The wall consists of squat piers;
- CLASS B: windows and doors are comparable. The wall consists of squat and slender piers;
- CLASS C: doors are predominant. The wall consists of slender piers.

5.3.0.6 Parameter 6, P6: stiffness of the spandrel beams

The parameter P_6 considers the spandrels' properties that affect the strength degradation and the walls' lateral resistance, influencing the masonry piers' coupling effect Capanna et al. (2021).

- CLASS A: presence of reinforced concrete or steel ring beams;

- CLASS B: presence of either a lintel characterized by a good texture of masonry, or a tension-resistant element;

- CLASS C: lack of tension-resistant elements and brittle masonry.

5.3.0.7 Parameter 7, P7: tensional state of the wall in plan

The tensile strength V_R benefits from the gravity load in the pier. Nevertheless, a considerable gravity load could trigger a collapse for exceedance of the compression strength due to seismic action. The parameter P_7 assesses the tensional state generated by gravity loads from to horizontal structures, see Eq. 5.5.

$$P_7 = \frac{\gamma_{slab} \cdot i_s}{t_m \cdot f_m} \tag{5.5}$$

where γ_{slab} is the specific weight of the horizontal structure, i is its influence length, t is the wall thickness and f_m is the compressive resistance of the masonry.

- CLASS A: $0 < P_7 < 5$ %. The tensile strength benefits from the gravity load.

- CLASS B: $5 < P_7 < 10$ %. The tensional state due to gravity load is considerable.

- CLASS C: $P_7 > 10$ %. The tensional state due to gravity load could trigger a collapse, under seismic action, due to attainment of the compression resistance.

5.3.0.8 Parameter 8, P8: tensional state in elevation of the wall

P_8 accounts for the tensional state due to the load of the upper floors. The vulnerability classes are defined as:

- CLASS A: $0 < P_7 < 5$ %, walls with gravity load due to wooden or steel floors and without upper walls;

- CLASS B: $5 < P_7 < 10$ %, walls with gravity load due to wooden or steel beams floors and upper walls;

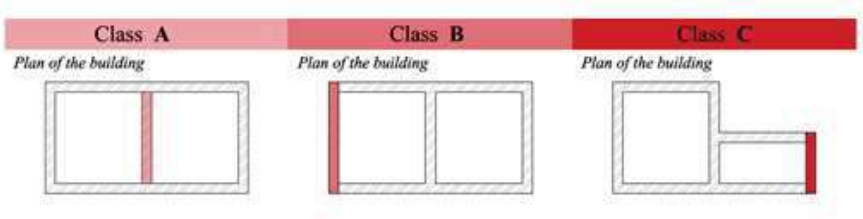

Figure 5.3. Illustration of the vulnerability classes for the parameter P_9.

- CLASS C: $P_7 > 10$ %, walls with upper walls and gravity load due to masonry vaults or reinforced concrete slabs.

5.3.0.9 Parameter 9, P9: position of the wall

Irregular shapes of buildings could exarcebete torsional phenomena under an earthquake action. Stiff floors affect the horizontal force's distribution among the walls, taking into account also the distance between mass and stiffness centroid. Conversely in the case of flexible horizontal structures, torsional phenomena are more negligible: walls' position is not a vulnerability source. The vulnerability classes, illustrated in Fig. 5.3, are defined as:

- CLASS A: the wall is located on an inner position;
- CLASS B: the wall is located on an exterior position;
- CLASS C: the wall is located on a corner position. The irregular shape of the building exacerbates possible torsional rotations of the buildings and stress concentrations for the wall.

5.3.0.10 Parameter 10, P10: site effects

The parameter P_{10} evaluates the soil and topographic conditions of the building. The vulnerability classes are defined based on the internal friction angle and soil type:

- CLASS A: rock soil with internal friction angle less than 15°. The site effects are absent.
- CLASS B: coherent soil, with ground natural slope > 15°.

- CLASS C: incoherent or heterogeneous soil and ground natural slope $> 15°$. The subsoil conditions lead to a significant seismic demand amplification.

5.3.1 Calibration of the Parameters' Weight

In this section, the relative influence of the parameters on the in-plane behaviour of walls is investigated. The wall behaviour can be assessed by defining a mechanical index I_M, see Eq. 5.6.

$$I_M = \frac{V_R}{V_S} \tag{5.6}$$

where V_R is the shear strength of the pier for diagonal cracking failure criterion and V_S is the horizontal earthquake force, evaluated from the elastic spectrum in acceleration for the proper vibration period of the wall. The following equation evaluates the ultimate strength, according to the Italian Design Code (Ministerial Decree of Public Works), see Eq. 5.7.

$$V_R = \frac{A \cdot 1.5 \cdot f_{vd0}}{\xi} \cdot \sqrt{(1 + \frac{\sigma_0}{1.5 \cdot f_{vd0}})} \tag{5.7}$$

where A signifies the resistant area of the wall, f_{vd0} is the shear strength with no axial force, σ_0 is the average tensional state, equal to the ratio between the gravity load and the area of the section, and ξ is a coefficient related to the pier geometrical ratio L/h between the width and the height of the pier. For each parameter of the predictive approach and for each vulnerability class, the mechanical index I_M has been evaluated. The weights cw have been established in proportion to the maximum discrepancy Δ between the maximum and minimum value among vulnerability classes, $I_{M,max}$ and $I_{M,min}$ respectively, for each of the ten parameter, see Eq. 5.8:

$$cw = \frac{\Delta}{0.67} = \frac{\frac{I_{M,max} - I_{M,min}}{I_{M,max}}}{0.67} \tag{5.8}$$

The assigned weights w have been derived from the calculated cw and rounded up and down, as reported in Table 5.2. Equation 5.9, empirically derived, is used to evaluate the vulnerability index for each wall, I_{Vw}, floor to floor (first summation), as the weighted sum of the ten parameters,

n	class A	class B	class C	Delta	cw	w
1	22.34	9.06	7.36	0.67	1.00	1.00
2	1.97	1.65	1.32	0.33	0.50	0.50
3	25.26	16.69	11.73	0.54	0.80	0.80
4	9.58	7.78	4.82	0.50	0.74	0.75
5	11.98	11.25	9.83	0.22	0.33	0.30
6	7.52	5.86	5.27	0.30	0.45	0.40
7	6.42	4.91	2.86	0.42	0.62	0.60
8	6.42	4.91	2.86	0.42	0.62	0.60
9	3.70	0.73	0.52	0.86	1.28	1.25
10	5.07	4.26	1.49	0.71	1.05	1.05

Table 5.2. Derivation of the weights for each parameter.

related to the three classes of growing vulnerability (from A to C), with the different scores associated c_i set equal to 0, 50 and 100 respectively (second summation):

$$I_V = \frac{n + 4.65}{6.65} \sum_{l=1}^{n} \sum_{1=1}^{10} (\frac{c_i \cdot w_i}{} 715) \tag{5.9}$$

where n is the number of floors and w_i are the assigned weights. The number 715 is the maximum value of the sum of the weighted parameters for the scores of the class C (equal to 100). Thus, I_{vw} results as the normalised value, varying from 0 to 1.00. The vulnerability index of the building, I_V, is assessed, for the main directions (x and y direction), as the sum of the walls' index weighted on their geometric area, A_m, see Eq. 5.10:

$$I_V = \frac{\sum_{j=1}^{m} I_{Vwm} \cdot A_m}{A_{tot}} \tag{5.10}$$

where m is the number of walls and I_{Vwm} is the vulnerability index for each wall, A_{tot} is the sum of the walls' resistant area, for the reference direction.

5.4 Discrete damage distributions and fragility curves through numerical results

The numerical results obtained via non-linear static analysis reported in the chapter 3, are herein used to derive discrete damage distributions and fragility curves for each structures of the buildings'sample. Standard normal cumulative distribution function ϕ was used to estimate the fragility

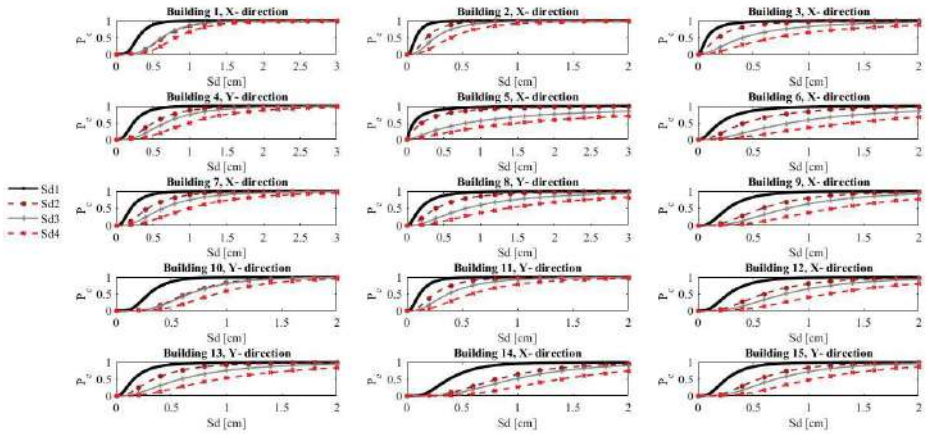

Figure 5.4. Fragility curves of buildings, referred to the direction with a lower seismic safety index.

function, as expressed in Eq. 5.11:

$$P(d_s|S_d) = \Phi\left(\frac{ln(S_d/\bar{S_{ds}}}{\beta_s}\right) \tag{5.11}$$

where d_s is the displacement at the threshold of damage state, $\bar{S_{ds}}$ is the median value of spectral displacement at d_s, bds is the standard deviation of the natural logarithm of spectral displacement at a certain damage state d_s. Expressions, reported in Equations 5.12, provide the limit damage state d_s, proposed by Lagomarsino and Giovinazzi (2006):

$$\begin{aligned} &(Sligth\ damage) && d_{s1} = 0.7D_y \\ &(Moderate\ damage) && d_{s2} = 1.5D_y \\ &(Severe\ damage) && d_{s3} = 0.5(D_u + D_y) \\ &(Extremely\ severe\ damage\ or\ collapse) && d_{s4} = D_u \end{aligned} \tag{5.12}$$

D_y signifies the yielding displacement and Du the ultimate displacement of the equivalent SDOF system, respectively, determined with push-over analysis. Fig.5.4 displays the fragility curves derived for each building.

Later, damage probability histograms were obtained for the spectral displacement required for the LS3 value to compare with the damage discrete distribution provided by the predictive method results. The Eq.5.11 was modified as reported in Eq.5.13:

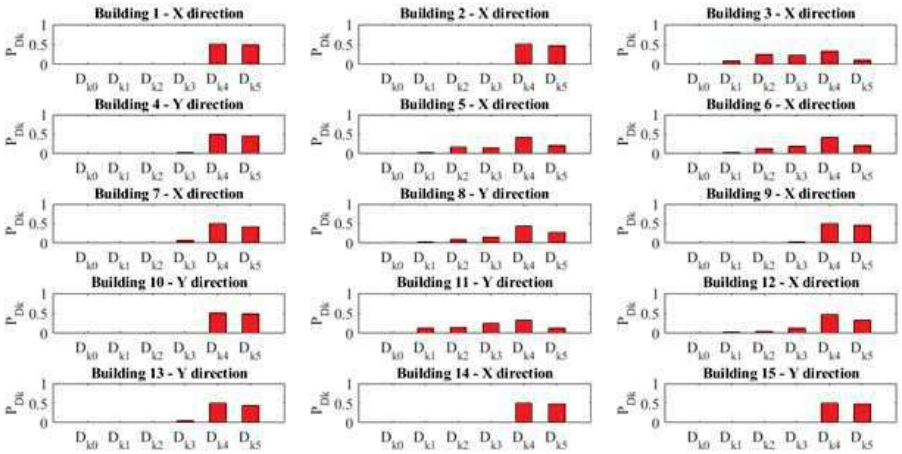

Figure 5.5. Damage discrete distribution referred to the direction with the minimum safety factor, for each building.

$$P(d_{sk}|D_{dmax}) = \Phi\left(\frac{ln(D_{max}/\bar{S_{dsk}})}{\beta_s}\right) \tag{5.13}$$

where k identifies the damage state as defined in the EMS-98 scaleGrünthal (1998), which ranges from 0 to 5 grade. The probability histograms of the damage limit state are derived from the cumulative distribution Lagomarsino and Giovinazzi (2006) using Equation 5.14:

$$\begin{aligned} P_{s4} &= P[D_{s4}|S_d^*] \\ P_{sk} &= P[D_{sk}|S_d^*] - P[D_{sk+1}|S_d^*] \\ P_{s0} &= 1 - P[D_{s1}|S_d^*] \end{aligned} \tag{5.14}$$

where k ranges from 1 to 3. The probability of damage P_{s4} is divided into parts: the collapse probability P5 and the one referred to the occurrence of heavy damage P4. The following expressions are used, see Equation 5.15:

$$\begin{aligned} P_{s4} &= P4 + P5 \\ P5 &= 0.09 \cdot sinh(0.6 \cdot \mu_{DS}) \cdot P_{s4} \end{aligned} \tag{5.15}$$

where $\mu_{DS} = \sum_{k=1}^{4} k \cdot p_{sk}$ The damage discrete distribution for each building, for the spectral displacement required for the LS3, is displayed in 5.5.

The Fig.5.5 highlights the preponderance of the building to experience the damage grade D_{k4}, with a mean damage probability equal to 46.2 %.

5.5 Application of the Predictive Method to the Building Sample

The predictive method was applied to the case-study. The vulnerability index was evaluated for each building. Table 5.3 reports the calculated empirical vulnerability indices, for the main directions, I_{vx} and I_{vy}, respectively. With the aim to identify the main sources of fragility of the buildings, the distribution of the parameters is presented in Fig.5.6. The figure points out the brittleness of the masonry and the lack of resistance of the spandrels, to which mitigation vulnerability measures should be taken. The macro-seismic methodLagomarsino and Giovinazzi (2006) was then applied, based on the predictive indices, to estimate the mean damage μ_D for each building, see Fig.5.7, using the Eq.5.16:

$$\mu_D = 2.5[1 + \tanh(\frac{I + 6.25V - 13.1}{Q})] \tag{5.16}$$

Where I is the seismic input in terms of macro seismic intensity, Q is the ductility coefficient (set to 2.3) and V is the vulnerability coefficient, evaluated as reported in Eq.5.17, from the vulnerability index i_v, expressed in a range between 0 and 100:

$$V = 0.58 + 0.0064 i_v \tag{5.17}$$

A binomial distribution estimated the probability p_k of occurrence of the damage grade D_k (k from 0 to 5) Grünthal (1998) as a function of μ_D, according to Eq.5.18:

$$p_k = \frac{5!}{k!(5-k)!}(\frac{\mu_D}{5}^k)(1 - \frac{\mu_D}{5})^{5-k} \tag{5.18}$$

where the symbol ! indicates the factorial operator.

.

In order to compare the numerically obtained binomial distributions with the experimental one, the mean damage μ_D is evaluated based on the peak ground acceleration of the site, set to 0.255g. The authors correlated the peak ground acceleration, a_g, with the macro-seismic intensity I,

Buildings	I_{Vx}	I_{Vy}
B1	0.43	0.39
B2	0.46	0.41
B3	0.36	0.43
B4	0.42	0.40
B5	0.40	0.37
B6	0.37	0.41
B7	0.45	0.48
B8	0.36	0.48
B9	0.54	0.48
B10	0.33	0.44
B11	0.33	0.35
B12	0.40	0.44
B13	0.35	0.39
B14	0.55	0.55
B15	0.34	0.44

Table 5.3. Vulnerability indices, in the main directions.

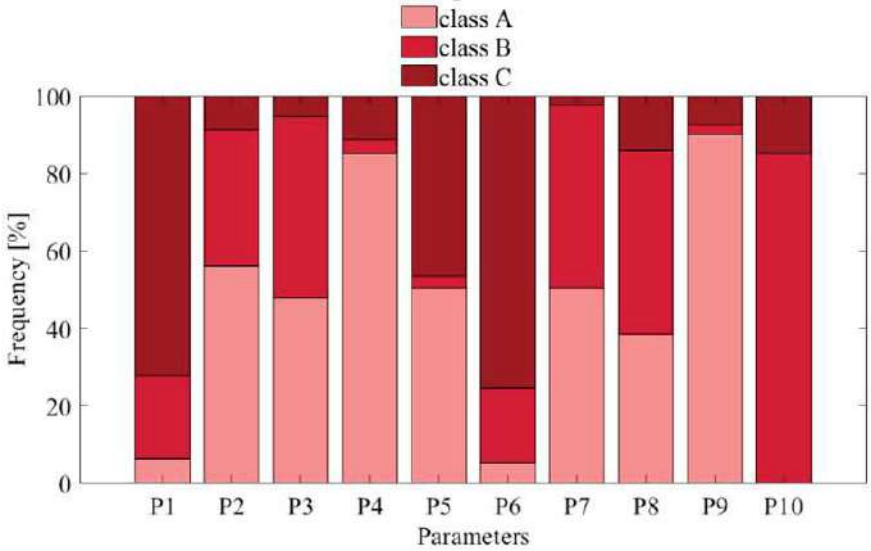

Figure 5.6. Damage discrete distribution referred to the direction with the minimum safety factor, for each building.

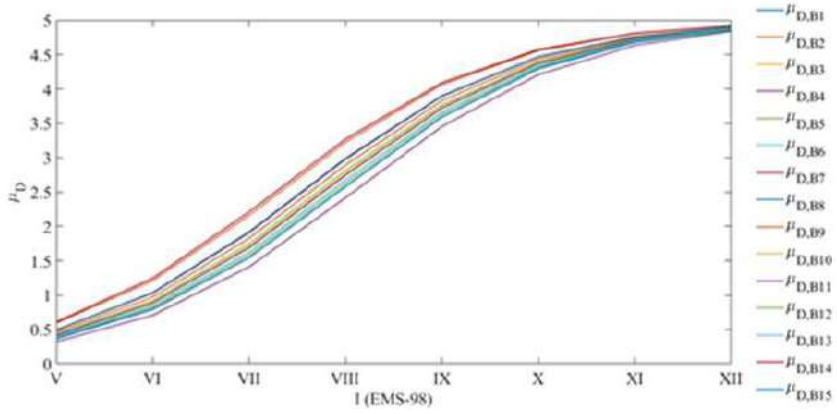

Figure 5.7. Mean damage curves for each building.

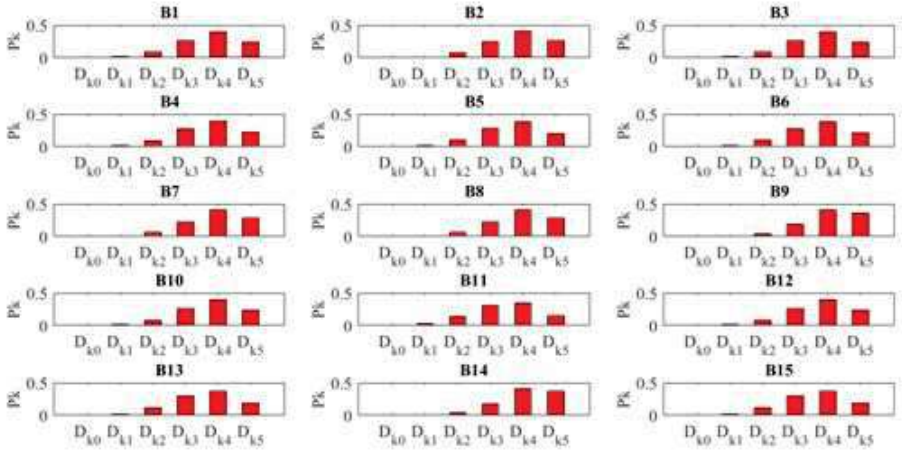

Figure 5.8. Damage discrete distributions for the buildings sample, referred to the IX grade of the EMS-98 scale, by means of the predictive approach.

following the correlation law in Eq.5.19Lagomarsino and Giovinazzi (2006).

$$a_g = (c_1 c_2)^{(I-5)} \tag{5.19}$$

C_1 and C_2 are constants, provided by Margottini et al.**?** and calibrated on Italian data, set to 0.03 and 1.75 respectively. The grade of the EMS-98 scale associated to the peak ground acceleration of the selected site corresponds to the IX grade: the related damage distributions are reported in Fig.5.8.

5.5.1 Comparison with Other Predictive Methods

Finally, the proposed approach was compared to others three approaches, available in literature: the G.N.D.T. method, proposed by Benedetti and PetriniBenedetti and Petrini (1984a), the approach proposed by Vicente et al.Maio et al. (2015); Vicente et al. (2014, 2008), which was widely used on large-scale assessment of Portuguese historical centres Ferreira et al. (2017), and finally the approach proposed by Formisano et al.Formisano et al. (2011, 2014), calibrated on Italian historical centres. The evaluated vulnerability indices are listed in Table 5.4 and the mean damage μ_D, evaluated for the mean value of the vulnerability indices of each approach, is plotted in Fig.5.9. Table 5.5 summarises the comparison among the empirical methods.

.

B	G.N.D.T	Vicente et al.	Formisano et al.	Proposed approach
B1	0.37	0.40	0.47	0.43
B2	0.49	0.41	0.43	0.46
B3	0.44	0.38	044	0.43
B4	0.35	0.42	0.35	0.42
B5	0.34	0.40	0.34	0.40
B6	0.40	0.31	0.40	0.41
B7	0.42	0.27	0.42	0.48
B8	0.32	0.38	0.38	0.48
B9	0.42	0.49	0.49	0.54
B10	0.43	0.26	0.43	0.44
B11	0.32	0.34	0.32	0.35
B12	0.41	0.32	0.41	0.44
B13	0.47	0.40	0.45	0.39
B14	0.48	0.46	0.50	0.55
B15	0.34	0.44	0.37	0.44

Table 5.4. Buildings' vulnerability indices evaluated by different approaches.

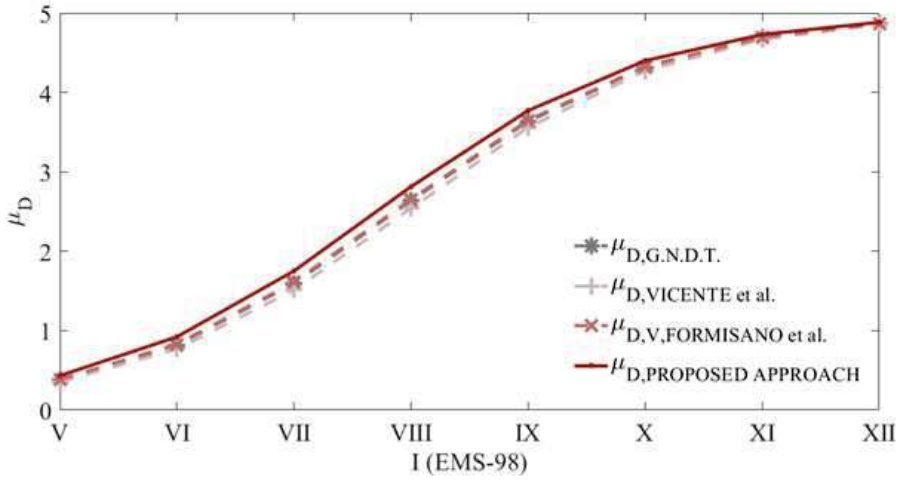

Figure 5.9. Mean damage curves evaluated by different approaches.

Approach	Min value	Max value	Mean value	σ
G.N.D.T.	0.32	0.49	0.40	0.057
Vicente et al.	0.26	0.49	0.37	0.067
Formisano et al.	0.32	0.50	0.40	0.054
Proposed approach	0.35	0.55	0.44	0.055

Table 5.5. Comparison among the different approaches: min value, max value, mean values, and standard deviation of the vulnerability indices.

The proposed approach reveals the highest value of the mean damage: the standard deviation σ is still within the range of the values found by the other procedures. The G.N.D.T. method represents the starting point for the other procedures that were derived by adjustments and modifications of the G.N.D.T. parameters. Therefore the discrepancy of the mean values of the vulnerability indices was appraised by comparing it to the G.N.D.T. index, equal to 0.40. The method proposed by Vicente et al., yielded a mean value of the vulnerability index affected by a discrepancy of –8.10 %.

.

The mean value, derived through the method proposed by Formisano et al., was equal to the G.N.D.T. index. The method proposed in this work yielded a mean value of the vulnerability index affected by a discrepancy of +9.09 %, proving to conservatively prediciting the mean damage μ_D. Finally, the application of the binomial probability distribution, for the mean value of the predictive indices, I_v equal to 0.44, allowed the estimation of the probability of occurrence of a certain damage value, evaluated for all grades of the macro seismic intensity of the European ScaleGrünthal (1998). The representation of the probabilities, displayed in Fig. 5.10, also called Damage Probability Matrix (DPM), yields the prediction of the likely damage scenarios for various earthquake intensities.

The estimated damage, illustrated in Fig.5.10, is also provided as fragility curves, reported in Fig.5.11, that reports the probability P (D > D_k) of exceeding an established damage grade, Dk when a certain earthquake with a seismic intensity IMCS occurs. P (D > D_k) is obtained from equations5.14, referring to the mean value of the predictive indices, I_v equal to 0.44. The DPM and fragility curves forecasted the damage scenarios on the expected seismic demand, providing a valuable tool for resilience-enhancing strategies. Based on the results discussed above, the reliability of the proposed

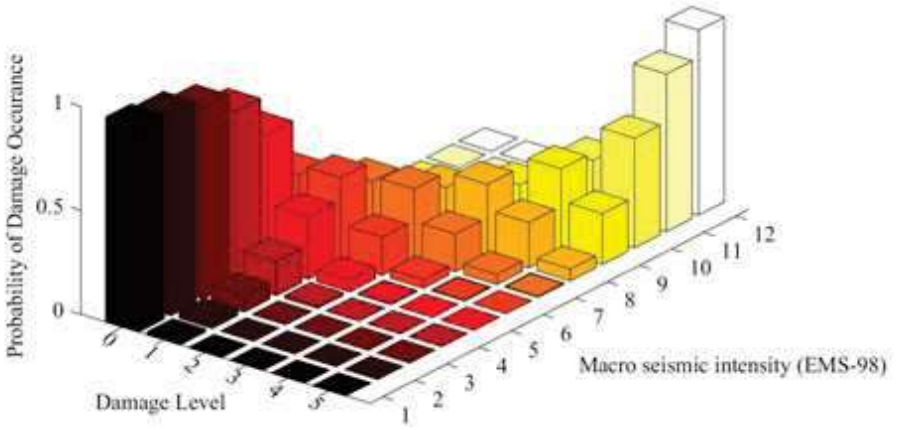

Figure 5.10. DPM for the predictive index $I_v = 0.44$.

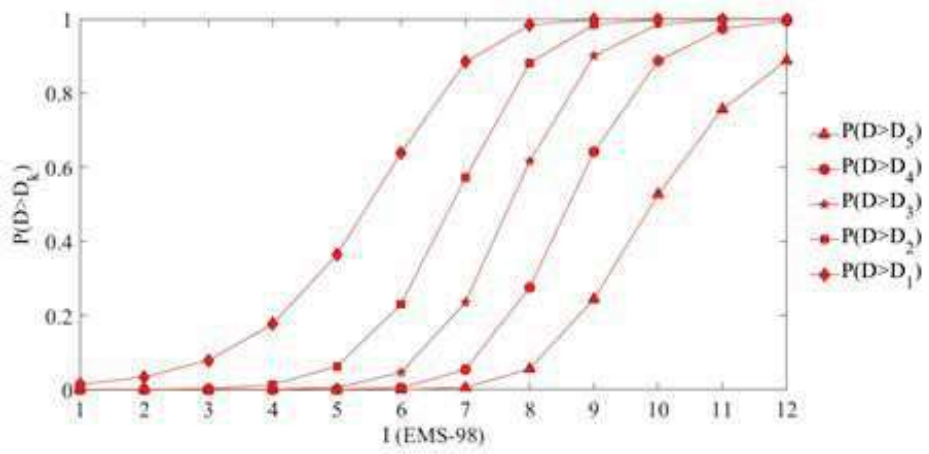

Figure 5.11. Fragility curves, for the predictive index $I_v = 0.44$, in terms of Macro Seismic intensity.

method was proved for large scale application.

5.6 Conclusion

The reduced seismic safety of the built masonry heritage requires some measure of mitigation of their seismic vulnerability. The damage suffered under recent earthquake actions highlighted the need of vulnerability assessment before an earthquake occurs. To this aim, predictive methods provide quick vulnerability assessment based on few structural parameters, known from field observations and geometric survey, to overcome excessive computational demand on large scale applications. In this paper, a novel predictive method is presented, which is focused on the in-plane response of masonry resistant bearing walls. The approach was applied to buildings,

located in the Central Italy, severely damaged by the 2016 earthquake. The seismic behaviour of the buildings was assessed also by numerical analysis. Damage discrete distributions were derived from fragility functions estimated from static non-linear analysis results. Vulnerability indices were evaluated as the weighted sum of ten parameters related to three classes of growing vulnerability (from A to C), yielding a vulnerability index for each wall and then for the entire building. The damage probabilities distributions, obtained from the predictive approach, confirmed the preponderance of occurrence of the damage grade D_{k4} derived from the numerical analysis. The comparison between the predictive mean probability of damage grade D_{k4} and the one derived from the numerical analysis highlights a difference of 13.5%, proving the reliability of the proposed method to predict the seismic damage. Finally, a comparison with other three predictive methods available in literature, was carried out in terms of mean damage derived by the macro seismic method: the G.N.D.T. and other two methods derived from the G.N.D.T. one by introducing some adjustiments and modifications. The differences between the mean values of the vulnerability indices and the G.N.D.T. one were calculated. The proposed method yielded a mean value of the vulnerability index affected by a discrepancy of 9.1 %, on the safe side when prediciting the mean damage μ_D. Finally, the representation of the damage probabilities, also called Damage Probability Matrix (DPM), and the empirical fragility curves yielded the prediction of the likely damage scenarios for various earthquake intensities that could support resilience-enhancing strategies for masonry construction at territorial scale.

5.7 Acknowledgements

The study presented in this chapter was published in the Journal *Civil Engineering and Environmental System*, Taylor and Francis:
"A Simplified Method for Seismic Assessment of Unreinforced Masonry Buildings.", I. Capanna, F. Di Fabio, M.Fragiacomo, 2022, 10.1080/10286608.2022.2047665.

A path to urban resilience strategies

Chapter abstract

A fast screening of fragilities of the built environment could be useful in forecasting of damage scenario under a ground motion to support authorities and decision makers to face effects of the seismic risk. Moreover, at this aim, the knowledge of the probability of reaching or exceeding a level of damage is useful to plan proper seismic risk mitigation measures. The simplified seismic assessment method developed in the PhD research activity is herein analysed to prove its capability to support risk mitigation policies, from emergency plans to resilience enhancement strategies. A path from the simplified seismic assessment to urban resilience improvement is suggested to highlight the main advantages and possible applications of the assessment seismic method proposed in this thesis. An estimation of seismic fragilities is performed for the selected buildings discussed in the chapter 3, representative of the entire class of URMs, through different assessment methods. Firstly, typological fragility curves for the macro-typology of URMs have been derived referred to the attainment of four limit states of interest, by means empirical and numerical approaches. A comparison between the obtained results in terms of probabilities of exceedance a limit state underlines the main advantages and limitations of each approach in the seismic vulnerability prediction on a large-scale application. Furthermore, in the light of the post-earthquake data gathered after the 2016 earthquake, the capability of the method to grasp the expected damage grade is confirmed. Afterwards, a vulnerability index-peak ground acceleration relation was developed using the empirical and the numerical assessment results of buildings' test site useful for the

entire URMs class. Still, the predictive method focuses on the evaluation of ten parameters, that affect the seismic performance of masonry buildings, of which seven ones could be modified by strengthening measures. Therefore, three different retrofitting solutions are introduced, and the correlated vulnerability reduction is appraised in terms of expected damage scenario, physical damage, loss of life, and unsafe buildings. An economic perspective was assumed to deepen the economic feasibility of the three strengthening solutions on a large scale of the built environment. The applications proposed corroborate the effectiveness of the method for seismic assessing on a territorial scale.

6.1 Introduction

Communities oftentimes face natural events and their disastrous effects. The most frequent shattering event in European countries are seismic events: the high structural vulnerability of the built heritage aggravates the losses in terms of casualties and safe buildings. An evaluation of seismic vulnerabilities of existing buildings allows to grasp their fragilities before an earthquake occurs. Predictive vulnerability assessments aim to detect the main vulnerabilities of buildings, focusing on few structural parameters in order to reduce time and effort required by a large scale of application. Therefore, simplified methods play a fundamental role in the framework of the seismic risk assessment, supporting social, urban, and economic evaluations. Furthermore, the knowledge of the weak points of the built environment allows to reduce the induced consequences of an earthquake for an urban area by introducing resilience enhancement measures, like effective emergency plans **?**. Due to the reasons above, predictive methods are useful for all phases of a seismic occurrence: (i) before an earthquake occurs, predictive method could support decisions about emergency management, like the design of the Emergency Limit Condition (ELC); (ii) after an earthquake, a fast surveying of the damage could address the restoration measures and the knowledge of the structural safety level could support the seismic risk mitigation policies, also with an economic perspective. All the activities deal with a large amount of input variables that qualify buildings, soil and urban components' conditions and their interactions: predictive models attempt to overcome the burden of a territorial application focusing on a more limited input information. Particularly, decision makers reserve interest in predictive models. In the light of the aforementioned, the robustness of a simplified method could be also investigated in forecasting the impact of a ground motion of a given intensity on an urban area from all points of view. In recent years, a growing attention has been reserved to the evaluation of the structural vulnerability of existing buildings through fragility assessment. A fragility function specifies the probability of a structure of attainment or exceedance a limit states of interest, depending upon a certain ground motion intensity measure Baker (2013). The knowledge

of the probability of the attainment or exceeding a limit state of interest allows to forecast damage scenario under a ground motion intensity. The estimation of fragility functions used with Geographic Information System (GIS) software could be extremely useful to support resilience enhancement strategies at urban scale. Currently, many scholars devote attention on the estimation of fragility functions for specific structural typologies of facilities. The derivation of typological fragility curves as representative of a homogeneous class of buildings, rather that stand-alone cases, allows to predict the seismic performance of an urban area reducing time and effort. In the paragraph *Typological fragility curves of URMs*, typological fragility estimation for the URMs class has been discussed. Typological fragility curves were derived referred to the attainment of four limit states of interest, through the proposed empirical method and static non-linear analysis. A comparison between the obtained results in terms of probabilities of exceedance a limit state underlines the main advantages and limitations of each approach in the seismic vulnerability prediction on large scale applications. In the paragraph *An hybrid calibration of the vulnerability model for URMs*, a relation between damage and peak ground acceleration is performed by means a combination of the empirical and numerical results providing an effective tool for assessing damage of URMs on a territorial scale. The relationship has been tested on the Central Italy test site, but the procedure could be properly repeated for URMs of other prone seismic area though a recalibration of the vulnerability model could be repeated to enhance its reliability. In the paragraph *Retrofitting solutions*, several applications of the method, useful to support resilience enhancement strategies, are discussed. The predictive method focuses on the evaluation of ten parameters, that affect the seismic performance of masonry buildings, of which seven ones could be modified by strengthening measures. Therefore, three different retrofitting solutions, SS, are introduced, and the correlated vulnerability reduction is appraised. In order to better understand the effectiveness of the strengthening solutions, a general building case is introduced with a vulnerability index equal to 1.00. After that, the SS influence on the buildings of the case study is investigated. A loss estimation in terms of expected damage scenario, physical damage, loss of life, and unsafe buildings, has been devel-

oped with reference to the different strengthened buildings' conditions. A cost-benefit analysis is carried out to also provide an economic insight of the strengthening measures proposed. Whereas the lack of reliable correlation between empirical damage and costs, a preliminary economic evaluation costs is developed to deepen the economic feasibility of the three strengthening solutions on a large scale of the built environment. The suggested path from vulnerability seismic assessment to urban resilience improvement highlights the main advantages of the method proposed in this thesis for possible implementations.

6.2 Typological fragility curves of URMs

About the estimation of the fragility functions, a significant part of the scientific literature focuses on the derivation of fragility curves through simplified analysis methods or alternative definition of the limit states Rota et al. (2010); **?**. Several approaches are used to derive fragility curves: empirical, analytical and hybrid ones. Empirical fragility methods aim to predict damage for specific levels of ground motion intensity based on post-earthquake damage data of specific buildings' typologies **???**, through simplified assessment of seismic performance. Analytical methods, also called mechanics-based methods, define the fragility functions based on structural or analytical models that appraisal the seismic behaviour of the structure **??**. Limit states are defined in terms of quantitative measure of structural performance, like displacements and deformation indicators **?**. Hybrid methods derive fragility curves using features of empirical and mechanics-based methods. Each method yields a proper level of accuracy. Empirical fragility assessment is calibrated on a specific area hit by an earthquake. In general, empirical fragility curves reflect uncertainties on structural data and ground shaking intensity. Analytical fragility assessment requires a numerical or mechanical modelling of the structure based on an in-depth knowledge of mechanical parameters and structural details, difficultly achievable at a territorial scale application. This paragraph also reports a comparison between empirical and numerical approaches to derive typological fragility curves for ordinary masonry buildings, through the investigation of the seismic behaviour of the buildings' sample, attempting

to mirror the entire class. The mean damage of the buildings' class was, in accordance with the European Macro seismic Scale classification, EMS-98, through the empirical approach proposed by the authors, to derive fragility curves for five damage states. After that, the fragility functions were estimated from the results of non-linear static analysis. A comparison between the typological empirical fragility curves and numerical ones reveals the main advantages and limitations in forecast damage scenarios and supporting resilience-enhancing strategies.

6.2.1 Derivation of fragility curves through empirical approach

In the last decades, a significant part of the scientific literature focused on the simplified estimation of the seismic vulnerability of masonry buildings, to face the estimation of the seismic vulnerability at territorial level. Empirical approaches attempt to overcome the effort of seismic vulnerability assessment on large-scale application resorting to few structural and mechanical parameters, known from visual inspections or geometric surveys. The authors proposed a simplified method finalized to provide a vulnerability index (ranging from 0 to 100) for the in-plane seismic behavior, based on ten parameters evaluated through quick formulations, related to three classes of growing vulnerability (from A to C), with different scores associated. The method was applied to each building of the case study. The mean value of the vulnerability indices, representative of the entire buildings' sample, was equal to 43.88. The expected mean damage of the typological class μ_D was estimated using the macro-seismic method Lagomarsino and Giovinazzi (2006). The average vulnerability curves and the confidence bounds associated are derived for different scenarios, expressed in terms of macro-seismic intensity, in Fig.6.1 (a), and in terms of peak ground acceleration in Fig.6.1 (b), evaluated according to Murphy O'Brien law correlation **?**.

The probability of occurring the damage grade D_k is estimated as a function of the μ_D. The typological fragility curves, derived by means the empirical method, are plotted in Fig.6.2: expressed in terms of macro-seismic intensity, in Fig.6.2 (a), in terms of peak ground acceleration in

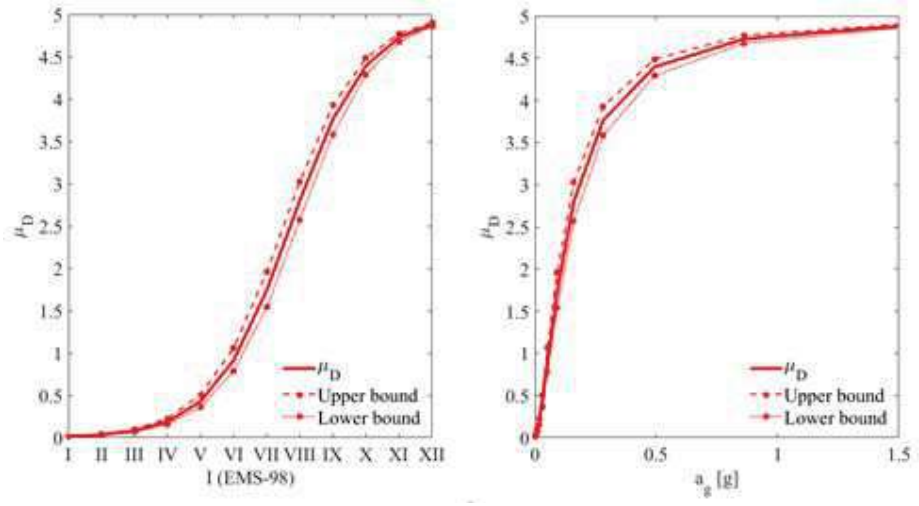

Figure 6.1. Mean typological damage curves: in terms of Intensity Measure (a); in terms of ag (b).

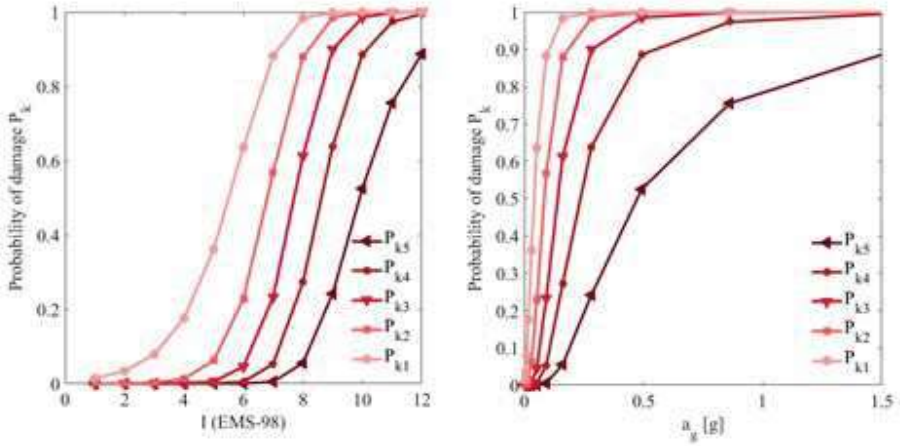

Figure 6.2. Typological fragility empirical curves: in terms of Intensity Measure (a); in terms of ag (b).

Fig.6.2 (b).

6.2.2 Seismic assessment by means mechanical approaches

Mechanics-based approaches appraisal the seismic structural performance of buildings accurately based on a numerical or analytical modeling. The achievement of a reliable estimation of the seismic behavior of a structure requires a deep knowledge of the structural system, detailed data, in-situ diagnostic tests, and a high computational effort. Therefore, the mechanical estimation of the seismic performance at territorial level represents a tricky application. Nevertheless, the authors derived the fragility curves of the URMs class through numerical analysis to compare the different

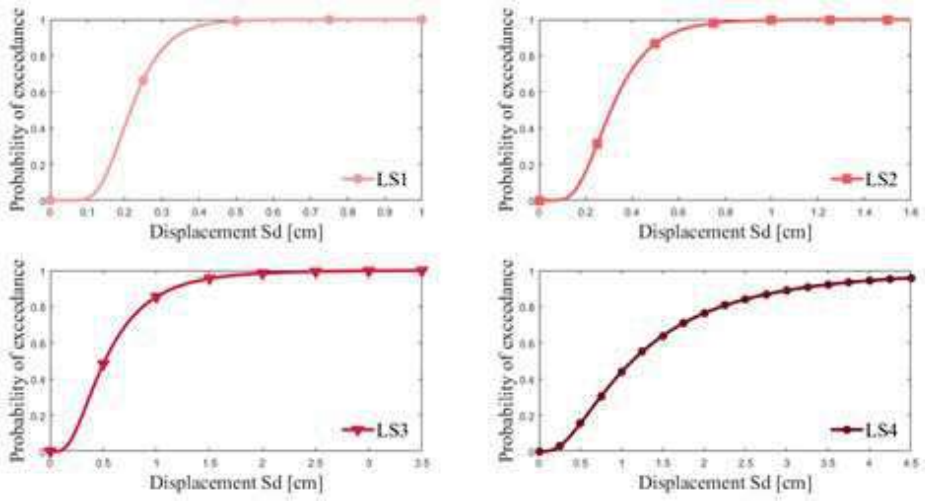

Figure 6.3. Typological fragility numerical curves for different limit states.

approaches. Static non-linear analysis was performed: for each structure, the analysis representative of the lowest safety level. The limit damage thresholds, considered in this application, are reported in Eq.6.1 :

$$\begin{aligned} (Sligth\ damage) \qquad & d_{s1} = 0.7D_y \\ (Moderate\ damage) \qquad & d_{s2} = 0.8D_y + 0.2D_u \\ (Severe\ damage) \qquad & d_{s3} = 0.5(D_u + D_y) \\ (Extremely\ severe\ damage\ or\ collapse) \qquad & d_{s4} = D_u \end{aligned} \tag{6.1}$$

The yielding and ultimate displacement, d_y and d_u, correspond to the average of the fifteen values, equal to 0.003 m and 0.011 m, respectively. The standard deviation is equal to 0.15 for the yielding displacement and 0.39 for the ultimate displacement. The typological fragility curves derived by means the numerical method are plotted in Fig. 6.3.

6.2.3 Comparative assessment of typological fragility curves

Fragility functions estimate the probability of a structure to attain or exceed limit states of interest, depending upon a certain ground motion Intensity Measure. In seismic risk assessment, probabilities of exceedance of limit states of interest are useful to predict the seismic behavior of the built environment before an earthquake occurs. The authors performed seismic fragility assessment for URMs class based on probabilities of exceedance

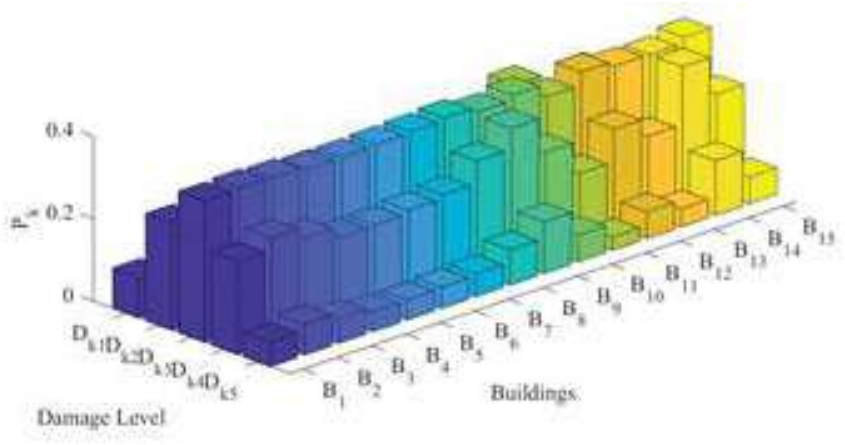

Figure 6.4. Discrete damage distributions for I=8.07.

derived through empirical and numerical approaches. Furthermore, a portfolio of the gathered information and data allows to detect the real damage scenario occurred after the 2016 earthquake. The suffered damage of each building of the stock was correlated to the Intensity Measure experienced by the attenuation law proposed by Crespellani **?**, see Eq. 6.2, to prove the reliability of the proposed empirical method in predicting seismic damage scenario:

$$I_{EMS-98} = 6.39 + 1.756Mw - 2.747\ln(R+7) \tag{6.2}$$

Where M_w is the moment magnitude occurred, set equal 6.2, and R is the distance from the epicenter, equal to 21.5 km. The discrete damage distributions for each building of the sample, evaluated for an intensity measure equal to 8.07, is reported in Fig. 6.4.

The percentage of buildings of the sample with a damage grade D_{k2} was equal to 6.67; with a damage grade D_{k3} was equal to 86.67, and with a damage grade D_{k4} equal to 6.67. The forecast damage shows a good agreement with the real suffered damage: the preponderant level of damage is D_{k3}, with a discrepancy equal to 6.97 % with the real damage. The results discussed above prove the capability and reliability of the empirical method to forecast the expected damage of buildings' sample. Obviously, this is a rough conclusion: a more accurate evaluation should consider damage for different intensity level. Moreover, the correlation law neglects the influence of possible site effects on damage scenario. Whereupon a

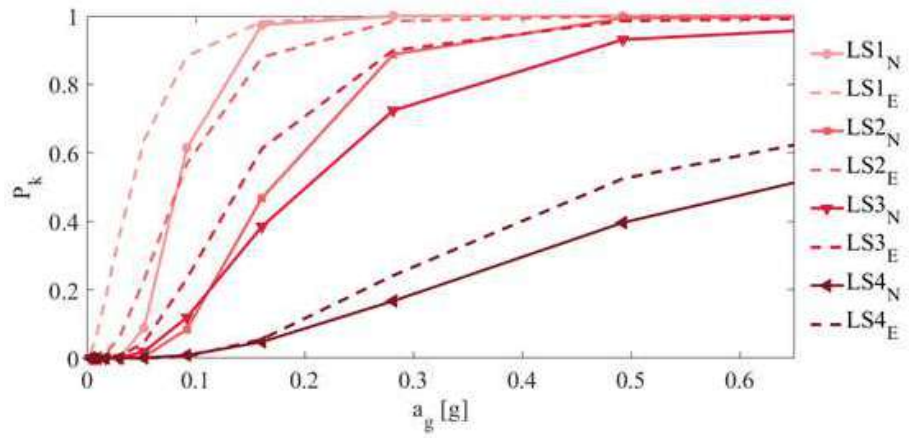

Figure 6.5. Fragility curves comparison.

comparison in terms of typological fragility curves is performed to compare empirical and mechanics-based methods, see Fig. 6.5, expressed in terms of a_g.

For a seismic demand encloses in the range 0-0.3 g, the discrepancy in terms of probability of exceedance for the LS1 reaches the value of 29.9 %; for the LS2 reaches the value of 47 %. The comparison highlights a difference of fragility curves, more remarkable for the LS1 and LS2. Whereas the fragility curves referred to the attainment of the LS3 and LS4 shows a better agreement. For a seismic demand higher than 0.3 g, the discrepancy in terms of probability of exceedance for the LS3 reaches the value of 19 %; for the LS4 reaches the value of 25 %. The empirical and numerical probability values of exceeding the limit state LS1 and LS2 may be regarded as too scattered to consider equivalently the two approaches. Overall, the empirical curves overestimate the probabilities of the collapse, on the safe side in predicting the damage scenario.

6.2.4 Comments on the comparison of typological curves

Fragility curves are derived for masonry buildings' class, by empirical and numerical methods. A simplified assessment of the seismic behavior of the buildings is performed, through an empirical method proposed by the authors, to provide a mean vulnerability index representative of the buildings' sample. Based on the empirical results, the mean damage was evaluated, according to the Macro Seismic Methodology, to derive empirical fragility curves of the buildings' class. After that, typological numerical fragility

curves are derived from the results of non-linear static analysis. Based on a comparison between the different methodologies, the typological fragility curves show different values of probability of exceedance, more scattered for the limit states LS1 and LS2. For a seismic demand encloses in the range 0-0.3 g, the discrepancy in terms of probability of exceedance for the LS1 reaches the value of 29.9 %; for the LS2 reaches the value of 47 %. Whereas the fragility curves referred to the attainment of the LS3 and LS4 shows a better agreement. For a seismic demand higher than 0.3 g, the discrepancy in terms of probability of exceedance for the LS3 reaches the value of 19 %; for the LS4 reaches the value of 25 %. Thus, the current research results show that a typological approach fails for the LS1 and LS2 states of interest. To improve the numerical fragility assessment of the buildings' typology, an investigation of the yielding displacements may be useful to propose an appropriate definition of the threshold for the slight and moderate damage states. The identification of suitable limit states for masonry buildings is still an open issue. Similarly, to improve the empirical fragility assessment, the ductile factor of the masonry structures, set equal to 2.3 in the empirical formulation of the expected mean damage, could be deepened: even within URMs class, buildings exhibit different ductile behaviour factors, showing the dispersion of the ductile parameter Q. Therefore, the empirical typological fragility assessment ensures accurate and quick seismic vulnerability prediction on large scale, reducing computation time of seismic analysis of buildings' class. For the LS1 and LS2 limit states, the current research points out that a typological approach requires more accurate quantitative parameters to grasp the buildings' seismic behaviour, with both approaches. To improve the fragility assessment of the entire URMs class, an investigation of the onset of the damage may be useful to propose an appropriate definition of the threshold for the slight and moderate damage states. Thus, the detected discrepancy between the adopted approaches could be removed improving observational, experimental, and numerical data to better deepen the seismic behaviour of the URMs local case study under investigation. The study presented in this paragraph was presented in the ConferenceCompdyn 2021, VIII ECCOMAS Thematic Conference on Computational Methods in Structural Dynamics and Earth-

quake Engineering:
"Comparative Assessment of empirical and mechanical approaches for the estimation of the seismic fragility of ordinary masonry buildings type of the inner Central Italy", I. Capanna, F. Di Fabio, M.Fragiacomo, Procediing of Compdyn 2021, Athens, Greece, 27-30 June, 2021.

6.3 An hybrid calibration of the vulnerability model for URMs

Simplified methods for seismic assessment deliver a conventional indicator of the structural safety, expressed as a vulnerability index. These methods could satisfy a fast screening of the seismic vulnerability at territorial level unlike other methods could fail due to their demanding computational effort. Nevertheless, a more comprehensive seismic knowledge of built heritage seismic performance is needed to set proper resilience enhancement strategies. Therefore, the improvement of predictive methods' capability of expressing seismic performance lays on a strong link between vulnerability indices and seismic intensity measures. Many scholars correlated empirical vulnerability indices to an intensity measure of seismic events by means different approaches. Several authors used observational data of damaged facilities by past earthquakes Cavaleri et al. (2017). Still, observational data are available only for built areas hit by past earthquakes. Therefore, information lacks lead to employ other methodologies to deliver a refined data, like numerical and experimental ones. Unfortunately, a reliable seismic assessment is difficult to achieve for covering all buildings' typologies. In all cases, a vulnerability model exploits vulnerability indices to correlate an intensity of the seismic event (e.g. peak ground acceleration) to an indicator of the seismic performance (e.g. mechanical or economical). The most representative seismic safety index is defined as the ratio between the peak ground acceleration corresponding to the collapse of the structure and the design ground acceleration. Moreover, two limit-levels of acceleration are significant for the damage analysis **?**: (i) the acceleration corresponding to the beginning of the damage of a structure, PGA_i; (ii) the acceleration corresponding to the collapse PGA_c. The vulnerability model proposed

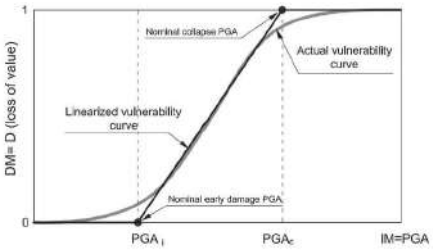

(a) Actual and vulnerability curve.

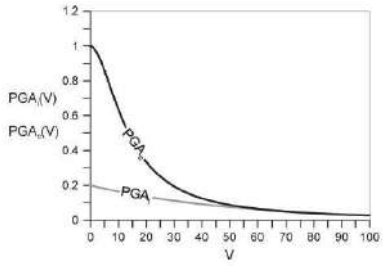

(b) Typical PGA-V relationship.

by Gaugenti and Petrini **?** is selected for the URMs under investigation. The approach correlates damage, acceleration, and vulnerability index by observing the damage to Italian masonry buildings under past earthquakes. An equivalent linearized curve**?**, see Fig. 6.6(a), expresses the acceleration-damage laws, defined according to expressions 6.3:

$$D(PGA,V) = \begin{cases} D = (PGA - PGA_i)/(PGA_c - PGA_i), & \text{if } PGA_i < PGA < PGA_c. \\ D = 0, & \text{if } PGA < PGA_c. \\ D = 1, & \text{if } PGA > PGA_c \end{cases} \tag{6.3}$$

The functional relationships, depicted in Fig. 6.6(b), correlate the PGA_i, see Eq.6.4, and PGA_c, see Eq. 6.5, to the vulnerability index:

$$PGA_c(V) = \beta_c V^{\gamma} + \alpha_c \tag{6.4}$$

$$PGA_i(V) = \alpha_i \exp(-\beta_i V) \tag{6.5}$$

The constants α_i , I, β_i, α_c, β_c and γ reflect the vulnerability connotation of the built asset and thus need specific calibration. The current paragraph merges the outcomes of the empirical and numerical seismic assessment previously carried out to calibrate the vulnerability model of the URMs of the test site. The vulnerability indices employed in the vulnerability model are derived through the empirical method proposed in the thesis. Afterwards, the vulnerability model was calibrated using the peak ground accelerations resulting from the static non-linear analysis of the buildings' class. The field of validity is extended to URMs typical of the Central Italy

Buildings	$I_{v,x}$	$PGA_{c,x}$ $[g]$	$I_{v,y}$	$PGA_{c,y}$ $[g]$
B1	0.23	0.78	0.47	1.52
B2	0.33	0.758	0.55	1.25
B3	0.95	0.75	0.65	1.25
B4	0.48	1.59	0.40	1.33
B5	0.42	1.39	0.91	2.97
B6	0.57	2.74	0.50	2.40
B7	0.39	1.87	0.55	1.78
B8	0.95	3.10	0.63	2.09
B9	0.31	1.03	0.55	1.81
B10	0.80	2.58	0.44	1.44
B11	1.60	5.26	0.89	2.94
B12	0.59	1.92	0.70	2.30
B13	0.42	1.37	0.37	1.21
B14	0.29	0.92	0.31	0.96
B15	0.51	1.73	0.33	0.85

Table 6.1. I_v, PGA_i, PGA_c (from static non-linear analyses)

thanks to the extensive numerical results that brace the calibration of the model.

6.3.1 Calibration of the vulnerability model for the selected URMs

The PGA_i and PGA_c were computed according to EC8 Herrmann and Bucksch (2014). Table 6.1 reports the vulnerability indices, the PGA_c, and the peak ground accelerations design of buildings, for the worst cases of pushover analyses, referred to the X-Direction and Y-Direction.

.

Fig.6.6 depicts the peak ground accelerations PGA_i and PGA_c in green and blue cloud points, respectively. The green trend line indicates the V-PGA_i relationship, whereas in blue V- PGA_c one. The calibration trend-lines lead to assess the parameters optimizing as reported in Fig. 6.6.

After the calibration of the vulnerability model, vulnerability curves for the investigated buildings are derived and depicted in Fig.6.7.

The relationship between the qualitative vulnerability index and the quantitative mechanical index, in terms of PGA, afford a powerful tool to face seismic fragility screening at territorial level. The derived vulnerability curves foresee the damage of buildings under an event of a specific seismic action. The calibration carried out for URMs representative of the built

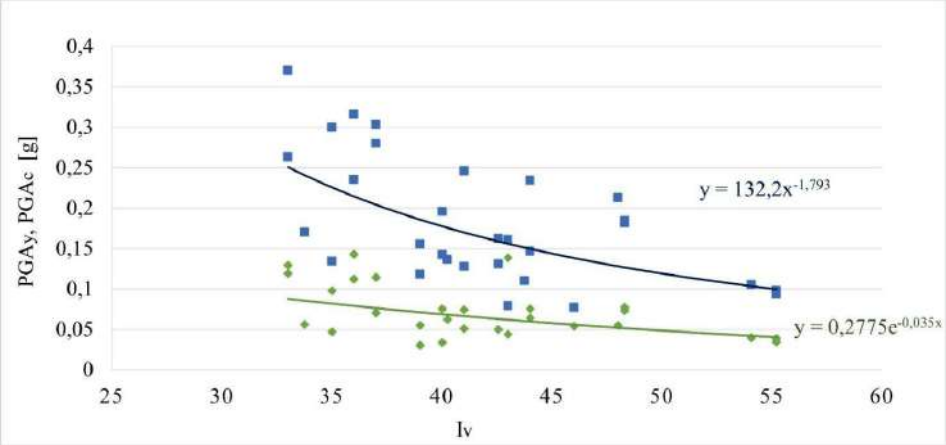

Figure 6.6. Calibration of the vulnerability model according to numerical results of the buildings' sample.

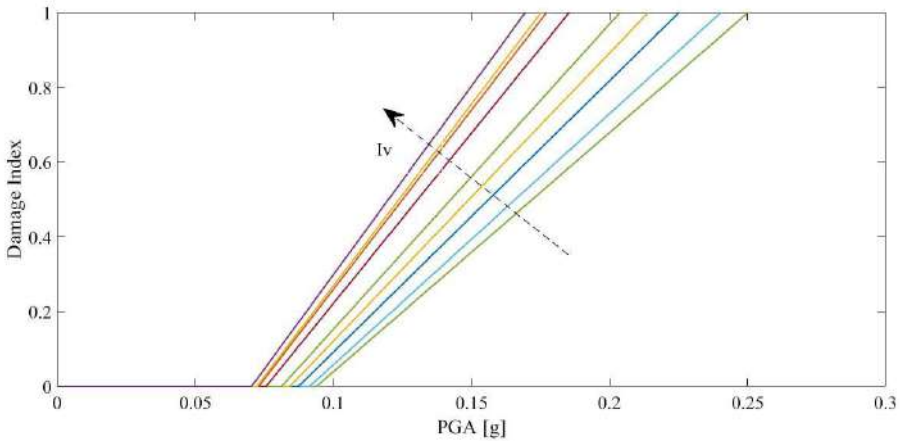

Figure 6.7. Calibration of the vulnerability model according to numerical results of the buildings' sample.

α_i	β_i	α_c	β_c	γ
0.2775	-0.035	0	132.2	-1.793

Table 6.2. Parameters optimizing PGA(V) relationship for the case-study.

layout of Central Italy could be extended to other URMs characterized by similar structural features. It is worth mentioning that for URMs with peculiar characteristics, a recalibration of the vulnerability model could be perform to avoid a loss of accuracy of the results.

.

6.4 Retrofitting solutions

The predictive method proposed by the authors evaluates the seismic vulnerability of masonry buildings based on the evaluation of ten parameters that affect the masonry walls' in-plane behaviour under a seismic action. Three classes of growing seismic vulnerability are introduced, from A to C, with the corresponding scores, equal to 0, 50 and 100, respectively. For each parameter, a weight is assigned for the relative importance among the ten parameters on the global in-plane behaviour. The predictive method consists of two phases: (i) the assessment of the vulnerabilities for each masonry wall of the analysed building, for its each main direction; (ii) the derivation of a global index representative of the entire building vulnerability from the masonry walls' indices. Damage scenario could be derived through the vulnerability indices to forecast the physical damage of buildings, particularly useful for strategies of resilience enhancement of the built environment. At this aim, the authors proposed three different strengthening solutions, SS, named SS1, SS2 and SS3, and their influence of damage scenario was investigated. The strengthening solutions are accounted on the seismic vulnerability index methodology: each package of strengthening measures decreases the vulnerabilities scores. The strengthening solutions are conceived to enhance the structural safety gradually. The strengthening solutions SS1 consist of limited interventions that mitigate the vulnerabilities locally, like closing of hollows into the walls and introduction of tension resistant element for masonry spandrels. The parameters modified by the

SS1 measures are P2, P3, P4, that allow a reduction of a class of vulnerability, and P6, that allows a reduction up to two classes. As well as the strengthening measures of the SS1 applied up to a reduction of two classes of vulnerability, the strengthening solutions SS2 consist of extended interventions of vertical and horizontal structures, like masonry consolidations, strengthening of masonry vaults, and floor stiffening, reducing the scores associated to the parameters P1, P7, P8 of a vulnerability class. The strengthening solutions SS3 are the most effective structural interventions that allow the reduction of the scores of the parameters indicated in the others strengthening measures up to two vulnerability classes. The knowledge of the influence of the strengthening solutions on the vulnerability indices is useful to analyse the impact of seismic retrofitting strategies, using damage scenarios for different levels of reinforcements. In order to better understand the effectiveness of the strengthening solutions, the maximum reduction of the vulnerability scores is apprised: equal to 142.5 for the SS1; 355 for the SS2 and 465 for the SS3. These values are normalised to the maximum value of the vulnerability index that ranges between 0 to 715. Therefore, the maximum reduction of the vulnerability indices is equal to 0.19 for the SS1; 0.49 for the SS2 and 0.65 for the SS3. Three different damage scenarios are derived to grasp the influence of the strengthening measures on the mean damage grades, μ_D. At this aim, the vulnerability index is set to 1.00, arbitrarily, to capture the maximum influence of the strengthening measures, see Fig.6.8, leading to a vulnerability index equal to 0.80 for a building reinforced with SS1, 0.50 with SS2, and 0.34 with SS3.

The mean damage curves highlight that the difference among the strengthening measures solutions is more marked in the ranges from IV to X macro seismic intensity. Fragility curves define the correlation between seismic intensity and expected damage in terms of a continuous probability function that expresses the probability of reaching or exceeding a given damage state. Probability of experiencing five damage grades as a function of the mean damage depicted in Fig. 6.8, is derived, see Fig. 6.9.

Fig. 6.9 shows that, for the most severe damage grades, the discrepancy in terms of reduction probabilities for the different SS enhances at

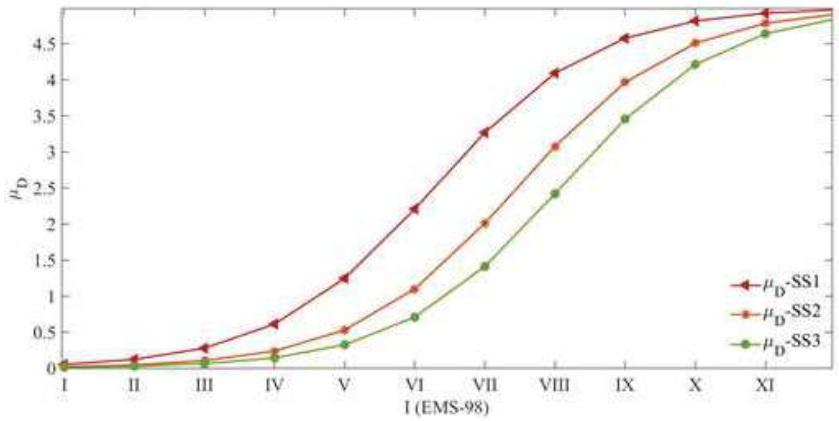

Figure 6.8. Maximum reduction of the mean damage for the different SS.

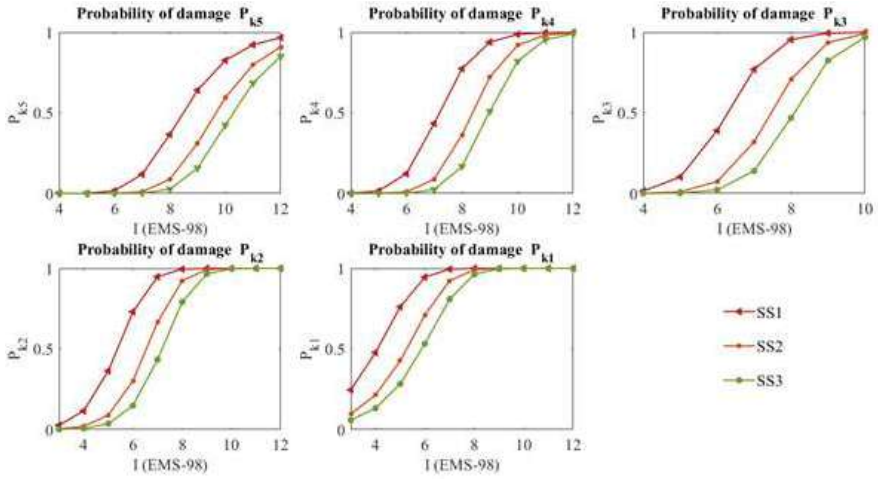

Figure 6.9. Maximum reduction of the probability of collapse for the different SS.

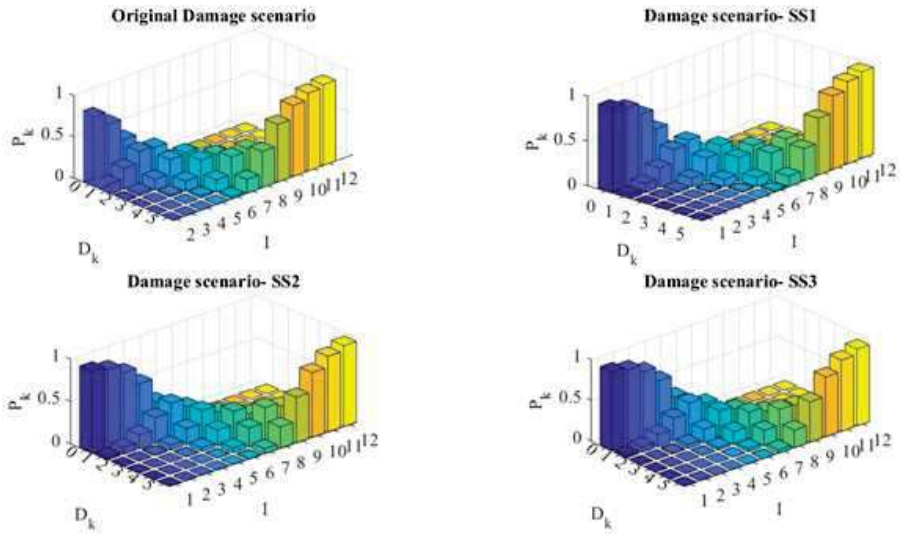

Figure 6.10. Damage scenario for the different SS.

higher macro seismic intensities, whereas it decreases at lower macro seismic intensities. For the slighter damage grades, the discrepancy in terms of probabilities for the different SS is more remarkable at lower macro seismic intensities. The impact of the strengthening solution at territorial scale is also represented in terms of damage probability matrix for the buildings' sample, see Fig.6.10.

Plotting damage scenario, depicted in Figures 6.10, through maps georeferenced by means of Geographic Information System (GIS) software, could be extremely useful to support resilience enhancement strategies at urban scale.

6.4.1 Impact of strengthening solutions on loss estimation

The forecast of the expected damage of buildings supports seismic mitigation strategies at territorial scale, providing the starting point for important tasks at urban scale, like plan emergency plan or resilience enhancement policy. The assessment of short-term use of buildings, in terms of collapsed and un-usable ones, is a fundamental information in the aftermath of a shattering earthquake and thus, required in a loss estimation activity. In this section the capability of the proposed method to perform a loss estimation is proved. The simplified method for seismic assessment of the unreinforced masonry buildings allows to investigate the buildings' vulnerability and its mitigation thanks the SS. The three strengthening solutions

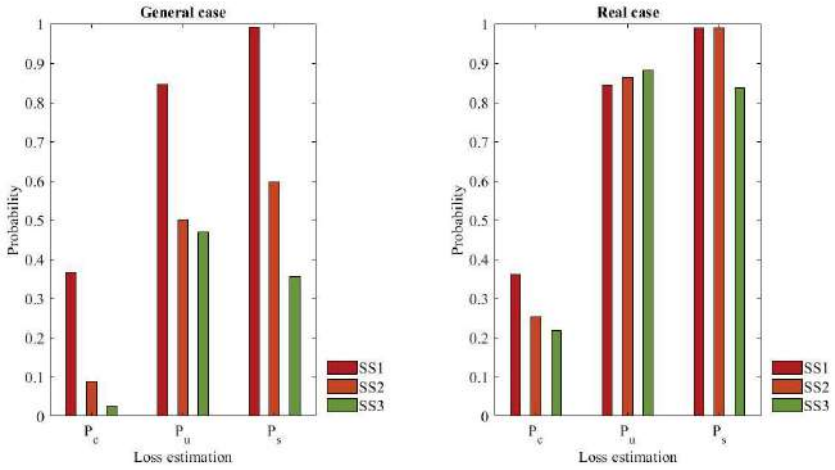

Figure 6.11. A generic loss estimation: probability of collapse, probability of un-usable buildings and probability of severely injured at varying of strengthening solutions.

differently affect the buildings' vulnerability leading to different damage probability. Based on the damage scenario reported in the previous paragraph, a loss estimation is carried out in terms of collapsed and un-usable buildings. The model adopted to perform loss estimation focuses on probability of exceeding a certain damage grades correlated to the probability of functional loss. The following equations, 6.6, were used to perform the loss estimation Vicente et al. (2014), depicted in 6.11:

$$\begin{aligned} P_{collapse} &= P(D_5) \\ P_{unsuablebuildings} &= P(D_3) * W_{i,3} + P(D_4) * W_{i,4} \\ P_{severelyinjured} &= 0.3 * P(D_5) \end{aligned} \tag{6.6}$$

Where P(D_i) is the probability of the occurrence of a certain damage grade and $W_{i,j}$ are multiplier factors that indicate the percentage of buildings associated with the damage grade D_i. The factors $W_{i,3}$ and $W_{i,4}$ are set equal to 0.4 and 0.6, respectively. The information provided by the loss estimation could be useful to authorities for housing recovery of the investigated urban area or allocating resources and disbursements in a seismic emergency.

6.4.2 Economic evaluations of the seismic retrofitting measures

The SS described in the previous paragraphs are here analysed from a financial perspective through a cost benefit analysis. Despite the lack of a reliable correlation between empirical damage and costs, a preliminary economic evaluation is developed to deepen the economic feasibility of the three strengthening solutions on a large scale of the built environment. A cost for each strengthening measure is introduced, considering the updated disposition of the Lazio Region. Based on the definition of the SS and their gradually reduction of the vulnerability classes (RVC), a mean cost for each SS is evaluated and listed in Table 6.3. The costs are counted for m^2 of area in plan of the structural elements affected by the interventions.

SS	Intervention	RVC	Mean cost	Max cost
SS1	closing of hollows	1 class	39.67	199.17
SS1	insertion of spandrels' element	2 class	159.50	199.17
SS2	closing of hollows	2 class	79.33	473.66
SS2	insertion of spandrels' element	2 class	159.60	473.66
SS2	reinforcement of masonry	1 class	234.83	473.66
SS2	stiffening of floors	1 class	63	473.66
SS3	closing of hollows	2 class	79.33	647.43
SS3	insertion of spandrels' element	2 class	159.50	647.43
SS3	reinforcement of masonry	2 class	408.60	647.43
SS3	stiffening of floors	2 class	88	647.43

Table 6.3. Economic evaluation for the different strengthening solutions.

The strengthening costs can be considered also as repair costs in the case of repairability evaluation of buildings. The costs probabilities for a certain seismic event characterized by an intensity I, $P[R|I]$ is evaluated as the product between the conditional probability of the cost for each damage level, $P[R|D_k]$ and the conditional probability of the damage condition for each level of vulnerability and seismic intensity, $P[D_k|I, I]$, see equation 6.7Vicente et al. (2014); **?**); **?**:

$$P[R|I] = \sum_{D_k=1}^{5} \sum_{I_v=0}^{100} P[R|D_k]P[D_k|I_v, I] \tag{6.7}$$

Instead, the benefits of the interventions could be appraised in terms of reduction of the mean damage expected. For each SS, a parameter called

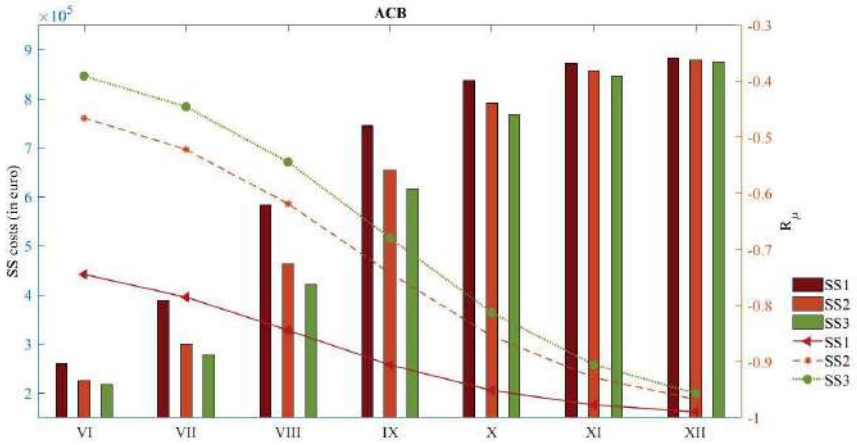

Figure 6.12. ACB of the case study at varying of strengthening solutions.

R_μ evaluates the reduction of the mean damage modifying the equation 6.8:

$$R_\mu = \frac{1 + \tanh(\frac{I+6.25V_{SS}-13.1}{Q})}{1 + \tanh(\frac{I+6.25V_0-13.1}{Q})} \tag{6.8}$$

Where V_{ss} is the vulnerability coefficient after the SS carried out and Vo is the vulnerability index before the SS application. A cost benefit analysis is also carried out for the buildings' sample of the case study, see Fig. 6.12. The vulnerability indices of the buildings' sample are equal to 33.93 after SS1, 18.77 SS2, and 13.31 for SS3.

The Fig. 6.12 shows that differences in terms of benefits and costs among the SS decrease at higher seismic intensities: the differences in terms of R_μ trends to decrease clearly.

6.5 A suggested implementation of the predictive method in seismic risk management

In the previous paragraphs, several applications of the assessment method are proposed and discussed, following the suggested procedures available in literature for all prone areas. In this paragraph, an use of the predictive method is proposed for the Italian area, integrating tools of National authorities to mitigate the seismic risk. In the frameworks of its activities, some Italian Institutions, like the Italian Fire Department, deal with the management of emergencies and urgent technical rescue of citizens. At this

aim, a reserved field is devoted to support the activities of the Italian Fire Department, through advanced geographical data, called Topography Service Applied to Rescue, TAS (in Italian "servizio di Topografia Applicata al Soccorso). In particular, the TAS allows to derive geo-referenced scenarios, that could also require the participation of the National System of Civil Protection, using a GIS tool called ArcGis Survey 123. The vulnerability analysis provided by the predictive assessment method could support Italian Institutions' activity. The main advantage of the empirical method is the fast evaluation of the seismic vulnerability of URMs. Afterwards, the vulnerability index is useful to derive damage scenario at varying the seismic demand, as already demonstrated. The authors propose the implementation of the assessment method in the tools of Institutions' activity to perform a proximity analysis of the built heritage respect to:

- emergency routes;
- strategic buildings: hospitals, prefectures, barracks of fire fighters and polices;
- areas with higher population density;
- industries or storage centers of substances dangerous for the environment;
- highways or airports.

considering that the seismic damage of URMs, as well as yielding an unsafe and unusable buildings, affect the functionality of the entire urban system. In fact, during a seismic event, the first difficulties to face are the rescue management due to the collapses of buildings that encumber the routes, the damage that affect strategic buildings and other resulting risks, like fires, landslides, and environmental disasters. The knowledge of the proximity of expected damaged buildings, based on a fast scenario of URMs derived through the empirical vulnerability index of the PhD research activity, could support the mitigation and managements of all risks that arise from a seismic event. Therefore, the implementation of the vulnerability index could be useful to draw the relationship of the existing URMs with the elements reported in the list above. The application proposed allows to

establish timely evacuation plans and rescue strategies of built areas taking into account the vulnerability level of the existing buildings and their position in the built environment.

6.6 Conclusion

In this chapter, an overview of the possible applications of the proposed simplified method is presented. A typological fragility assessment is carried out to derive typological fragility curves of URMs. A comparison between numerical and empirical curves shows that, for a seismic demand encloses in the range 0-0.3 g, the discrepancy in terms of probability of exceedance for the LS1 reaches the value of 29.9 %; for the LS2 reaches the value of 47 %. Whereas the fragility curves referred to the attainment of the LS3 and LS4 shows a better agreement. For a seismic demand higher than 0.3 g, the discrepancy in terms of probability of exceedance for the LS3 reaches the value of 19 %; for the LS4 reaches the value of 25 %. Thus, the current research results show that the empirical typological fragility assessment ensures accurate and quick seismic vulnerability prediction on large scale, reducing computation time of seismic analysis of buildings' class. A vulnerability model of reference is calibrated on the empirical and numerical seismic assessment results. The field of validity of the relationship between damage, vulnerability index and peak ground motion is extended to URMs typical of the Central Italy and buildings with similar structural features thanks to the extensive numerical results that brace the calibration of the model. Afterwards, the feasibility of the simplified method in resilience improvement strategies was corroborated through several applications. Therefore, three different retrofitting solutions are introduced, and a correlated loss estimation is carried out in terms of expected damage scenario, physical damage, loss of life, and unsafe buildings. The information provided by the loss estimation could be useful to authorities for housing recovery of the investigated urban area or allocating resources and disbursements in a seismic emergency. Whereas the restoration of public or residential buildings may affect national economy, the economic feasibility of the three strengthening solutions on a large scale of the built environment was deepen form an economic perspective: the cost benefit analysis proposed offers a prelim-

inary overview of the possible mitigation seismic risk options. Finally, an implementation of the empirical assessment method proposed in the TAS suggests a meaningful way to manage other risks resulting from a seismic events, thanks a proximity analysis of URMs respect to the built environment. The suggested path from vulnerability seismic assessment to resilience enhancement application confirms the potentialities of the method proposed in this thesis for possible implementations.

Mechanics-based method for seismic assessment of URMs

Chapter abstract

The core of the research discussed in this PhD thesis is the development of a multicriteria method for seismic assessment of URMs, through different levels of accuracy and effort analysis. The first level of the method grasps the seismic vulnerability empirically, particularly effective for quick seismic analysis through a rough knowledge of building. This chapter presents the last development of the multi-criteria method developed. The mechanical vulnerability method, here presented, aims to predict the seismic capacity of masonry walls more accurately respect to the empirical method, for a refined seismic assessment. Its starts from the seismic assessment of each masonry wall of the analyzed building, for its each main directions, to achieve the seismic assessment of the entire building, in terms of shear capacity and peak ground acceleration capacity. Furthermore, based on the evidence discussed in the previous chapter, different formulations are proposed to derive the seismic capacity of the URMs at varying resistance of floors. The reliability of the method in evaluating the seismic response is investigated through different approaches applied to the copious buildings' sample that covers different structural configurations, for a total of 15 URMs and 95 masonry walls analysed. 380 static non-linear analysis are performed to deliver robust data for the investigation of the accuracy of the proposed method. Lastly, a comparison between the derived results confirms the reliability of the mechanics-based method. Thus, the last method ends the path to predict the seismic capacity of URMs at territorial level, suggested in this research activity.

7.1 Introduction

The discussion of URMs' seismic response deserves a dedicated attention due to randomness of the structural parameters and the complexity of their seismic behavior, sometimes exasperated by the sensitivity of numerical tools to the input variables Felice et al. (2017). Despite the intrinsic differences between masonry buildings, two seismic response may occur, see Fig.7.1: local mechanism, also called *out-of-plane response*; (ii) global mechanism, also called *in-plane response*. (i) The seismic response of URMs without connections between wall-to-wall and wall-to-floor, inspected after an earthquake, shows some common features, driven by collapse mechanisms and damage patterns of different structural parts, named *macro-elements*, with independent behavior**??**. Vulnerability descends from material and structural details. In fact, observed seismic damage highlights the brittleness of the masonry and the lack of connection among different structural compounds**?**. Field observations often reveal similar damage mechanisms, despite the uniqueness of each construction. The recurring failure modes, like out-of-plane overturning and local collapse, involve only exterior walls, depending their geometric configuration. Several simplified mechanical procedures may be found in literature to assess the out-of-plane behaviorD'Ayala and Speranza (2003). (ii) The seismic response of URMs with a box like behavior consists of an in-plane response of each bearing walls. The global behavior is affected by the high stiffness, low tensile and shear strength, low ductility, and low capacity of bearing reverse loading of the structure Rota et al. (2010). Three parameters accurately describes the seismic behavior of URMs: (i) the elastic displacement defines the attainment of the first significant crack at which the stiffness decreases; (ii) the maximum resistance reveals the achievement of the building performance; (iii) instead, the ultimate displacement specifies the 80 % of the maximum resistance. Thus, the in-plane response of URMs is more difficult to appraisal than local mechanisms and few research studies have been reserved effort to found simplifications in numerical or mechanical modelingRota et al. (2010).

Numerical and mechanical modelling capture the seismic behaviour in

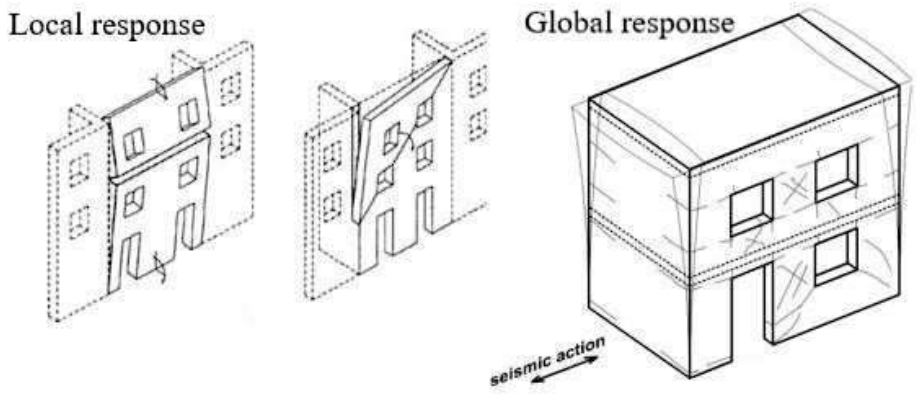

Figure 7.1. Seismic response of URMs: local and global mechanisms.

non-linear field, although an in in-depth knowledge of the structure is required to perform a reliable analysis. Nevertheless, these modelling strategies require high effort and time consuming. As repeatedly stated, the seismic evaluation of numerous buildings through numerical or mechanical approaches is a tricky activity at territorial scale. Considering the outcomes of other procedures, the authors chose to develop a simplified mechanical method, focusing on the outcomes of the proposed empirical one. Furthermore, some simplifications are removed from the modelling strategies available in literature to propose a more refined method. For example, the RE.SIS.TO method appraisals the seismic behaviour through a modelling of a URM carrying out analyses for single stories to grasp the first story that attains the failure condition.

The aim of the method proposed is performing a blind prediction of the seismic capacity of a URM with flexible floor (wooden, iron or vaults). The reliability of the method in evaluating the seismic response is confirmed through a comparison with the results of static no-linear analysis of the buildings' sample, that covers different structural configurations, for a total of 15 URMs and 95 masonry walls analysed. Overall, 380 static non-linear analysis are performed to deliver robust data. In the next paragraphs, the mechanics-based strategy is carefully discussed. The mechanical method concludes the multi-criteria approach for seismic assessment of URMs proposed in this PhD thesis with suggestions of meaningful applications on seismic risk mitigation.

7.2 Proposed mechanics-based method criteria

The authors proposed a mechanics-based method for the prediction of masonry walls under a seismic action. The aim of the last method is a more performing seismic analysis than the empirical method. The main purpose of the method is the derivation of structural indicators of the seismic performance of URMs. The advantages of the method are the accuracy in grasping the seismic fragilities of URMs and the limited time and efforts compared to numerical analyses.

The method could be applied to URMs with flexible floors. An adequate in-plane stiffness and effective connections floors-to-walls improve the box-like behavior of URMs leading to a better distribution of horizontal forces to the bearing masonry walls **?**. The seismic performance of URMs of pre-anti seismic code is primarily influenced by masonry walls' behavior due to the negligible role of flexible floors. A flexible floor not ensure the forces' distribution among bearing walls, leading to an independent in-plane behavior of each bearing wall. This structural behavior justifies the analysis of each single masonry wall. The method evaluates the seismic behavior of URMs in terms of shear strength and Peak Ground Acceleration (PGA) capacity. The mechanics-based method follows the same two phases of the empirical one: (i) the derivation of a vulnerability index for each masonry wall of the analysed building, in each main direction; (ii) the derivation of a global index representative of the entire building vulnerability as the minor masonry walls' indices.

7.2.1 Mechanics formulations of the mechanics-based method

URMs with flexible floors denote a partial or total absent coupling effect among masonry walls due to the low resistance and stiffness of floors, leading to a weak like box-behavior of the structure. Therefore, the seismic capacity of the structure is strongly related to the activation of the first failure mechanism of masonry walls. Also the scientific community confirms the critical role of flexible diaphragms in the overall seismic response of the masonry buildings **???**. Due to the reasons above, the authors chose to focus on each masonry wall, in order to grasp the activation of the fail-

ure mode that overcome the first damage threshold, affecting the seismic performance of a URM with flexible floors.

Masonry's mechanical properties, the resistance of masonry spandrels, and the geometrical configuration play a crucial role in both the in-plane and out-of-plane seismic response. Several recent studies have investigated the influence of the mechanical characteristics on the evaluation of the seismic behavior Capanna et al. (2021); **?**. Conversely, few studies have attempted to inspect opening size and position effect on the in plane failure modes **????**. First of all, the in-plane response of masonry walls with openings can be discretized by three structural compounds: vertical panels, also called piers, that support dead and seismic loads; horizontal panels, also named spandrels, that link the vertical panels; and rigid nodes, that are the masonry portions confined between vertical and horizontal panels, undamaged under seismic actions. The authors introduced a classification of the walls based on geometrical configurations typical of URMs. These buildings consist of more openings in the exterior walls, distributed in a regular configuration. Sometimes, the interior spaces, over the years, have been modified, leading to the realization of new openings into the walls and more articulated and irregular layout of walls, specially at the ground floors.

The three references walls, established based on the disposition of the openings. They are previously discussed in chapter 5. In the first layout typology, called *Class A*, the wall behavior is regular along the height. It consists in a squat and a slender piers, mainly. The second layout typology, named *Class B*, offers a not negligible reduction of the shear resistance and stiffness in elevation, leading to a high difference of the displacements between the floors. The third layout typology, called *Class C* entails the worst seismic behaviour: the remarkable enhancement of stiffness, along the height, causes a localized collapse or a soft floor. In the light of the above mentioned, a simplified constitutive law of each masonry wall class has been proposed to describe the behavior under horizontal actions. A mechanical definition of the constitutive laws was derived for each masonry walls differently, in terms of the elastic displacement, $d_{y,eq}$, see Eq.7.2, ultimate displacements, $d_{u,eq}$, see Eq.7.3, stiffness k_{eq}, see Eq.7.4, and the maximum

shear resistances $V_{r,eq}$, see Eq.7.1. The validation of the constitutive laws has been proved based on the equivalent area criterion, considering equal areas below the both systems' curves.

$$V_{eq} = \begin{cases} = V_{max,sq}, & \text{Class A} \\ = \sum_{k=1}^{j} V_{r,i}, & \text{Class B} \\ = \sum_{k=1}^{j} V_{r,i}, & \text{Class C} \end{cases} \tag{7.1}$$

$$d_{y,eq} = \begin{cases} = d_{y,sq}, & \text{Class A} \\ = mean(d_{y,i}), & \text{Class B} \\ = \dfrac{V_{eq}}{K_{eq}}, & \text{Class C} \end{cases} \tag{7.2}$$

$$d_{u,eq} = \begin{cases} = d_{u,sq}, & \text{Class A} \\ = mean(d_{u,i}), & \text{Class B} \\ = mean(d_{u,i}), & \text{Class C} \end{cases} \tag{7.3}$$

$$k_{eq} = \begin{cases} = k_{eq,sq}, & \text{Class A} \\ = \dfrac{V_{eq}}{d_{eq}}, & \text{Class B} \\ = \sum_{k=1}^{j} k_i, & \text{Class C} \end{cases} \tag{7.4}$$

where i indicates each masonry piers, sq and sl indicate the squat and slender piers of the Class A wall, respectively. After this evidences, the authors proposed a schematize of walls as an equivalent single degree of freedom (ESDOF). At each floor of the wall, the proper constitutive law may be assigned at varying the wall class. The mass of the ESDOF, m^*, is evaluated according to the Eq.7.5:

$$m^* = A_{eff} * \gamma * t * h_f \tag{7.5}$$

where γ is the specific weight of the masonry, t the thickness of the wall and h its height. Based on this simplified model, a blind prediction of the mechanical behavior has been derived. The horizontal forces are assigned as a force system distributed along the height of the WSDOF, following the equation Eq.7.6:

$$F_i = F_{b,e} * \frac{z_i * m^*}{\sum(z_i * W_i)} \tag{7.6}$$

where $F_{b,e}$ is the seismic force at the base of the wall, W_i is the seismic weigh of the floor, z_i is the height of the floor from the base of the structure. An index of the wall i_d, see Eq.7.7, express the attainment of the first damage:

$$i_d = min(i_{d,i}) = min(\frac{F_i}{V_i}) \tag{7.7}$$

where $i_{d,i}$ indicates an index of each floor of the wall. Finally, the capacity peak ground acceleration is evaluated considering a behaviour factor equal to 2. The index representative of the seismic safety i_v is evaluated as the ratio between capacity and demand peak ground acceleration. Flexible floors ensure an absent coupling effect among masonry walls. Therefore, the masonry wall with the worst seismic performance is considered representative of vulnerability level of the entire building, $i_{v,m}$, evaluated as the minimum value of walls' indices i_{v,m_i}. In order to confirm the reliability of the blind prediction proposed, a comparison with numerical and analytical methods was carried out.

7.2.2 Validation of the mechanical method

The capability of the mechanics-based method proposed was investigated. 9 URMs of the buildings' sample have flexible floors. The buildings analysed for this research activity are listed in Table 7.1. For each of them, for X-Direction and Y-Direction, the number of masonry walls (n_x and n_y) have been specified.

.

Therefore, the mechanical method proposed has been validated based on the numerical results of non-linear static analysis. The numerical data used consists of 24 analysis for 59 masonry walls, for a total of 1416 analysis. Table 7.2 reports the main numerical outputs of the pushover analysis for the lowest safety level, for each masonry wall: the yielding force F_y, the yielding and ultimate displacements, d_y and d_u, of the equivalent single degree-of-freedom (SDOF) system, the safety factor ψ_u, and the capacity

Buildings	n_x	n_y
B1	2	5
B2	3	4
B3	3	4
B4	2	4
B9	4	4
B11	3	4
B13	4	2
B14	3	4
B15	2	2

Table 7.1. Characterization of the buildings' sample.

peak ground acceleration PGA_c referred to the LS3. Similarly, Table 7.3 reports the main numerical outputs for buildings B5, B9 and B15, for which the empirical method fails.

.

.

As already mentioned, the complexity of seismic behavior of URMs exasperates the sensitivity of numerical tools to the input variables. The authors performed a parametric analysis, in a previous research activity Capanna et al. (2021), to investigate the sensitivity of the seismic response of historical URMs by varying a suite of modelling parameters, which express the scatter of the mechanical properties typical of the investigated construction typology. Furthermore, the parametric assessment, discussed in the Chapter 4, to address the choice of the parameters involved in the model updating, also highlights the influence of mechanical parameters on the the dynamic behavior of URMs. Moreover, different modeling strategies are employed by software packages, leading to a scatter of the numerical results: different numerical software packages could provide different numerical results. The data set of numerical anlaysis is herein used to prove the reliability of the proposed method in evaluating the structural behavior of URMs. The numerical results may lead to inaccurate comparison, in the light of the sensitivity of numerical tools to the input variables and modelling strategies. Therefore, the authors performed seismic analysis of the buildings sample also through an analytical approach developing a calculation code to perform static no linear analysis based on the code formulations dei Trasporti e delle Infrastrutture (2008); Herrmann and Bucksch (2014);

Buildings	**Wall**	**Wall**	F_y $[kN]$	d_y $[cm]$	d_u $[cm]$	ψ_u	PGA_c $[g]$
B1	X1	A	210	0.5	2.44	0.90	2.30
B1	X2	A	275	0.39	0.95	0.69	1.76
B1	Y1	A	122.06	0.5	2.82	1.10	2.98
B1	Y2	A	148.10	0.65	2.48	0.85	2.15
B1	Y3	C	62	1.02	4.23	0.68	1.76
B1	Y4	A	153.72	0.45	1.50	0.98	2.5
B1	Y5	A	176.48	0.54	1.99	1.13	2.88
B2	X1	C	152.77	0.20	0.92	1.35	2.44
B2	X2	A	152.45	0.19	1.06	2.15	3.88
B2	X3	C	47.14	0.26	0.78	0.62	1.11
B2	Y1	A	100.11	0.19	1.03	2.07	3.73
B2	Y2	A	52.88	0.21	1.22	1.12	2.01
B2	Y3	A	30	0.08	0.82	1.54	2.78
B2	Y4	A	62.26	0.44	2.04	1.09	1.97
B4	X1	C	100.20	0.63	4.91	0.70	1.79
B4	X2	A	192.45	0.32	0.86	0.66	1.68
B4	Y1	A	138	0.69	2.30	0.93	1.95
B4	Y2	A	120.75	1.23	2.06	0.45	1.15
B4	Y3	A	114.89	1.59	4.44	0.81	2.07
B4	Y4	A	69.75	0.75	4.46	1.02	2.59
B11	X1	C	140	0.44	3.46	1.31	3.34
B11	X2	C	366	0.26	1.28	1.64	4.18
B11	X3	C	167	0.66	3.94	1.20	3
B11	Y1	C	106	0.19	1.37	1.70	4.3
B11	Y2	C	74	0.38	3.99	0.78	1.99
B11	Y3	C	103	0.48	4.19	1.10	2.80
B11	Y4	C	103	0.34	2.91	1.24	3.18
B13	X1	A	223.54	0.31	2.13	1.28	3.14
B13	X2	A	142.09	0.45	2.31	0.92	2.23
B13	X3	B	81.33	0.22	2.24	0.83	2.03
B13	X4	A	157.66	0.39	2.64	1.22	2.98
B13	Y1	A	59.70	0.75	4.82	0.41	1
B13	Y2	A	216.45	0.20	0.52	0.55	1. 36
B14	X1	A	256	0.93	3.27	0.71	1. 73
B14	X2	B	140	0.48	2.63	0.967	2.37
B14	X3	A	257.66	0.45	1.14	0.439	1.07
B14	Y1	C	75	2.53	6.77	0.55	1.35
B14	Y2	B	175.16	1.12	1.99	0.39	0.95
B14	Y3	B	205.83	0.82	1.54	0.48	1.17
B14	Y4	C	96	0.75	2.58	0.43	1.06

Table 7.2. Results of numerical static non-linear analyses for each masonry wall of the selected buildings.

Buildings	**Wall**	**Class**	F_y **[kN]**	d_y **[cm]**	d_u **[cm]**	ψ_u	PGA_c**[g]**
B3	X1	A	213.85	0.13	0.98	1.64	3.17
B3	X2	A	220.39	0.21	0.36	0.48	0.93
B3	X3	A	198.34	0.12	1.88	1.82	3.50
B3	Y1	A	79	0.17	1.56	1.96	1.96
B3	Y2	A	150.84	0.14	1.16	2.33	1.96
B3	Y3	A	82	0.18	2.58	1.84	1.93
B3	Y4	A	82	0.14	3.16	1.69	3.26
B9	X1	A	128.98	0.39	2.08	0.96	2.46
B9	X2	A	101.95	0.09	3.04	5.59	13.48
B9	X3	C	195.66	0.59	4.09	0.78	1.99
B9	X4	C	163	0.89	6.45	0.8	2.5
B9	Y1	C	154.82	0.12	2.19	0.62	2.54
B9	Y2	A	632.42	0.50	1.77	0.85	2.19
B9	Y3	A	433.58	0.45	2.03	1.08	2.76
B9	Y4	C	436.61	0.42	0.90	0.51	1.31
B15	X1	A	257.82	0.29	1.27	1.01	2.58
B15	X2	A	73.98	0.69	4.13	0.63	1.61
B15	Y1	A	138.67	0.37	1.11	0.74	1.87
B15	Y2	A	74.05	0.54	3.72	0.66	1.7

Table 7.3. Results of numerical static non-linear analyses for each masonry wall of the selected buildings.

per le Costruzione (2018). In this way, the author could better understand the results. The comparison of the masonry analysis results underlines that the simplified mechanical method yielded results affected by a discrepancy minor of 35 % for 28 masonry walls. Moreover, the method fails in the seismic evaluation for some masonry walls that belong to three URMs (B3, B9 and B15). In Fig.7.2, the plan of the three buildings are reported.

Some considerations can be drawn about the structural configuration of these three buildings. B3 presents a structural configuration that consists of two parts linked by a stair. Therefore, under seismic action, the two main parts attain to an independent seismic behavior as two structural units. B9 shows an L-shaped plan and an irregular configuration along the height. Furthermore the presence of some masonry walls not built down to foundations leads to a complex dynamic behavior. The numerical model consists of some stiff links to transfer the load of the these masonry walls to bearing ones. This aspect is not taken account by the proposed mechanical model. Therefore, the distribution of the vertical load is different

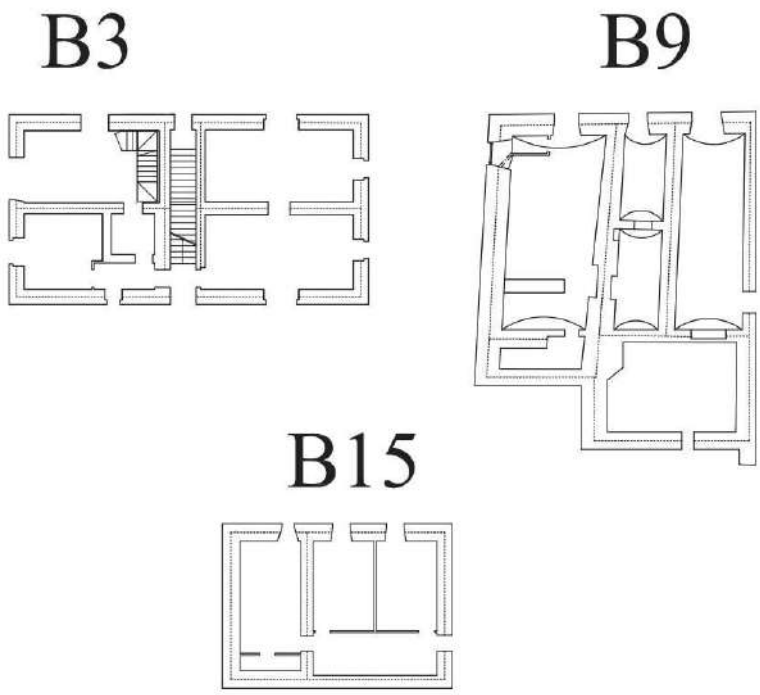

Figure 7.2. Geometric plan of the ground floor of the B3, B9 and B15 URMs.

between the numerical and mechanical evaluation leading to different tensional state and shear strength. B15 consists of a reinforced concrete roof that contributes to the structural behavior of the URM and the high load at the roof height engenders amplification phenomena of the seismic action and a preponderant irregular behavior along the height, difficult to grasp by means a simplified evaluation.

In the light of above, the proposed mechanical method is reliable to evaluate the seismic safety level for URMs that exhibit seismic performance driven by a regular behaviour in plan and in elevation. Nevertheless, the mechanical approach predicts the vulnerability index, $i_{v,m}$, referred to the entire buildings, in a satisfying agreement with numerical results, $i_{v,n}$. Table7.4 reports results of all seismic analysis through numerical, empirical and mechanical analysis.

.

Moreover, Table7.4 confirms the higher accuracy of the mechanical approach in evaluating seismic vulnerability level than the empirical one. Fig.7.3 plots the the mean damage μ_D, for the mean value of the vulnerability indices of selected buildings, evaluated through each approach (empirical $\mu_{D,L1}$, mechanical $\mu_{D,L2}$ and numerical $\mu_{D,N}$), reporting a graphical

Buildings	$i_{v,n}$	$i_{v,e}$	$i_{v,m}$
B1	0.23	0.43	0.36
B2	0.34	0.46	0.40
B3	0.65	0.43	0.59
B5	0.41	0.42	0.35
B9	0.30	0.54	0.25
B11	0.94	0.35	0.37
B13	0.31	0.39	0.25
B14	0.27	0.55	0.23
B15	0.25	0.44	0.15

Table 7.4. Results of all seismic analysis.

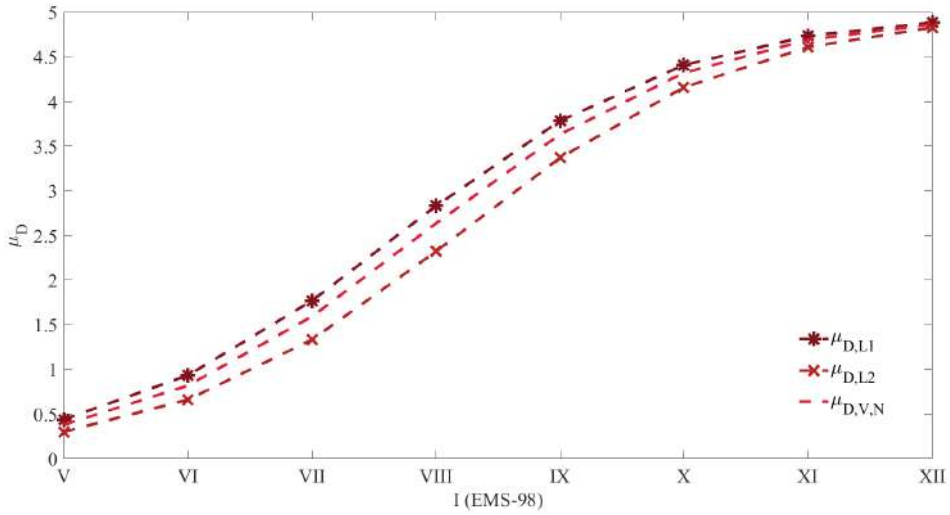

Figure 7.3. Mean damage curves for each approach.

comparison among the methods.

In the light of above, the mechanical approach reliably predicts the seismic vulnerability level of a URMs. Its accuracy delivers vulnerability indices in agreement with the numerical ones and the localization of the most vulnerable masonry wall. Therefore, the mechanical method could drive a more refined analysis to design strengthening measures aimed to enhance the seismic safety of URMs.

7.3 Suggestions for further applications of the mechanical method

The mechanical method provides a simplified analysis of URMs that grasps their structural behavior accurately, with a limited effort. The benefits of

the method embraces meaningful applications. Mainly, the method could be provide a practice oriented way to investigate the vulnerability level of URMs. The application of the empirical method provides a screening of seismic vulnerabilities of URMs, to which the application of the mechanical method could follow for URMs with flexible floors. The mechanical method grasps the vulnerability level less roughly than the empirical one. A knowledge of a quantitative vulnerabilities indices, representative of the structural expected seismic performance, could support seismic evaluations in forecasting the mitigation strategies quantitatively. Based on the results of mechanical approach, the strengthening measure could be addressed to masonry walls affected by worse seismic performance. As a further development of the research activity, the authors intend to consider the influence of stiffness floors in the mechanical method. This achievement could extend the application of the mechanical method to the whole URMs typology.

Research significance and future outcomes

Chapter abstract

The last chapter wants to tread the path followed by the carried out PhD activity. The research achievements have been discussed from a critical point of view. A discussion of the obtained results evidences the advantageous of the proposed assessment method that could promote further developments and applications. At the same time, the limitations of the assessment method have been underlined, with the aim to overcome them with targeted studies. Several applications of the simplified vulnerability method have been suggested. The last aim of the chapter is the definition of the role of the two criteria of the proposed method in seismic risk mitigation field.

8.1 Research significance and future outcomes

The seismic risk is an insurmountable issue to face for authorities, rescuer, technicians, and citizens. The impact of the seismic risk on human life needs to be mitigated to reduce decades, casualties, damaged buildings, homeless, and economic losses. The main fragility of the built environment is its inability to withstand seismic actions, confirmed by its aftermaths. Thus, the only strategy, that could satisfy this request, resides in the reduction of the structural vulnerabilities to mitigate the seismic risk. This achievement is firstly possible through the knowledge of the seismic vulnerability level of the built heritage, that represents the preliminary activity to undertake for the improvement of seismic performance. Worldwide, researchers reserve effort in developing seismic assessment methods increasingly performing. The discussed thesis, that places in this research field of earthquake engineering, attempted to propose a multi criteria vulnerability method to satisfy needs of authorities and stakeholders. Their interest arises from different goals to achieve. Authorities need to know the seismic risk from a territorial point of view. Their activities focus on the management of the built area, in previous and post emergency conditions. Therefore, a screening of the seismic vulnerabilities of URMs support the authorities: (i) before an earthquake occurs, in emergency management, like the design of the Emergency Limit Condition (ELC); (ii) after an earthquake, in surveying damage and assigning seismic risk mitigation measures. Authorities (like administrations, rescuer, etc.) need the knowledge of the seismic risk level from a territorial point of view. Other stakeholders (like technicians and citizens) require the investigation of the seismic risk from a local point of view. For example, technicians undertake vulnerability assessment of one or few buildings to evaluate the vulnerability level, in the design of straightening interventions, to improve seismic performance. Well, the Eq.8.1 defines the seismic risk, see Fig. 8.1.

$$R = \frac{f * M}{K} \tag{8.1}$$

where f is the frequency of occurrence of the earthquake, M the magnitude of seismic damage and K is a constant that expresses the awareness

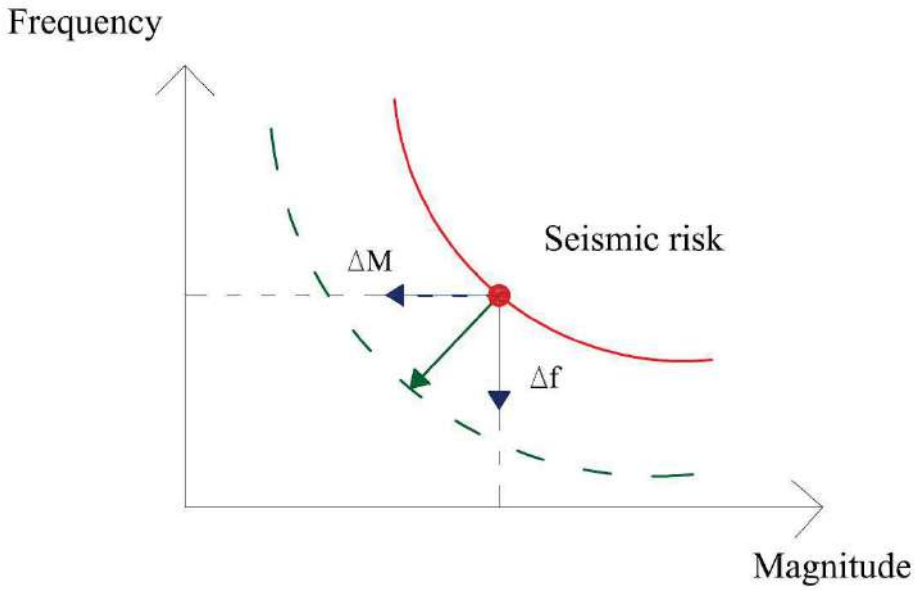

Figure 8.1. Seismic risk curve.

of the risk. The seismic risk could be mitigated by the reduction of the Magnitude ΔM and K.

Therefore, the knowledge of the seismic vulnerabilities enhances the awareness to face earthquakes. In mathematical terms, K takes into account this evidence. Whereas, ΔM is ensured through the seismic mitigation of the built environment fragilities. The multi criteria assessment method attempts to reduce the seismic risk acting on ΔM and K.

The empirical vulnerability assessment method for URMs bases on the evaluation of few structural parameters, which can be determined from visual inspection and a geometry survey. It seeks to overcome the application effort of a vulnerability assessment on a large scale. The method could be used to predict likely seismic damage scenarios for various earthquake intensities, useful for resilience-enhancing strategies for masonry construction at territorial scale. A path has been proposed to improve urban resilience through the proposed seismic assessment method. Typological fragility curves for the macro-typology of URMs, retrofitting solutions and losses' estimations embrace a suite of activities that could support the authorities in their evaluation at territorial level. The mechanical approach completes the multi criteria assessment method. It provides the seismic capacity of masonry walls more accurately respect to the empirical method, for a refined seismic assessment. The method represents a practice oriented way to

investigate the vulnerability level of URMs, with flexible floors. Still, the mechanical method delivers a robust prediction of the seismic performance, in order to establish strengthening decisions more accurately.

Therefore, the multi criteria assessment methods supplies a powerful path to follow to reduce the seismic risk. The empirical method allows to know seismic vulnerabilities at territorial level quickly. This achievement mainly influences the enhancement of the awareness, K, of the seismic risk. Based on the first screening empirically derived, the mechanical method allows to undertake a more refined seismic assessment, on which strengthening measure could be accurately appraised. This assessment could be useful to appraise the magnitude of effect of the seismic risk, that could be mitigated through strengthening interventions (in Eq.8.1 the termsΔM.)

In the light of above, the multi criteria method could be support seismic risk management activities to deepen the fragilities of built areas.

[Blank page]

Bibliography

Acito, M., Bocciarelli, M., Chesi, C., and Milani, G. (2014). Collapse of the clock tower in finale emilia after the may 2012 emilia romagna earthquake sequence: Numerical insight. *Engineering Structures*, 72:70–91.

Agency, F. (1997). Nehrp guidelines for the seismic rehabilitation of buildings (fema publication 273).

Aşıkoğlu, A., Vasconcelos, G., Lourenco, P., and Del Re, A. (2020). *Seismic response of an unreinforced masonry building with structural irregularity; Blind prediction by means of pushover analysis*, pages 1037–1045.

Allemang, R. and Brown, D. (1982). A correlation coefficient for modal vector analysis. *Proceedings of the 1st International Modal Analysis Conference*.

Aloisio, A. and Fragiacomo, M. (2021). Reliability-based overstrength factors of cross-laminated timber shear walls for seismic design. *Engineering Structures*, 228:111547.

Aloisio, A., Pasca, D. P., Tomasi, R., and Fragiacomo, M. (2020a). Dynamic identification and model updating of an eight-storey clt building. *Engineering Structures*, 213.

Aloisio, A., Pasquale, A., Alaggio, R., and Fragiacomo, M. (2020b). Assessment of seismic retrofitting interventions of a masonry palace using operational modal analysis. *International Journal of Architectural Heritage*.

Angiolilli, M., Lagomarsino, S., Cattari, S., and Degli Abbati, S. (2021). Seismic fragility assessment of existing masonry buildings in aggregate. *Engineering Structures*, 247:113218.

Augenti, N. and Parisi, F. (2009). Seismic vulnerability and damage of masonry buildings.

Baker, J. (2013). Efficient analytical fragility function fitting using dynamic structural analysis. *Earthquake Spectra*, 31.

Barbalić, M., Polić, S., Barbalić, D., Vukmanić, L., and Majerović, T. (2016). Risk assessment of fluvial floods for the risk assessment for disaster management.

Basar, T., Deb, S., Das, P., and Sarmah, M. (2021). Seismic response control of low-rise unreinforced masonry building test model using low-cost and sustainable un-bonded scrap tyre isolator (u-sti). *Soil Dynamics and Earthquake Engineering*, 142:106561.

Benedetti, D. and Petrini, V. (1984a). Sulla vulnerabilita di edifici in muratura: proposta di un metodo di valutazione. *Industria Costruzioni*, 18:66–74.

Benedetti, D. and Petrini, V. (1984b). Vulnerability of masonry buildings: Proposal of a method of assessment (in italian). *L'Industria Costruzioni*, 149:66–74.

Booth, E., Saito, K., Spence, R., Madabhushi, G., and Eguchi, R. (2011). Validating assessments of seismic damage made from remote sensing. *Earthquake Spectra*, 27:S157–S177.

Bozza, A., Asprone, D., and Manfredi, G. (2015). Developing an integrated framework to quantify resilience of urban systems against disasters. *Natural Hazards*, 78.

Bramerini, F., Conte, C., Castenetto, S., and Naso, G. (2014). Analisi della condizione limite per l'emergenza (cle): considerazioni preliminari sui dati raccolti.

Brando, G., De Matteis, G., and Spacone, E. (2017). Predictive model for the seismic vulnerability assessment of small historic centres: Application to the inner abruzzi region in italy. *Engineering Structures*, 153:81–96.

Brandonisio, G., Lucibello, G., Mele, E., and Luca, A. (2013). Damage and performance evaluation of masonry churches in the 2009 l'aquila earthquake. *Engineering Failure Analysis*, 34:693–714.

Cacace, F., Zuccaro, G., De Gregorio, D., and Perelli, F. (2018). Building inventory at national scale by evaluation of seismic vulnerability classes distribution based on census data analysis: Binc procedure. *International Journal of Disaster Risk Reduction*, 28.

Calò, M., Malomo, D., Gabbianelli, G., and Pinho, R. (2021). How detailed should your masonry model be? *Proceedings of the 14th Caandian Masonry Symposium, Montreal, Canada*.

Calderoni, B., Cordasco, E., Pacella, G., Musella, C., and Sandoli, A. (2017). L'efficacia della modellazione a puntone delle fasce di piano degli edifici in muratura soggetti a forze orizzontali.

Capanna, I., Aloisio, A., Di Fabio, F., , and Fragiacomo, M. (2021).

Cardone, D., Gesualdi, G., and Perrone, G. (2017). Cost-benefit analysis of alternative retrofit strategies for rc frame buildings. *Journal of Earthquake Engineering*, 23.

Carpenter, S., Walker, B., Anderies, J., and Abel, N. (2001). From metaphor to measurement: Resilience of what to what? *Ecosystems*, 4:765–781.

Cavaleri, L., Di Trapani, F., and Ferrotto, M. (2017). A new hybrid procedure for the definition of seismic vulnerability in mediterranean cross-border urban areas. *Natural Hazards*, 86.

Chang, S., Mcdaniels, T., Fox, J., Dhariwal, R., and Longstaff, H. (2013). Toward disaster-resilient cities: Characterizing resilience of infrastructure systems with expert judgments. *Risk analysis : an official publication of the Society for Risk Analysis*, 34.

Chelleri, L., Olazabal, M., Kunath, A., Minucci, G., Waters, J., and Yumalogava, L. (2012). *Multidisciplinary perspectives on Urban Resilience*.

Chever, L. (2012). Use of seismic assessment methods for planning vulnerability reduction of existing building stock. *In Proceedings of the 15th WCEE-World Conference of Earthquake Engineering, Lisbon, Portugal, 2012*, pages 1 – 10.

Chiarabba, C., Jovane, L., and Di Stefano, R. (2005). A new view of italian seismicity using 20 years of instrumental recordings. *Tectonophysics*, 395:251–268.

Chieffo, N., Clementi, F., Formisano, A., and Lenci, S. (2019). Comparative fragility methods for seismic assessment of masonry buildings located in muccia (italy). *Journal of Building Engineering*, 25.

Coburn, A., Sspence, R., and Pomonis, A. (1994). Vulnerability and risk assessment.

Colonna, S., Imperatore, S., and Ferracuti, B. (2018). The 2016 central italy earthquake: Damage and vulnerability assessment of churches.

Commission, C. (1996). Atc-40: The seismic evaluation and retrofit of concrete buildings. *ATC*, 2.

Cornell, C. (1967). Engineering seismic risk analysis. 58.

Cornell, C. and Krawinkler, H. (2000). Progress and challenges in seismic performance assessment. *PEER Center News*, 3.

Cosenza, E., Del Vecchio, C., Di Ludovico, M., Dolce, M., Moroni, C., Prota, A., and Renzi, E. (2018). The italian guidelines for seismic risk classification of constructions: technical principles and validation. *Bulletin of Earthquake Engineering*, 16.

Cremen, G. and Baker, J. (2018). A methodology for evaluating component-level loss predictions of the p-58 seismic performance assessment procedure. *Earthquake Spectra*, 35.

Croce, P., Landi, F., and Formichi, P. (2019). Probabilistic seismic assessment of existing masonry buildings. *Buildings*, 9:237.

da porto, F., Donà, M., Rosti, A., Rota, M., Lagomarsino, S., Cattari, S., Borzi, B., Onida, M., Gregorio, D., Perelli, F., Gaudio, C., Ricci, P.,

and Speranza, E. (2021). Comparative analysis of the fragility curves for italian residential masonry and rc buildings. *Bulletin of Earthquake Engineering*, 19.

D'Alençon, R. and Rota, F. (2015). Heritage and catastrophes: Prevention, emergency, restoration and transformation in 2009 l'aquila earthquake.

D'Altri, A., Sarhosis, V., Milani, G., Rots, J., Cattari, S., Lagomarsino, S., Sacco, E., Tralli, A., Castellazzi, G., and Miranda, S. (2019). Modeling strategies for the computational analysis of unreinforced masonry structures: Review and classification. *Archives of Computational Methods in Engineering*, 27.

D'Ayala, D. (2013). *Assessing the seismic vulnerability of masonry buildings*, pages 334–365.

D'Ayala, D. and Speranza, E. (2003). Definition of collapse mechanisms and seismic vulnerability of historic masonry buildings. *Earthquake Spectra*, 19.

DE Martino, G., Di Ludovico, M., Prota, A., Moroni, C., Manfredi, G., and Dolce, M. (2015). Damage distribution and repair costs of private buildings after l'aquila earthquake.

DE Martino, G., Di Ludovico, M., Prota, A., Moroni, C., Manfredi, G., and Dolce, M. (2017). Analysis of the relationship between empirical damages and repair costs on rc private buildings after l'aquila earthquake.

De Matteis, G., Brando, G., Corlito, V., Criber, E., and Guadagnuolo, M. (2019). Seismic vulnerability assessment of churches at regional scale after the 2009 l'aquila earthquake. *International Journal of Masonry Research and Innovation*, 4:174.

De Risi, M. T., Del Gaudio, C., and Verderame, G. (2019). Evaluation of repair costs for masonry infills in rc buildings from observed damage data: the case-study of the 2009 l'aquila earthquake. *Buildings*, 9:122.

Decanini, L., Liberatore, L., Mollaioli, F., and Monti, G. (2010). 2009 l'aquila earthquake -seismic demand and damage characterization.

dei Trasporti e delle Infrastrutture, M. (2008). Ntc2008, norme tecniche per le costruzioni. Technical report, DM 14/01/2008, In Italian.

Deierlein, G., Krawinkler, H., and Cornell, C. (2003). A framework for performance-based earthquake engineering.

Del Gaudio, C., DE Martino, G., Di Ludovico, M., Manfredi, G., Prota, A., Ricci, P., and Verderame, G. (2019). Empirical fragility curves for masonry buildings after the 2009 l'aquila, italy, earthquake. *Bulletin of Earthquake Engineering*, 17.

Del Gaudio, C., Ricci, P., and Verderame, G. (2015a). Observed and predicted earthquake damage scenarios: the case study of l'aquila municipality. pages 185–196.

Del Gaudio, C., Ricci, P., and Verderame, G. (2017). First remarks about the expected damage scenario following the 24 th august 2016 earthquake in central italy.

Del Gaudio, C., Ricci, P., Verderame, G., and Manfredi, G. (2015b). Development and urban-scale application of a simplified method for seismic fragility assessment of rc buildings. *Engineering Structures*, 91.

Del Vecchio, C., Di Ludovico, M., Pampanin, S., and Prota, A. (2017). Repair costs of existing rc buildings damaged by the l'aquila earthquake and comparison with fema p-58 predictions. *Earthquake Spectra*, 34.

Di Bucci, D., Burrato, P., Vannoli, P., and Valensise, G. (2010). Tectonic evidence for the ongoing africa-eurasia convergence in central mediterranean foreland areas: A journey among long-lived shear zones, large earthquakes, and elusive fault motions. *Journal of Geophysical Research (Solid Earth)*, 115:12404–.

Di Ludovico, M., DE Martino, G., Prota, A., Manfredi, G., and Dolce, M. (2021a). Relationships between empirical damage and direct/indirect costs for the assessment of seismic loss scenarios. *Bulletin of Earthquake Engineering*, pages 1–26.

Di Ludovico, M., DE Martino, G., Prota, A., Manfredi, G., and Dolce, M. (2021b). Relationships between empirical damage and direct/indirect

costs for the assessment of seismic loss scenarios. *Bulletin of Earthquake Engineering*, pages 1–26.

Di Ludovico, M., Digrisolo, A., Moroni, C., Graziotti, F., Manfredi, V., Prota, A., Dolce, M., and Manfredi, G. (2019). Remarks on damage and response of school buildings after the central italy earthquake sequence. *Bulletin of Earthquake Engineering*, 17.

Di Ludovico, M., Prota, A., Moroni, C., Manfredi, G., and Dolce, M. (2017). Reconstruction process of damaged residential buildings outside historical centres after the l'aquila earthquake: part i—"light damage" reconstruction. *Bulletin of Earthquake Engineering*, 15.

Di Sarno, L., da porto, F., Guerrini, G., Calvi, P., Camata, G., and Prota, A. (2019). Seismic performance of bridges during the 2016 central italy earthquakes. *Bulletin of Earthquake Engineering*, 17.

Dolce, M., Prota, A., Borzi, B., da porto, F., Lagomarsino, S., Magenes, G., Moroni, C., Penna, A., Polese, M., Speranza, E., Gerardo, ., Verderame, G., and Zuccaro, G. (2021). Seismic risk assessment of residential buildings in italy. *Bulletin of Earthquake Engineering*.

Dolce, M., Speranza, E., Giordano, F., Borzi, B., Bocchi, F., Conte, C., Meo, A., Faravelli, M., and Pascale, V. (2017). Da.d.o – a web-based tool for analyzing and comparing post-earthquake damage database relevant to national seismic events since 1976 - da.d.o - uno strumento per la consultazione e la comparazione del danno osservato relativo ai più significativi eventi sismici in italia dal 1976.

Domaneschi, M., Cimellaro, G., and Scutiero, G. (2019). A simplified method to assess generation of seismic debris for masonry structures. *Engineering Structures*, 186:306–320.

Du (2020). Probabilistic seismic hazard assessment for singapore. *Natural Hazards*, 103.

Economidou, M., Atanasiu, B.and Despret, C. M. J., Nolte, I., and Rapf, O. (2011). Europe's buildings under the microscope. a country-by-

countryreview of the energy performance of buildings. *Buildings Performance Institute Europe (BPIE)*.

Ercolino, M., Magliulo, G., and Manfredi, G. (2016). Failure of a precast rc building due to emilia-romagna earthquakes. *Engineering Structures*, 118:262–273.

Felice, G., De Santis, S., Lourenco, P., and Mendes, N. (2017). Methods and challenges for the seismic assessment of historic masonry structures. *International Journal of Architectural Heritage*.

Ferreira, T., Maio, R., and Vicente, R. (2017). Seismic vulnerability assessment of the old city centre of horta, azores: calibration and application of a seismic vulnerability index method. *Bulletin of Earthquake Engineering*, 15:2879–2899.

Ferreira, T., Vicente, R., Mendes Silva, R., Varum, H., and Costa, A. (2013). Seismic vulnerability assessment of historical urban centres: Case study of the old city centre in seixal, portugal. *Bulletin of Earthquake Engineering*, 11:1–21 LA.

Fiorentino, G., Forte, A., Pagano, E., Sabetta, F., Baggio, C., Lavorato, D., Nuti, C., and Santini, S. (2018). Damage patterns in the town of amatrice after august 24th 2016 central italy earthquakes. *Bulletin of Earthquake Engineering*, 16.

Formisano, A. (2012). School damage assessment of school buildings after 2012 emilia romagna earthquake. *Journal of Earthquake Engineering*, 2-3:72–86.

Formisano, A., Feo, P., Grippa, M., and Florio, G. (2010). L'aquila earthquake: A survey in the historical centre of castelvecchio subequo. *COST ACTION C26: Urban Habitat Constructions under Catastrophic Events - Proceedings of the Final Conference*, pages 371–376.

Formisano, A., Florio, G., Landolfo, R., and Mazzolani, F. (2011). Numerical calibration of a simplified procedure for the seismic behaviour assessment of masonry building aggregates.

Formisano, A., Florio, G., Landolfo, R., and Mazzolani, F. (2014). Numerical calibration of an easy method for seismic behaviour assessment on large scale of masonry building aggregates. *Advances in Engineering Software*, 80.

Forte, G., Chioccarelli, E., Falco, M., Cito, P., Santo, A., and Iervolino, I. (2019). Seismic soil classification of italy based on surface geology and shear-wave velocity measurements. *Soil Dynamics and Earthquake Engineering*, 122:79–93.

Fragomeli, A., Galasco, A., Graziotti, F., Guerrini, G., Kallioras, S., Magenes, G., Malomo, D., Mandirola, M., Manzini, C. F., Marchesi, B., Milanesi, R., Morandi, P., Penna, A., Rossi, A., Rosti, A., Rota, M., Senaldi, I., Tomassetti, U., Cattari, S., and Sorrentino, L. (2017). Performance of masonry buildings in the seismic sequence of central italy 2016 - part 2: case studies of affected municipalities. *Progettazione Sismica*, 8:75–95.

Friswell, M. and Mottershead, J. (1995). *Finite Element Model Updating in Structural Dynamics (Solid Mechanics and Its Applications)*.

Gaetani d'Aragona, M., P. M. and Prota, A. (2020). Stick-it: A simplified model for rapid estimation of idr and pfa for existing low-rise infilled rc building typologies. *Engineering Structures*, 223:111182.

Galadini, F., Falcucci, E., Gori, S., Zimmaro, P., Cheloni, D., and Stewart, J. (2018). Active faulting in source region of 2016–2017 central italy event sequence. *Earthquake Spectra*, 34.

Gambarotta, L. and Lagomarsino, S. (1996). On dynamic response of masonry panels. *Proceedings of the national conference on 'Masonry mechanics between theory and practice', Messina, Italy*.

Gambarotta, L. and Lagomarsino, S. (1997). Damage models for the seismic response of brick masonry shear walls. part i: the mortar joint model and its applications. *Earthquake Engineering and structural dynamics*, 26:423–439.

Gattesco, N., Rinaldin, G., and Claudio, A. (2014). Experimental and numerical characterization of the cyclic behaviour of unreinforced and reinforced masonry spandrels.

Giovinazzi, S., Marchili, C., Pietro, A., Giordano, L., Costanzo, A., Porta, L., Pollino, M., Rosato, V., Lückerath, D., Milde, K., and Ullrich, O. (2021). Assessing earthquake impacts and monitoring resilience of historic areas: Methods for gis tools. *ISPRS International Journal of Geo-Information*, 10:461.

Girardi, M., Padovani, C., Pellegrini, D., Porcelli, M., and Robol, L. (2018). Finite element model updating for structural applications. *Journal of Computational and Applied Mathematics*, 370.

GNDT-SSN (1994). Scheda di esposizione e vulnerabilità e di rilevamento danni di primo e secondo livello (muratura e cemento armato). *GNDT-SSN*.

Grünthal, G. (1998). *European Macroseismic Scale 1998 (EMS-98). European Seismological*.

Hazus, E. L. E. M. (1997). Technical manual. *National Institute of Building for the Federal Emergency Management Agency, Washington (DC)*.

Herrmann, H. and Bucksch, H. (2014). *Eurocode 8 - Design of structures for earthquake resistance*.

Holling, C. (1973). Resilience and stability of ecological systems. ann rev ecol syst 4: 1-23. *Annual Review of Ecology and Systematics*, 4:1–23.

Iervolino, I., Manfredi, G., Polese, M., Prota, A., and Verderame, G. (2014). L'aquila earthquake: A wake-up call for european research and codes. *Geotechnical, Geological and Earthquake Engineering*, 32:129–142.

Jiménez, B., Pelà, L., and Hurtado, M. (2018). Building survey forms for heterogeneous urban areas in seismically hazardous zones. application to the historical center of valparaíso, chile. *International Journal of Architectural Heritage*, 12:1076–1111.

Kappos, A., Panagopoulos, G., Panagiotopoulos, C., and Penelis, G. (2006). A hybrid method for the vulnerability assessment of r/c and urm buildings. *Bulletin of Earthquake Engineering*, 4:391–413.

Lagomarsino, S. and Giovinazzi, S. (2006). Macroseismic and mechanical models for the vulnerability assessment of current buildings. *Bulletin of Earthquake Engineering*, 4:415–443.

Lang, D., Kumar, A., Sulaymanov, S., and Meslem, A. (2017). Building typology classification and earthquake vulnerability scale of central and south asian building stock. *Journal of Building Engineering*, 15.

Leggieri, V., Ruggieri, S., Zagari, G., and Uva, G. (2021). Appraising seismic vulnerability of masonry aggregates through an automated mechanical-typological approach. *Automation in Construction*, 132:103972.

Lemos, J. (2007). Discrete element modeling of masonry structures. *International Journal of Architectural Heritage - INT J ARCHIT HERIT*, 1:190–213.

Locati, M., CAMASSI, R. D., Rovida, A. N., Ercolani, E., BERNARDINI, F. M. A., Castelli, V., Caracciolo, C. H., Tertulliani, A., Rossi, A., Azzaro, R., et al. (2016). Dbmi15, the 2015 version of the italian macroseismic database.

Lourenco, P., Rots, J., and Blaauwendraad, J. (1994). *Assessment of a Strategy for the Detailed Analysis of Masonry Structures*, pages 359–369.

Lucibello, G., Brandonisio, G., Mele, E., and Luca, A. (2013). Seismic damage and performance of palazzo centi after l'aquila earthquake: A paradigmatic case study of effectiveness of mechanical steel ties. *Engineering Failure Analysis*, 34:407–430.

Lulić, L., Ožić, K., Kišiček, T., Hafner, I., and Stepinac, M. (2021). Post-earthquake damage assessment—case study of the educational building after the zagreb earthquake. *Sustainability*, 13:6353.

Magenes, G., Penna, A., Senaldi, I., Rota, M., and Galasco, A. (2014). Shaking table test of a strengthened full-scale stone masonry building

with flexible diaphragms. *International Journal of Architectural Heritage*, 8.

Maio, R., Ferreira, T., Vicente, R., and Estêvão, J. (2016). Seismic vulnerability assessment of historical urban centres: case study of the old city centre of faro, portugal. *Journal of Risk Research*, 19:551–580.

Maio, R., Vicente, R., Formisano, A., and Varum, H. (2015). Seismic vulnerability of building aggregates through hybrid and indirect assessment techniques. *Bulletin of Earthquake Engineering*, 13.

Martino, S., Battaglia, S., D'Alessandro, F., Della Seta, M., Esposito, C., Martini, G., Pallone, F., and Troiani, F. (2020). Earthquake-induced landslide scenarios for seismic microzonation: application to the accumoli area (rieti, italy). *Bulletin of Earthquake Engineering*, 18.

Mascandola, C., Luzi, L., Felicetta, C., and Pacor, F. (2021). A gis procedure for the topographic classification of italy, according to the seismic code provisions. *Soil Dynamics and Earthquake Engineering*, 148:106848.

Mauro, D. (2012). The seismic prevention program. in proceedings of the 15th world conference on earthquake engineering in lisboa.

Mcdaniels, T., Chang, S., Cole, D., Mikawoz, J., and Longstaff, H. (2008). Fostering resilience to extreme events within infrastructure systems: Characterizing decision contexts for mitigation and adaptation. *Global Environmental Change*, 18:310–318.

McGuire, R. (2008). Probabilistic seismic hazard analysis: Early history. *Earthquake Engineering and Structural Dynamics*, 37:329 – 338.

Mendes, N. and Lourenco, P. (2010). Seismic assessment of masonry "gaioleiro" buildings in lisbon, portugal. *Journal of Earthquake Engineering*, 14:80–101.

Meslem, A., D'Ayala, D., Vamvatsikos, D., Porter, K., and Rossetto, T. (2016). *Guidelines for Analytical Vulnerability Assessment - Low/Mid-Rise*.

Mihalić Arbanas, S., Oštrić, M., and Krkac, M. (2011). Seismic microzonation: A review of principles and practice. *Geofizika*, 28:5–20.

Moreira, S., Ramos, L., Oliveira, D., and Lourenco, P. (2014). Experimental behavior of masonry wall-to-timber elements connections strengthened with injection anchors. *Engineering Structures*, 81:98–109.

Moscatelli, M., Albarello, D., Mugnozza, G., and Dolce, M. (2020). The italian approach to seismic microzonation. *Bulletin of Earthquake Engineering*, 18.

Mouzakis, C., Adami, C.-E., Karapitta, L., and Vintzileou, E. (2018). Seismic behaviour of timber-laced stone masonry buildings before and after interventions: shaking table tests on a two-storey masonry model. *Bulletin of Earthquake Engineering*, 16.

Narjabadifam, P., Hoseinpour, R., Noori, M., and Altabey, W. (2021). Practical seismic resilience evaluation and crisis management planning through gis-based vulnerability assessment of buildings. *Earthquake Engineering and Engineering Vibration*, 20:25–37.

Novelli, V., D'Ayala, D., Makhloufi, N., Benouar, D., and Zekagh, A. (2014). A procedure for the identification of the seismic vulnerability at territorial scale. application to the casbah of algiers. *Bulletin of Earthquake Engineering*, pages 1–26.

Ordaz, M. and Reyes, C. (1999). Earthquake hazard in mexico city: observations vs. computations. *Bulletin of the Seismological Society of America*, 89:1379–1383.

Ozyetgin Altun, A. and Tezer, A. (2018). A preliminary study on defining urban resilience for urban planning: The case of sultanbeyli, istanbul.

Pagliaroli, A. (2018). Key issues in seismic microzonation studies: Lessons from recent experiences in italy. *Rivista Italiana di Geotecnica*, 1/2018:5–48.

Parisi, V. (2013). *Federal Emergency Management Agency (FEMA)*, pages 321–322.

Pasticier, L., Amadio, C., and Fragiacomo, M. (2008). Non-linear seismic analysis and vulnerability evaluation of a masonry building by means of

the sap2000 v. 10 code. *Earthquake engineering and structural dynamics*, 37(3):467–485.

Paupério, E., Romão, X., Tavares, A., Vicente, R., Guedes, J., Rodrigues, H., Varum, H., and Costa, A. (2012). Survey of churches damaged by the may 2012 emilia-romagna earthquake sequence.

P.Code (2005). Eurocode 8: Design of structures for earthquake resistance-part 1: general rules, seismic actions and rules for buildings. Technical report, Brussels Eur. Comm. Stand.

Peeters, B. and De Roeck, G. (2001). Stochastic system identification for operational modal analysis: A review. *Journal of Dynamic Systems Measurement and Control-transactions of The Asme - J DYN SYST MEAS CONTR*, 123.

Penna, A., Calderini, C., Sorrentino, L., Carocci, C., Cescatti, E., Sisti, R., Borri, A., Modena, C., and Prota, A. (2019). Damage to churches in the 2016 central italy earthquakes. *Bulletin of Earthquake Engineering*, 17.

per le Costruzione, N. T. (2018). Aggiornamento delle norme tecniche per le costruzioni. Technical report, decreto 17-1-2018, Gazzetta Ufficiale 42, 20-02-2018, Ordinary Suppl.

Peter, F. (1999). Capacity spectrum method based on inelastic demand spectra. *Earthquake Engineering and Structural Dynamics*, 28:979 – 993.

Peter, F. (2000). A nonlinear analysis method for performance-based seismic design. *Earthquake Spectra - EARTHQ SPECTRA*, 16.

Peter, F. and Fischinger, M. (1987). Non-linear seismic analysis of rc buildings: Implications of a case study. *European Earthquake Engineering*, 1:31–43.

Pina-Henriques, J. and Lourenco, P. (2005). Masonry micro-modelling adopting a discontinuous framework.

Pina-Henriques, J. and Lourenco, P. (2006). Masonry compression: A numerical investigation at the meso-level. *Engineering Computations*, 23:382–407.

Polese, M., Gaetani d'Aragona, M., and Prota, A. (2019). Simplified approach for building inventory and seismic damage assessment at the territorial scale: An application for a town in southern italy. *Soil Dynamics and Earthquake Engineering*, 121:405–420.

Pondrelli, s., Visini, F., Rovida, A., D'Amico, V., Pace, B., and Meletti, C. (2020). Style of faulting of expected earthquakes in italy as an input for seismic hazard modeling. *Natural Hazards and Earth System Sciences*, 20:3577–3592.

Pulatsu, B., Bretas, E., and Lourenco, P. (2016). Discrete element modeling of masonry structures: Validation and application. *Earthquakes and Structures*, 11:563–582.

Rapone, D., Brando, G., Spacone, E., and De Matteis, G. (2018). Seismic vulnerability assessment of historic centers: description of a predictive method and application to the case study of scanno (abruzzi, italy). *International Journal of Architectural Heritage*, 12:1–25.

Reynolds, T., Harris, R., Chang, W.-S., Bregulla, J., and Bawcombe, J. (2015). Ambient vibration tests of a cross-laminated timber building. *Proceedings of the Institution of Civil Engineers-Construction Materials*, 168(3):121–131.

Risi, R., Sextos, A., Zimmaro, P., Simoneli, A., and Stewart, J. (2018). The 2016 central italy earthquake sequence: Observations of incremental building damage.

Rizzano, G., Sabatino, R., and Zambrano, M. (2009). L'influenza delle fasce di piano sulla resistenza di pareti in muratura.

Roca, P., Cervera, M., Gariup, G., and Pelà, L. (2010). Structural analysis of masonry historical constructions. classical and advanced approaches. *Archives of Computational Methods in Engineering*, 17:299–325.

Roselli, P., Marzocchi, W., Mariucci, M., and Montone, P. (2018). Earthquake focal mechanism forecasting in italy for psha purposes. *Geophysical Journal International*, 212:491–508.

Rossetto, T., D'Ayala, D., Gori, F., Persio, R., Han, J., Novelli, V., Wilkinson, S., Alexander, D., Hill, M., and Stephens, S. (2014). The value of multiple earthquake missions: The eefit l'aquila earthquake experience. *Bulletin of Earthquake Engineering*, 12:1–29.

Rossi, L., Holtschoppen, B., and Butenweg, C. (2019). Official data on the economic consequences of the 2012 emilia-romagna earthquake: a first analysis of database sfinge. *Bulletin of Earthquake Engineering*, 17.

Rossi, L., Stupazzini, M., Parisi, D., Holtschoppen, B., Ruggieri, G., and Butenweg, C. (2020). Empirical fragility functions and loss curves for italian business facilities based on the 2012 emilia-romagna earthquake official database. *Bulletin of Earthquake Engineering*, 18:1–29.

Rosti, A., Del Gaudio, C., Rota, M., Ricci, P., Di Ludovico, M., Penna, A., and Verderame, G. (2021a). Empirical fragility curves for italian residential rc buildings. *Bulletin of Earthquake Engineering*, 19:1–19.

Rosti, A., Rota, M., and Penna, A. (2021b). Empirical-fragility curves for italian urm buildings. *Bulletin of Earthquake Engineering*, 19.

Rota, M., Penna, A., and Magenes, G. (2010). A methodology for deriving analytical fragility curves for masonry buildings based on stochastic nonlinear analyses. *Engineering Structures*, 32:1312–1323.

Rota, M., Penna, A., and Strobbia, C. (2008). Processing italian damage data to derive typological fragility curves. *Soil Dynamics and Earthquake Engineering*, 28:933–947.

Ruggieri, S., Cardellicchio, A., Leggieri, V., and Uva, G. (2021a). Machine-learning based vulnerability analysis of existing buildings. *Automation in Construction*, 132:103936.

Ruggieri, S., Porco, F., Uva, G., and Vamvatsikos, D. (2021b). Two frugal options to assess class fragility and seismic safety for low-rise reinforced concrete school buildings in southern italy. *Bulletin of Earthquake Engineering*, 19.

Ruggieri, S., Tosto, C., Rosati, G., Uva, G., and Ferro, G. (2020). Seismic vulnerability analysis of masonry churches in piemonte after 2003 valle

scrivia earthquake: Post-event screening and situation 17 years later. *International Journal of Architectural Heritage*.

Saretta, Y., Sbrogiò, L., and Valluzzi, M. (2021). Assigning the macroseismic vulnerability classes to strengthened ordinary masonry buildings: An update from extensive data of the 2016 central italy earthquake. *International Journal of Disaster Risk Reduction*, 62:102318.

Senaldi, I., Magenes, G., Penna, A., Galasco, A., and Rota, M. (2014). The effect of stiffened floor and roof diaphragms on the experimental seismic response of a full scale unreinforced stone masonry building. *Journal of Earthquake Engineering*, 18.

Sextos, A., Risi, R., Pagliaroli, A., Foti, S., Passeri, F., Ausilio, E., Cairo, R., Capatti, M. C., Chiabrando, F., Chiaradonna, A., Dashti, S., de Silva, F., Dezi, F., Durante, M., Giallini, S., Lanzo, G., Sica, S., Simonelli, A., and Zimmaro, P. (2018). Local site effects and incremental damage of buildings during the 2016 central italy earthquake sequence. *Earthquake Spectra*, 34.

Shabani, A., Kioumarsi, M., and Zucconi, M. (2021). State of the art of simplified analytical methods for seismic vulnerability assessment of unreinforced masonry buildings. *Engineering Structures*, 239:112280.

Silva, V., Akkar, S., Baker, J., Bazzurro, P., Castro, J., Crowley, H., Dolsek, M., Galasso, C., Lagomarsino, S., Monteiro, R., Perrone, D., Pitilakis, K., and Vamvatsikos, D. (2019). Current challenges and future trends in analytical fragility and vulnerability modeling. *Earthquake Spectra*, 35.

Sorrentino, L., Cattari, S., da porto, F., Magenes, G., and Penna, A. (2019). Seismic behaviour of ordinary masonry buildings during the 2016 central italy earthquakes. *Bulletin of Earthquake Engineering*, 17.

Spence, R., Bommer, J., Del Re, D., Bird, J., Aydinoglu, M. N., and Tabuchi, S. (2003). Comparing loss estimation with observed damage: A study of the 1999 kocaeli earthquake in turkey. *Bulletin of Earthquake Engineering*, 1:83–113.

STADATA (2011). *3muri User Manual: a computer program for analysis of structures in masonry and mixed materials through a non-linear (pushover) and static analysis.*

Suckale, J., Grunthal, G., Regnier, M., and Bosse, C. (2005). *Probabilistic Seismic Hazard Assessment for Vantau.*

Terzic, V., Gillengerten, J., Saldana, D., Kumavat, N., Villanueva, P., Chrupalo, T., Bonneville, D., and Hortacsu, A. (2020). Fema p-58: Performance estimation tool as a design aid.

Tiberti, S. and Milani, G. (2017). Historic city centers after destructive seismic events, the case of finale emilia during the 2012 emilia-romagna earthquake: Advanced numerical modelling on four case studies. *The Open Civil Engineering Journal*, 11:1059–1078.

Tocchi, G., Polese, M., Di Ludovico, M., and Prota, . (2021). Regional based exposure models to account for local building typologies. *Bulletin of Earthquake Engineering.*

Valluzzi M.R., Sbogiò, L. and Saretta, Y. (2021). Interventions strategies for the seismic improvement of masonry buildings baed on fme validation: the case study of a terraced building struck by the 2016 central italy earthquake. *Buildings*, 11.

Verderame, G., Ricci, P., Luca, F., Del Gaudio, C., and De Risi, M. T. (2014). Damage scenarios for rc buildings during the 2012 emilia (italy) earthquake. *Soil Dynamics and Earthquake Engineering*, 66:385–400.

Vettore, M., Donà, M., Carpanese, P., Follador, V., da porto, F., and Valluzzi, M. (2020). A multilevel procedure at urban scale to assess the vulnerability and the exposure of residential masonry buildings: The case study of pordenone, northeast italy. *Heritage*, 3:1433–1468.

Vicente, R., D'Ayala, D., Ferreira, T., Varum, H., Costa, A., Silva, J., and Lagomarsino, S. (2014). *Seismic Vulnerability and Risk Assessment of Historic Masonry Buildings*, pages 307–348.

Vicente, R., Parodi, S., Lagomarsino, S., Varum, H., and Mendes Silva,

R. (2008). Seismic vulnerability assessment, damage scenarios and loss estimation case study of the old city centre of coimbra, portugal.

Vicente, R., Parodi, S., Lagomarsino, S., Varum, H., and Mendes Silva, R. (2011). Seismic vulnerability and risk assessment: Case study of the historic city centre of coimbra, portugal. *Bulletin of Earthquake Engineering*, 9:1067–1096.

Walker, B., Holling, C., Carpenter, S., and Kinzig, A. (2003). Resilience, adaptability and transformability in social-ecological systems. *Ecol. Soc.*, 9.

Whitney, R. and Agrawal, A. (2015). Seismic performance of flexible timber diaphragms: Damping, force-displacement and natural period. *Engineering Structures*, 101:583–590.

Yi, T., Moon, F., Leon, R., and Kahn, L. (2006). Analyses of a two-story unreinforced masonry building. *Journal of Structural Engineering-asce - J STRUCT ENG-ASCE*, 132.

Zanini, M., Hofer, L., and Pellegrino, C. (2019). The use of seismic risk maps in the development of seismic risk reduction programs.

Zuccaro, G., Dolce, M., De Gregorio, D., Speranza, E., and Moroni, C. (2015). La scheda cartis per la caratterizzazione tipologico-strutturale dei comparti urbani costituiti da edifici ordinari. valutazione dell'esposizione in analisi di rischio sismico.

Zucconi, M., Sorrentino, L., and Ferlito, R. (2017). Principal component analysis for a seismic usability model of unreinforced masonry buildings. *Soil Dynamics and Earthquake Engineering*, 96:64–75.

List of Publications

Publications list

Research papers in Journals

- Identification and Model Update of the Dynamic Properties of the San Silvestro Belfry in L'Aquila and Estimation of Bell's Dynamic Actions, A.Aloisio, I. Capanna, R. Cirella, R. Alaggio, F. Di Fabio, M. Fragiacomo, Applied Sciences, 2020, 10, 4289, doi:10.3390/app10124289.
- Sensitivity Assessment of the Seismic Response of a Masonry Palace via Non-Linear Static Analysis: A Case Study in L'Aquila (Italy), I. Capanna, A. Aloisio, F. Di Fabio, M. Fragiacomo, Infrastructures, 2021, 6(8), 10.3390/infrastructures6010008.
- Operational Modal Analysis, Model Update and Fragility Curves Estimation, through Truncated Incremental Dynamic Analysis, of a Masonry Belfry, I. Capanna, R.Cirella, A. Aloisio, R. Alaggio, F. Di Fabio, M. Fragiacomo, Buildings, 2021, 11, 120,10.3390/buildings11030120.
- Operational Modal Analysis and Non-Linear Dynamic Simulations of a Prototype Low-Rise Masonry Building, I. Capanna, R. Cirella, A. Aloisio, F. Di Fabio, M.Fragiacomo, Buildings, 2021, 11(10): 471, 10.3390/buildings1100471.
- A Simplified Method for Seismic Assessment of Unreinforced Masonry Buildings, I. Capanna, F. Di Fabio, M.Fragiacomo, Civil Engineering and Environmental System, 2022, 10.1080/10286608.2022.2047665.

International Proceedings

- The St. Silvestro belfry in L'Aquila: from the rehabilitation works to the actual performance in terms of dynamic properties and fragility functions estimation, I. Capanna, R. Cirella, A. Aloisio, R.Alaggio, F. Di Fabio, M. Fragiacomo, EASD Procedia, Eurodyn 2020, 3218-3227, XI International Conference on Structural Dynamics, Athens, Greece, 23-26 November, 2020.

- Comparative Assessment of empirical and mechanical approaches for the estimation of the seismic fragility of ordinary masonry buildings type of the inner Central Italy, I. Capanna, F. Di Fabio, M.Fragiacomo, Proceeding of Compdyn 2021, VIII ECCOMAS Thematic Conference on Computational Methods in Structural Dynamics and Earthquake Engineering, Athens, Greece, 27-30 June, 2021.

National Conference contribute

- Use of shape memory alloy devices in heritage structures: application in S.Silvestro belfry in L'Aquila, I. Capanna, F. Di Fabio, Proceeding of XVIII Convegno ANIDIS , Ascoli Piceno, Italia, 15-19 September, 2019.

[Blank page]

<APPENDIX>

A.1 Macro-element formulation implemented in the 3Muri software

In this appendix, the formulation, implemented in the 3Muri software, to analyse masonry building, is discussed. The macro-element formulation is accurately descripted in the user manual of the programme of which the main points are reported.

The panel, see Fig.A.1, with a b width and s thickness, consists of three parts with different mechanical behaviour. The parts called 1 and 3, of infinitesimal thickness and infinity stiffness to shear action, denote axial deformability. The part called 2, with height h and infinity stiffness to axial and flexural actions, denotes shear deformability. The macro-element consists of three degrees of freedom of nodes i and j, concentrated at the interface nodes.

Piers and spandrels are modelled as non-linear beam element, with:

- Initial stiffness (elastic);
- Bilinear constitutive law, with maximum values of shear and bending moment, evaluated at the ultimate limit state;
- Redistribution of the internal forces, according to the element equilibrium;
- Detection of damage limit states, considering global and local damage;

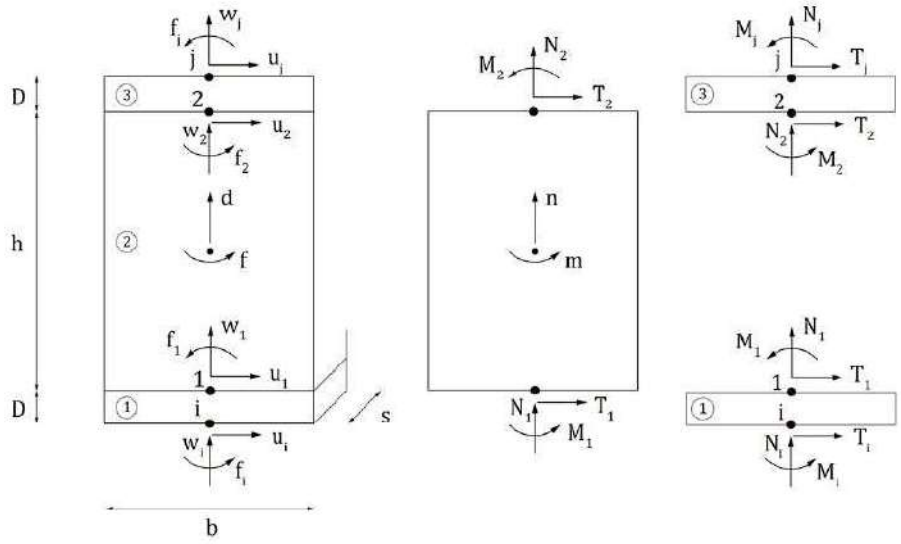

Figure A.1. Model of the macro-elementSTADATA (2011).

- Stiffness degradation in plastic range;
- Ductility control in terms of maximum drift, differents for failure mechanisms, according to Italian Code and EC8;
- Collapse of the element at reaching the ultimate drifts, without the interruption of the global analysis.

At reaching the minimum of the strength criteria of elements (flexural-rocking, shear-sliding or diagonal shear cracking), the non-linear behaviour is activated.

A.1.1 Flexural: Rocking behaviour

Eq.A.1 defines the ultimate flexural moment:

$$M_u = 0.5 * \sigma_0 * t * D^2 * (1 - \frac{\sigma_0}{0.85 * f_d}) = \frac{ND}{2} * (1 - \frac{N}{N_u}) \qquad (A.1)$$

where σ_0 is the mean vertical stress for gravitational loading, referred to the section at the middle of the piers' height; D and t are the width and the thickness of the wall, respectively; f_m is the mean compression strength of the masonry, N is the axial compressive force (positive for the compression). This approach foresee a non-linear re-distribution of stresses,

considered as a rectangular stress block with a reduction factor equal to 0.85. For existing structures (like the case studies of the PhD research activity), the mean compression strength f_m is divided by the confidence factor FC, different at varying the knowledge level, following the Normative Code Dispositions. According to Eq.A.2, the global equilibrium could be satisfied and thus, the shear value associated is:

$$V_i = -V_j = \frac{M_i + M_j}{h} \tag{A.2}$$

A.1.2 Shear: Mohr-Coulomb Criterion

The ultimate shear, expressed according to Mohr-Coulomb criterion, is evaluated as A.3:

$$V_u = D^{'} t f_v = D^{'} t(f_{v0} + \mu\sigma_n) = D^{'} t(f_{v0} + \mu_N \tag{A.3}$$

where $D^{'}$ is the length of the compressed section of the pier, f_v is the shear strength of the masonry, f_{v0} is the shear strength of the masonry with no compression, μ is the friction factor (kn general equal to 0.4), and σ_n is the normal mean compressive tensional state. The length $D^{'}$ is evaluated according to Eq.A.4:

$$l' = 3(\frac{l}{2} - e) = 3(\frac{l}{2} - \frac{|M|}{N}) \tag{A.4}$$

If the shear V exceeds the ultimate shear value, V_u, the bending moments value, M_i and M_j, could be changed to ensure the equilibrium. Consequently, a reduction of the moments cause a reduction of the eccentricity e and the enhancement of the l' value that could be expressed according to the Eq.A.5:

$$l^{'} = 3(\frac{l}{2} - e) = 3(\frac{l}{2} - \frac{\alpha V_h}{N}) \tag{A.5}$$

where α is a coefficient equal to: 0.5 for double bending constraints; 1 for cantilever.

The shear strength V_R is defined as the Eq.A.6. If V=V_R, the shear strength V_R is defined as the Eq.A.7.

$$V_R = (f_{v0} + 0.4 * \sigma_0) l' * t = f_{v0} * l^{'} * t + 0.4N \tag{A.6}$$

$$V_R = 3(\frac{l}{2} - \frac{\alpha V_R h}{N}) f_{v0} t + 0.4N = 1.5 * f_{v0} lt + 0.4N - 3\alpha f_{v0} ht \frac{V_R}{N} \tag{A.7}$$

The expressionA.7 could be manipulated in A.8.

$$V_R = \frac{1}{2} N \frac{3 f_{v0} lt + 0.8N}{3\alpha F_{v0} ht + N} \tag{A.8}$$

l' could be expressed as, see Eq.A.9, that indicates the length of the compressed section of the panel at the limit condition of shear failure:

$$l_R^{'} = \frac{3}{2}(l - \frac{3\alpha f_{v0} lt + 0.8\alpha N}{3\alpha f_{v0} ht + N} h) \tag{A.9}$$

Furthermore, respecting the Mohr-Coulomb criterion, the shear tension f_v must not exceed the limit value $f_{v,lim}$. If the $f_v > f_{v,lim}$, the shear value must be fixed as $V_{lim} = f_{v,lim} l^{'} t$. The effective compressed length l' has to be consistent with the value of V_{lim} and, thus, different from $l_R^{'}$. The limit compressed length $l_{lim}^{'}$, under the condition of failure mode, could be evalauted imposing $V = V_{lim}$, see Eq.A.10 and A.11.

$$V_{lim} = \frac{3}{2} N \frac{f_{v,lim} lt}{3\alpha F_{v,lim} ht + N} \tag{A.10}$$

$$l_{lim}^{'} = \frac{3}{2}(l - \frac{3\alpha f_{v,lim} lt}{3\alpha f_{v,lim} ht + N} h) \tag{A.11}$$

The shear V_u is the minimum between V_{lim} and V_R. The moment M_{max} is evaluated as, see Eq.A.12:

$$M_{max} = T_u \alpha h M_{min} = T_u (1 - \alpha) ht = T_u \tag{A.12}$$

The resistant criteria lays on the behaviour laws depicted in Fig.A.2.

A.1.3 Shear: Turnsek and Cacovic Criterion

Turnsek and Cacovic Criterion models the shear failure mode for existing buildings. The ultimate shear is evaluated according the Eq.A.13:

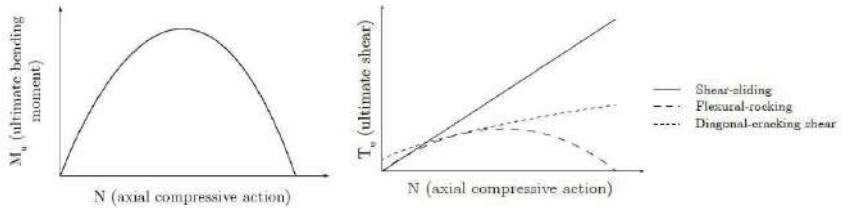

Figure A.2. Comparison between resistant criteria for macro-elementsSTADATA (2011).

$$V_u = \frac{1.5 * f_{v0} * t * D}{\epsilon} * \sqrt{1 + \frac{\sigma_0}{1.5 * f_{v0}}} \tag{A.13}$$

where σ_0 is the mean vertical stress for gravitational loading; D and t are the width and the thickness of the wall, respectively; f_{v0} indicates the design shear strength with no axial force, and ϵ is a coefficient related to the element geometrical ratio, assumed as H/D, where H is the height of the vertical masonry element.

A.1.4 Shear: Masonry spandrel beams

For spandrels beams, the shear strength could be expressed according to Eq.A.14:

$$V_{u,spandrel} = htf_{v0} \tag{A.14}$$

where h is the height of the section of the spandrel and t its thickness. The maximum bending moment could be expressed according to Eq.A.15

$$M_{u,spandrel} = \frac{hH_p}{2}(1 - \frac{H_p}{0.85 f_h ht}) \tag{A.15}$$

where H_p is the minimum value between:

- the tensile strength of tensional resistant element (like iron tie or beam);
- $0.4 * fh * f * t$, where f_h is the compression strength of the masonry referred to the horizontal direction.

A.2 Three dimensional nodes formulation implemented in the 3Muri software

The EquationsA.16, A.17, A.18 express the five dregrees of freedom of the three-dimensional nodes (u_x, u_y, u_z, ω_x and ω_y) and the three degrees of freedom of the two-dimensional nodes:

$$u = u_x * cos\omega + u_y * cos\omega \tag{A.16}$$

$$w = u_z \tag{A.17}$$

$$\phi = \phi_x sin\omega - \phi_y cos\omega \tag{A.18}$$

where u,v and ϕ indicate the displacement components. Fig.A.3 shows the reference axis along of which the forces are transmitted among macro-elements that belong to a single wall or a two walls.

Fig.A.3 (b) indicates the overall reference axis at which the forces transmitted refer. The forces trasmitted follow the expressions A.19:

$$F_x = F_{h1}cos\theta_1 + F_{h2}cos\theta_2 F_y = F_{h1}sin\theta_1 + F_{h2}sin\theta_2 F_z = F_v^1 + F_v^2 M_x = M_1 sin\theta_1 + M_2 sin\theta_2 M_y \tag{A.19}$$

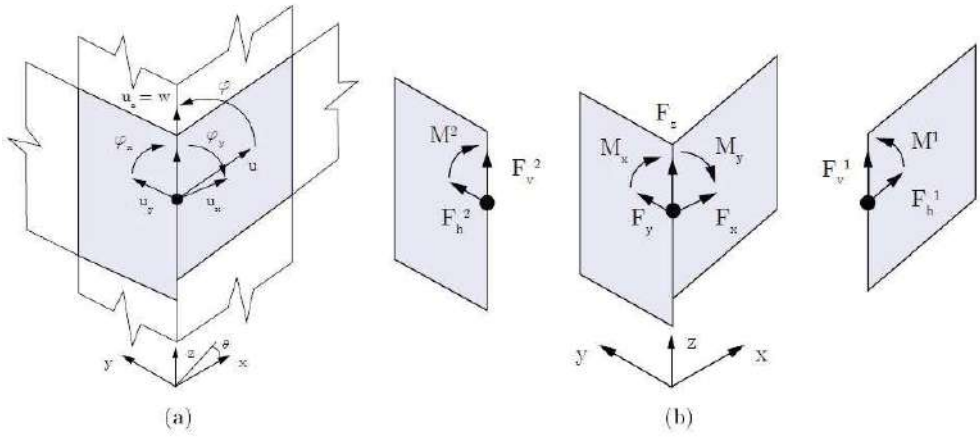

Figure A.3. Displacements-forces components: (a) for a single wall; (b) for two walls. STADATA (2011).

<APPENDIX>

B.1 Capacity Spectrum Method Formulation

This appendix reports the Capacity Spectrum method formulation that are used to derive push over curves of the analysed buildings during the research activity. The paragraphs below partially report the recommendations by European Code (EC8) Herrmann and Bucksch (2014) and the Italian Building Codes dei Trasporti e delle Infrastrutture (2008); per le Costruzione (2018).

The method was introduced by ATC-40 and implemented in HAZUS methodology for earthquake loss estimation Hazus (1997). The Capacity Spectrum method founds application in Non-linear static analysis. First of all, a capacity curve of an analyzed building which plots the base shear force versus the displacement of a control node. Then, the capacity curve is converted from a multi-degree-of-freedom (MDOF) in a single-degree-of-freedom (SDOF). The pushover curve is defined for 70% of the maximum base shear force value of the MDOF to consider equal areas below the both systems' curves. In the following paragraphs, each steps of the method is reported.

B.1.1 Performance Point for Non-linear static analysis

The performance point, PP, of a structure indicates the demand displacement, determined from the elastic response spectrum. Firstly, the normalisation of forces and displacements is carried out follow th Eq.B.1 and

Eq.B.2, respectively.

$$\bar{F_i} = m_i \Phi_i \tag{B.1}$$

$$\bar{F_n} = m_n \Phi_n \tag{B.2}$$

where m_i is the mass of the i-th storey, Φ_n is equal to 1, therefore $\bar{F_n} = m_n$.

B.1.2 The Equivalent SDOF system

In this chapter are reported the formulation to convert the MDOF in SDOF. The mass of an equivalent SDOF, m^*, is evaluated according to the Eq.B.3:

$$m^* = \sum mi\Phi_i = \sum \bar{F_i} \tag{B.3}$$

The mass participation factor Γ is evaluated according to Eq.B.4:

$$\Gamma = \frac{m^*}{\sum m_i \Phi_{i2}} = \frac{\sum \bar{F_i}}{\sum (\frac{\bar{F_i}^2}{m_i})} \tag{B.4}$$

Lastly, the force at the base F_b^* and the displacement d_n^* of the SDOF are evaluated according to the Eq.B.5 and Eq. B.6, respectively.

$$F_b^* = \frac{F_b}{\Gamma} \tag{B.5}$$

$$d_n^* = \frac{d_n}{\Gamma} \tag{B.6}$$

where F_b and d_n indicate the base shear force and the displacement of control node of the MDOF, respectively.

B.1.3 The idealized elasto-perfectly plastic curve between force and displacement

The yield Force F_y^*, that indicates the ultimate strength of the idealized system, is equal to the base shear at the plastic mechanism occurred. The formulation of the elastic stiffness of of the idealized system considers the equivalence of the areas of the idealized curve and actual one. The yield

displacement, dy* of the idealized system is evaluated according to the Eq.B.7:

$$d_y^* = 2(d_u^* - \frac{E_m^*}{F_y^*}) \tag{B.7}$$

where E_m^* is the deformation energy value evalauted up to the end of the elastic range.

B.1.4 The period of the idealized equivalent SDOF system

The period T^* of the idealized equivalent system SDOF is evaluated according to the Eq.B.8:

$$T^* = 2\Pi\sqrt{\frac{m^*}{k^*}} \tag{B.8}$$

where the secant stiffness k^* is equal to, see Eq.B.9:

$$k^* = \frac{F_y^*}{d_y^*} \tag{B.9}$$

B.1.5 Demand displacement of the idealized equivalent SDOF system

The performance point of the structure, with a period T_* and unlimited elastic behavior is evaluated according to the Eq.B.10:

$$d_{e,max}^* = S_e(T)^*[\frac{T^*}{2\Pi}] \tag{B.10}$$

where $S_e(T)^*$ is the elastic acceleration response spectrum at the period T^*. For the evaluation of the performance point d_{max}^*, different formulations are proposed, at varying the relationship between T^* and T_c^*, see Eq.B.11,B.12:

$$d_{max}^* = d_{e,max}^* = S_{De}(T)^* \tag{B.11}$$

if $T^* > T_c^*$; alternatively,

$$d_{max}^* = \frac{d_{e,max}^*}{q^*}[1 + (q^* - 1)\frac{T_c}{T^*}] \geq d_{e,max}^* \tag{B.12}$$

if $T^* < T_c^*$.

q^* is the behaviour factor evaluated as, see Eq.B.13:

$$q^* = \frac{S_e(t^*)m^*}{F_y^*} \tag{B.13}$$

It is imposed that $d_{max}^* < 3 * d_{e,max}^*$.

B.1.6 Demand Displacement of the MDOF system

The displacement demand of the control node of the MDOF is, see Eq.B.14:

$$d_{max} = \Gamma d_{max}^* \tag{B.14}$$

B.1.7 Energy dissipation

The final step of the Capacity Spectrum Method foresees the evaluation of the structural safety level of the structure: the energy dissipation effects could be considered, in the non-linear structural field, to evaluate the seismic demand. Therefore, the inelastic spectrum is drawn, starting from the elastic response spectrum of as SDOF, in the ADRS format (S_{ae} versus S_{de}), reduced by a reduction factor R_μ that takes into account the ductility of the structure, see Eq.B.15,B.16,B.17,B.18:

$$S_a = \frac{S_{ae}}{R_\mu} \tag{B.15}$$

$$S_d = \frac{\mu}{R_\mu} * S_{de} \tag{B.16}$$

$$S_{de} = \mu + * \frac{T^2}{R_{4*\pi^2}} * S_a \tag{B.17}$$

$$R_\mu = \frac{S_{ae}(T^*)}{S_{ay}} \tag{B.18}$$

where μ is the ductility factor (ratio between the ultimate and yielding displacement). Furthermore, R_μ depends on the fundamental period of the structure, and thus, on its stiffness, see Eq.B.19,B.20:

$$R_\mu = (\mu - 1)\frac{T^*}{T_c} + 1 for T^* < T_c \tag{B.19}$$

$$R_\mu = \mu for T^* > T_c \tag{B.20}$$

where T_c is the response spectrum transition period between the constant acceleration and constant velocity branches. Finally, the displacement demand S_d is evaluated as Eq.B.21,B.22:

$$S_d = \frac{S_{ae}}{R_\mu}[1 + (R_\mu - 1)\frac{T_c}{T^*}] for T^* < T_c \tag{B.21}$$

$$S_d = S_{de}(T^*) for T^* > T_c \tag{B.22}$$

=